Development of a high-throughput shotgun-mass spectrometry method for qualitative and quantitative analysis of major mammalian brain gangliosides

D i s s e r t a t i o n s s c h r i f t

zur Erlangung des akademischen Grades

Doctor rerum medicinalium (Dr. rer. med.)

vorgelegt

der Medizinischen Fakultät Carl Gustav Carus

der Technischen Universität Dresden

von

Herrn M.Sc. Christopher Spiegel

aus Heidelberg

Dresden, 2019

2. Blatt (2. Seite)

1. Gutachter: Prof. Dr. Kai Simons

2. Gutachter: Prof. Dr. Daniel Müller

Tag der mündlichen Prüfung: (Verteidigungstermin): 12.05.2020

gez.: Prof. Dr. Björn Falkenburger----------

Vorsitzender der Promotionskommission

Anmerkung:

Die Eintragung der Gutachter und Tag der mündlichen Prüfung (Verteidigung) erfolgt nach Festlegung von Seiten der Medizinischen Fakultät Carl Gustav Carus der Technischen Universität Dresden. Die oben genannten Eintragungen werden durch die Doktoranden nach der Verteidigung zwecks Übergabe der fünf Pflichtexemplare an die Zweigbibliothek Medizin in gedruckter Form oder handschriftlich vorgenommen.

Table of Contents

Abbreviation	**Full Name**
ABC	Ammonium Bi-carbonate
AD	Alzheimer's Disease
AMD	Automated multiple development machines
CerS	Ceramide Synthases
CERT	Ceramide transfer protein
Cmah	CMP-N-acetylneuraminic acid hydroxylase
CNS	Central nervous system
CV	Coefficient of variance
DRM	Detergent resistant membranes
DsiaT	Drosophila sialyltransferase
ECM	Extracellular matrix
Elisa	Enzyme-linked immunosorbent assay
ER	Endoplasmatic reticulum
ESI	Electrospray ionization
FACS	Fluorescent-activated cell sorting
GD	Gaucher's Disease
GPMVs	Giant plasma membrane vesicles
GSL	Glycosphingolipid
HPLC	High-performance liquid chromatography
HPTLC	High-performance thin layer chromatography
LOD	Limit of detection
LOQ	Limit of quantification
LSD	Lysosomal storage disease
MS	Mass spectrometer
MS/MS	Tandem MS (for molecule fragmentation)
NeuAC	N-acetylneuraminic acid
NeuGC	N-glycolylneuraminic acid
NPLC	Normal phase liquid chromatography
PA	Phosphatidic acid

PC	Phosphatidylcholine
PE	Phosphatidylethanolamine
PI	Phosphatidylinositol
PNS	Peripheral nervous system
PS	Phosphatidylserine
RF	Response factors
RPLC	Reverse phase liquid chromatography
Sia	Sialic acid
SM	Sphingomyelin
SPE	Solid phase extraction
TAG	Triacylglyceride
TOF	Time of flight
Trks	Tyrosine kinases

Acknowledgements

I want to express my gratitude to a group of very special people, without them, their support and understanding I would not have been able to work on and finish this project.

Firstly, my supervisors and mentors Kai Simons and Christian Klose for everything they taught me, their patience and support. My colleagues Tomek Sadowski, Mathias Gerl and Ronny Herzog for all the interesting discussions, the time they took for me and the support they gave me.

My gratitude also goes to Ludger Johannes for providing me with the C17-Ganglioside Standards, which were a crucial contribution to this project and without which it would not have been possible to develop the protocol as far as it is. I would also like to thank Mikael Simons for providing the mouse brain samples for the final global lipidomics experiment.

A very special thank you extends to my parents, who were always there for me and I cannot even imagine where I would be without their love and support.

But above all, I want to thank my wife. You give a dreamer the necessary roots.

1. Introduction

Cells are the fundamental units of life. These small, membrane-enclosed entities are filled with an aqueous solution and are brimming with staggering variety of chemicals, minerals, ions, proteins, nucleic acids and lipids. For a living cell it is fundamental to separate itself from its environment in such a way that interactions with the surroundings remain possible. This is achieved by encapsulating the cytoplasm with a lipid membrane. Cells depend on their selectively permeable membranes to import nutrients and to export by- or waste products, as well as for cell adhesion, cell signaling and for many other processes. Intensive research has provided insights into the underlying processes and allowed to extend our knowledge about functions of these versatile permeability barriers. Nevertheless, many aspects are still far from being understood. The cellular outer membrane, called plasma membrane, not only contains a lipid bilayer but also harbors multitude of proteins that are key to its functional capabilities (Daum et al., 1998). While the cell membrane research of the last decades has been mainly focused on proteins, lipids have been largely neglected. This is changing due to the emergence of new technologies (Ivanova et al., 2009; Schuhmann et al., 2012; Surma et al., 2015). But what is a lipid? A lipid is a small amphipathic molecule, consisting of a hydrophilic head group and a membrane-embedded hydrophobic moiety. Lipids have been systematized into 8 primary categories: fatty acyls, glycolipids, glycerophospholipids, sphingolipids, sterol lipids, prenol lipids, saccharolipids, and polyketides (Fahy et al., 2005).

Of special interest for this dissertation are glycolipids that additionally contain sialic-acid and are then called glycosphingolipids (GSLs) or also gangliosides. Gangliosides are ubiquitously present on all human cells, but most abundantly in the neuronal and hepatic cells.

1.1. Discovery and definition of Glycosphingolipids (GSLs)

Glycolipids consist out of one or more carbohydrate residues that are connected via glycosidic linkage with a hydrophobic or amphipathic lipid moiety (Fahy et al., 2005). Glycolipids possessing either a ceramide or sphingoid base as a lipid moiety are termed glycosphingolipids (Yu et al., 2011). The lipid moiety usually serves as an anchor in the plasma membrane, while the sugar residues are part of the extracellular matrix (ECM), with the first sugar residue partly embedded into the lipid bilayer of a cell (Alberts et al., 2002). Hence, they contribute to the cell- and species-specific profile at the cell surface. This profile undergoes constant changes, reflecting the stage of development, differentiation, and even oncogenic transformation, thus indicating the importance of these lipid molecules for cell-cell and cell-matrix interactions

(Cohen and Varki, 2010). In addition, glycolipids are important signal molecules for cell adhesion, modulation of membrane receptors and signal transduction (Eich et al., 2016).

Gangliosides are sialic acid containing glycosphingolipids, which are in turn a subgroup of glycolipids. The name ganglioside was given by the German scientist Ernst Klenk in 1942, after he for the first time isolated lipids from ganglion brain cells and determined their chemical structure (Klenk, 1942).

Close to 200 ganglioside species have been identified in vertebrates while considering only their different carbohydrate structures ("IUPAC-IUB Joint Commission on Biochemical Nomenclature (JCBN) Nomenclature of glycolipids," 1998). If also the heterogeneity, e.g. the chain length and saturation of the hydrophobic lipid moiety is considered, the molecular structural complexity of gangliosides increases multifold.

1.2. Structure and biosynthesis of glycolipids

Glycolipids are biomolecules consisting of hydrophobic or amphipathic lipid moieties linked to one or more carbohydrate residues through a glycosidic linkage. Hence, they contribute to both, the cellular lipidome and the glycome/sialome. (Cohen and Varki, 2010). Glycosphingolipids (GSLs) contain a great variety of carbohydrate sequences, including gangliosides and are classified based on their basic carbohydrate structure (see Table 1).

Series	Core Structure	Abbreviation
Arthro	GlcNAcβ1,3Manβ1,4Glcβ1,1´Cer	At
Gala	Galα1,4Galβ1,1´Cer	Ga
Neogala	Galβ1,6Galβ1,6Galβ1,1´Cer	
Ganglio	Galβ1,3GalNAcβ1,4Galβ1,4Glcβ1,1´Cer	Gg
Globo	GalNAcβ1,3Galα1,4Galβ1,4Glcβ1,1´Cer	Gb
Isoglobo	GalNAcβ1,3Galα1,3Galβ1,4Glcβ1,1´Cer	iGb
Lacto	Galβ1,3GlcNAcβ1,3Galβ1,4Glcβ1,1´Cer	Lc
Neolacto	Galβ1,4GlcNAcβ1,3Galβ1,4Glcβ1,1´Cer	nLc
Muco	Galβ1,3Galβ1,4Galβ1,4Glcβ1,1´Cer	Mc
Mollu	Fucα1,4GlcNAcβ1,2Manα1,3Manβ1,4Glcβ1,1´Cer	Mu
Schisto	GalNAcβ1,4Glcβ1,1´Cer	
Spirometo	Galβ1,4Glcβ1,3Galβ1,1´Cer	

Table 1. Carbohydrate structure of glycosphingolipids.

Gangliosides are synthesized in the Golgi apparatus by specific glycosyltransferases, the expression of which controls the steady-state levels of gangliosides at the cell surface.

An important part of gangliosides are the sialic acids bound to their sugar moieties. Sialic acids (Sia) are also very interesting molecules and their distribution in nature is worth noting. An abundant expression of sialic acids only occurs in the deuterostome lineage (vertebrates and a few higher invertebrates) (Angata and Varki, 2002). In other lineages (bacteria, archaea, plants, fungi, protozoa and protostomes) the expression of Sia is only detected in a small minority of species (Vimr et al., 2004). Of these few Sia^+ non-deuterostome lineage species the ones associated with human or animal hosts, e.g. gram-negative bacteria, are by far the majority and often the causative agents for serious illnesses (Varki, 2008). For example, neuroinvasive bacteria (*Escherichia coli* K1 and *Neisseria meningitidis* serogroup B) express high-molecular weight homopolymers of α2-8- and/or α2-9 lined neuraminic acid (NeuAc) called polysialic acid (polySia) (Vimr et al., 2004). These Sia polymers have a size and charge that support bacterial dissemination by downmodulation of complement activity (Allen et al., 1987; Schneider et al., 2007). Furthermore, *Neisseria meningitidis* produces a serogroup B with such a remarkable structural similarity to the α2-8-linked polySia capsule that it impedes with the initiation of an immune response in human hosts (Ziak et al., 1996). Also other pathogenic bacteria, such as *Campylobacter jejuni*, have been identified to be capable to express remarkably complex sialoglycans on lipooligosaccharides of their outer membranes (Yuki, 2007). The similarity of these glycans to vertebrate brain sialoglycans can induce autoimmune neuropathies (Yuki and Hartung, 2012).

Distribution of sialic acids in invertebrates is so rare, that for a long time it was perceived as practically non-existing, except in a few higher species (Angata and Varki, 2002). Only after sequencing of the *Drosophila* genome, it became clear that they possess similar genes required for the mammalian sialoglycan biosynthesis (Koles et al., 2009) and even a single sialyltransferase (*DSiaT*) (Repnikova et al., 2010). A subsequent glycan analysis of *Drosophila* glycoproteins confirmed the expression of the sialic acid N-acetylneuraminic acid (*NeuAc*) (Kračun et al., 1984; Aoki et al., 2007). Interestingly, expression of *DSiaT* gene only occurs in a small group of differentiated central nervous system neurons (Repnikova et al., 2010). The phenotype accompanying a loss of *DSiaT* function is characterized by a progressive loss of coordination and temperature-sensitive paralysis, as well as locomotor defects (Repnikova et al., 2010). Such symptoms could origin from possible defects in the formation and physiology of voltage-gated sodium channels in neuromuscular junctions. These findings point to key

functions of sialic acids and help to highlight the evolutionary role of sialyation in the nervous system.

Interestingly, most vertebrates including human's closest evolutionary relatives, bonobos and chimps, express two different sialic acids, N-glycolylneuraminic acid (*NeuGc*) and N-acetylneuraminic acid (*NeuAc*), in significant amounts, while humans only express NeuAc (Chou et al., 2002). The reason for this difference in the human sialome is due to an exon deletion in the gene encoding for CMP-*N*-acetylneuraminic acid hydroxylase (*CMAH*) (Okerblom et al., 2017), which is converting *N*-acetyl to *N*-glycolyl. According to the molecular clock comparison, a technique used to validate the evolutionary diversion of two or more species based on mutation rates of DNA or amino acid sequences for proteins from fossils or archeological dates, the branching of the human line from the chimpanzee *CMAH* gene took place around ~3 million years ago (Chou et al., 2002). The most common hypothesis for that circumstance is the occurrence of a catastrophic pandemic pathogen at the beginning of the human lineage that targeted NeuGc. By giving rise to natural selection against a functional *CMAH* gene (Varki, 2010), this event has been termed the "sialoquake" by Varki (Varki, 2009). Also, the glycan mediated binding specificities of related human and non-human pathogens support this theory, since evolutionary changes in sialic acid binding proteins of the immune system postdate the loss of *CMAH*. But it is remarkable that the expression of NeuGc is likewise diminished in the brain of non-human species to the advantage of NeuAc, even though NeuGc is the predominant sialic acid in all other tissues. In mice for example the expression of *Cmah* gene is high in liver, thymus, spleen and kidney, but its transcripts are undetectable in the brain (Kwon et al., 2014). Nevertheless, the question why NeuAc is predominantly expressed over NeuGc in human brains is still not fully answered; possible explanations could lie in the specific function of NeuAc in molecular recognition processes in the brain (Davies and Varki, 2015).

1.3. Ceramidase expression patterns

Besides the prior mentioned sugar moieties, the second major building block of gangliosides are ceramides, which play an essential role in sphingolipid metabolism in general and contribute significantly to membrane signaling. In mammals, ceramide is synthesized by a family of six ceramide synthases (CerS), each of them being responsible for specific acyl chain length it synthesizes (Levy and Futerman, 2010; Cingolani et al., 2016) (see Figure 1). The hypothesized role of ceramide as a signaling molecule made it to the center of ongoing studies regarding its involvement in regulating differentiation, proliferation and apoptosis of cells.

(Kolesnick, 2002; Pettus et al., 2002). These molecules constitute out of a sphingoid long chain base that is connected via an amide bond to a fatty acid. *De novo* synthesis of ceramide takes place in the endoplasmic reticulum (ER), while additional steps of sphingomyelin and glycosphingolipid synthesis continue in the Golgi apparatus (Futerman and Riezman, 2005). The transport from the ER to the Golgi apparatus proceeds either by vesicular trafficking or by ceramide transfer protein (CERT) across membrane contact sites between the two organelles (Hanada et al., 2003). *De novo* pathway begins with the condensation of L-serine and palmitoyl transferase (Hanada, 2006) generating 3-ketosphinganine, which is then reduced to sphinganine via 3-ketosphinganine reductase (Dolgachev et al., 2004) and followed by acylation of sphinganine via sphinganine *N*-acyl transferase to dihydroceramide. The acylation step of sphinganine by N-acyl transferase is a key reaction in this pathway, which is carried out by the prior mentioned six CerS. Futerman and Levy (Levy and Futerman, 2010) showed, that each member of the CerS family possesses a distinct set of features and described their individual tissue distribution (see Figure 2). As shown in Figure 2, CerS1 is the most dominant ceramide synthase in the brain, followed by CerS4 and CerS2; these enzymes - except CerS2 - facilitate the addition of C18 or, respectively, C20 fatty acids to the C18 sphinganine (see Figure 1) resulting in a majority of C36 and C38 ceramides in the central nervous glycosphingolipids.

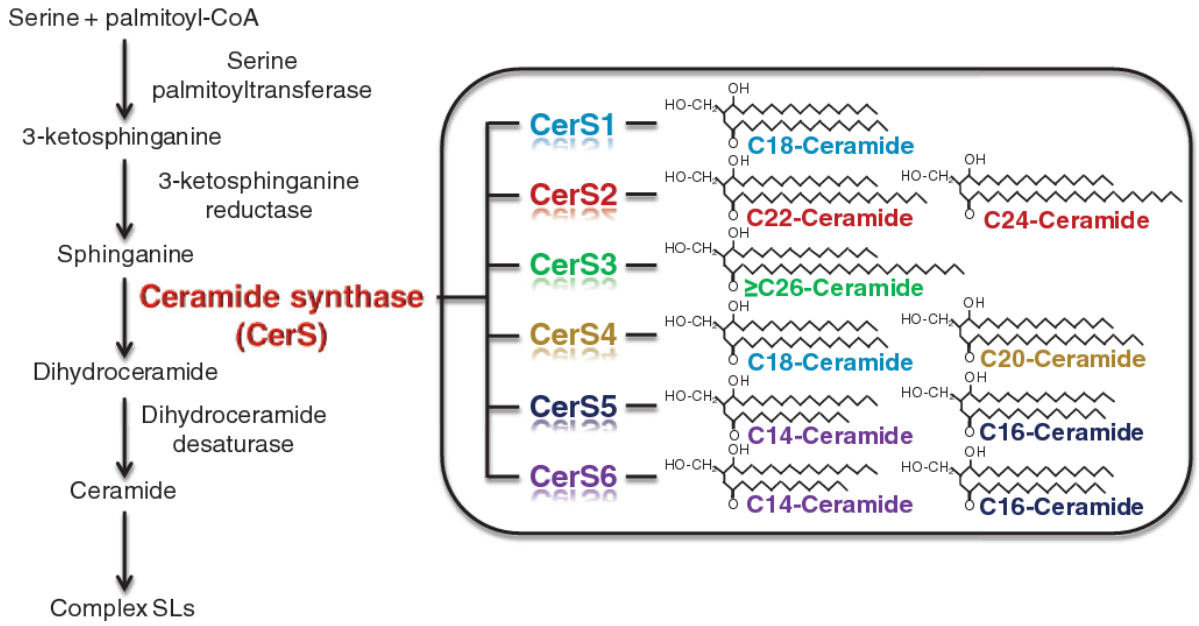

Figure 1. The ceramide synthase (CerS) family consists out of 6 enzymes, each specific for the addition of different acyl chain lengths. Due to this fact, ceramides can possess a variety of chain lengths and different degrees of saturation and α-hydroxylation. Figure was adapted from (Cingolani et al., 2016).

The above findings were also supported by Ikeda *et al.*, who analyzed the total lipid extracts of the mouse brain by employing the reverse phase liquid-chromatography coupled with electrospray-ionization fragmentation mass spectrometry (RPLC/ESI-MS/MS) and multiple reaction monitoring (MRM) of 25 week-old C57BL/6 mice (Ikeda et al., 2008). Results of this study are summarized in Figure 3 which shows that the d18:1-18:0 is the dominating ceramide species in mouse brain, followed by d20:1-18:0, in particular in the more complex gangliosides, namely GM1, GD1, GT1 and GQ1. The biosynthetic pathway of gangliosides is illustrated in Figure 4. Ceramide (Cer) is the starting molecule for all *de novo* ganglioside synthesis with the stepwise addition of monosaccharides to Cer. Gangliosides are divided into 4 groups:0-, a-, b-, and c-series, depending on the number of neuraminic acid molecules connected to the lactosylceramide (LacCer) before the addition of GalpNAc by GM2/GD2 synthase occurs. Continuation of the ganglioside biosynthesis pathway after LacCer is sequentially performed by the enzymes β4GalNAc T1, β3Gal T4, and the sialyltransferases ST3Gal II and ST8Sia V (see Figure 4).

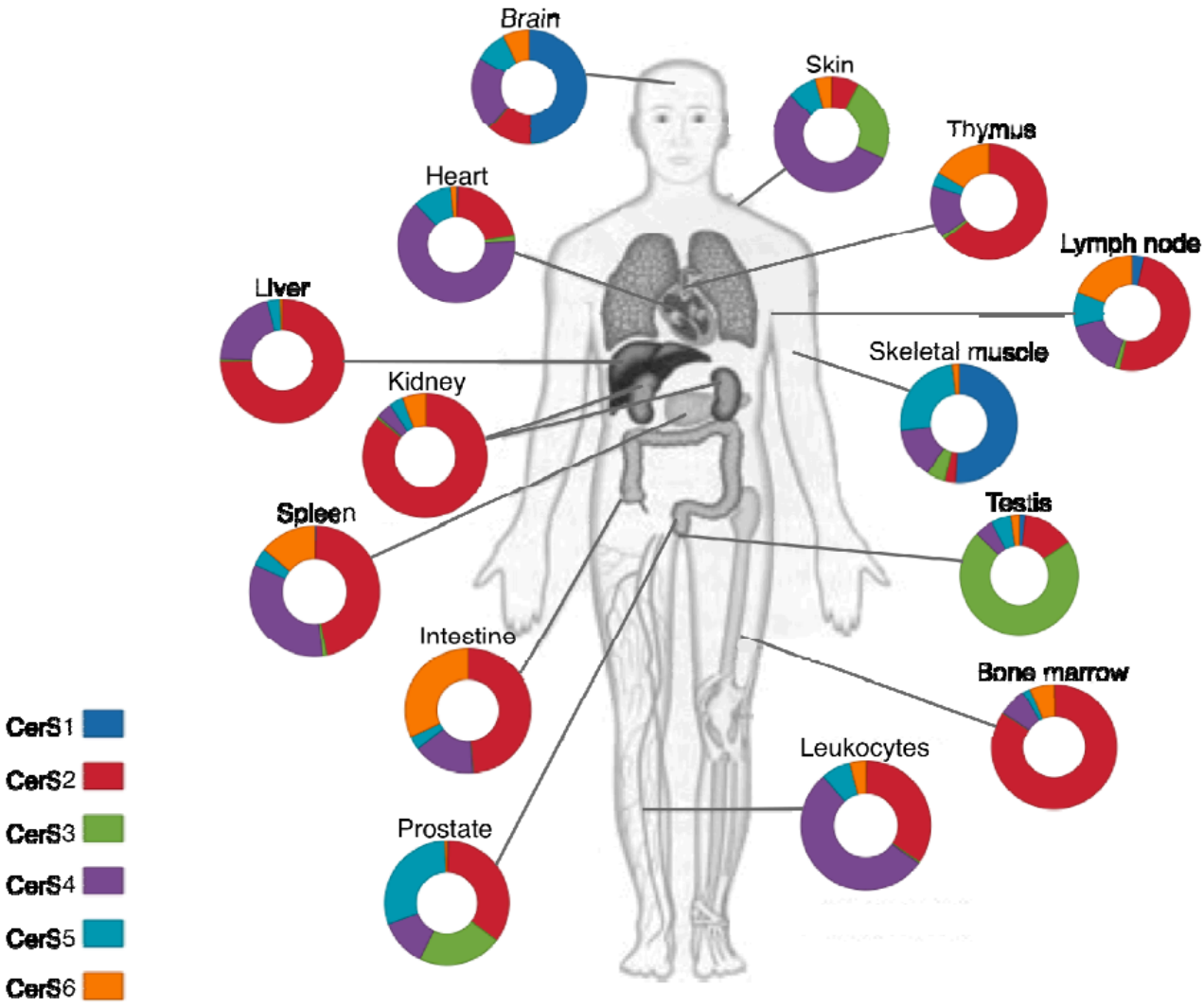

Figure 2. The distribution of ceramide synthases is represented in pie charts for each human organ, each member of the CerS family is color coded as shown in the legend. Figure was adapted from (Levy and Futerman, 2010).

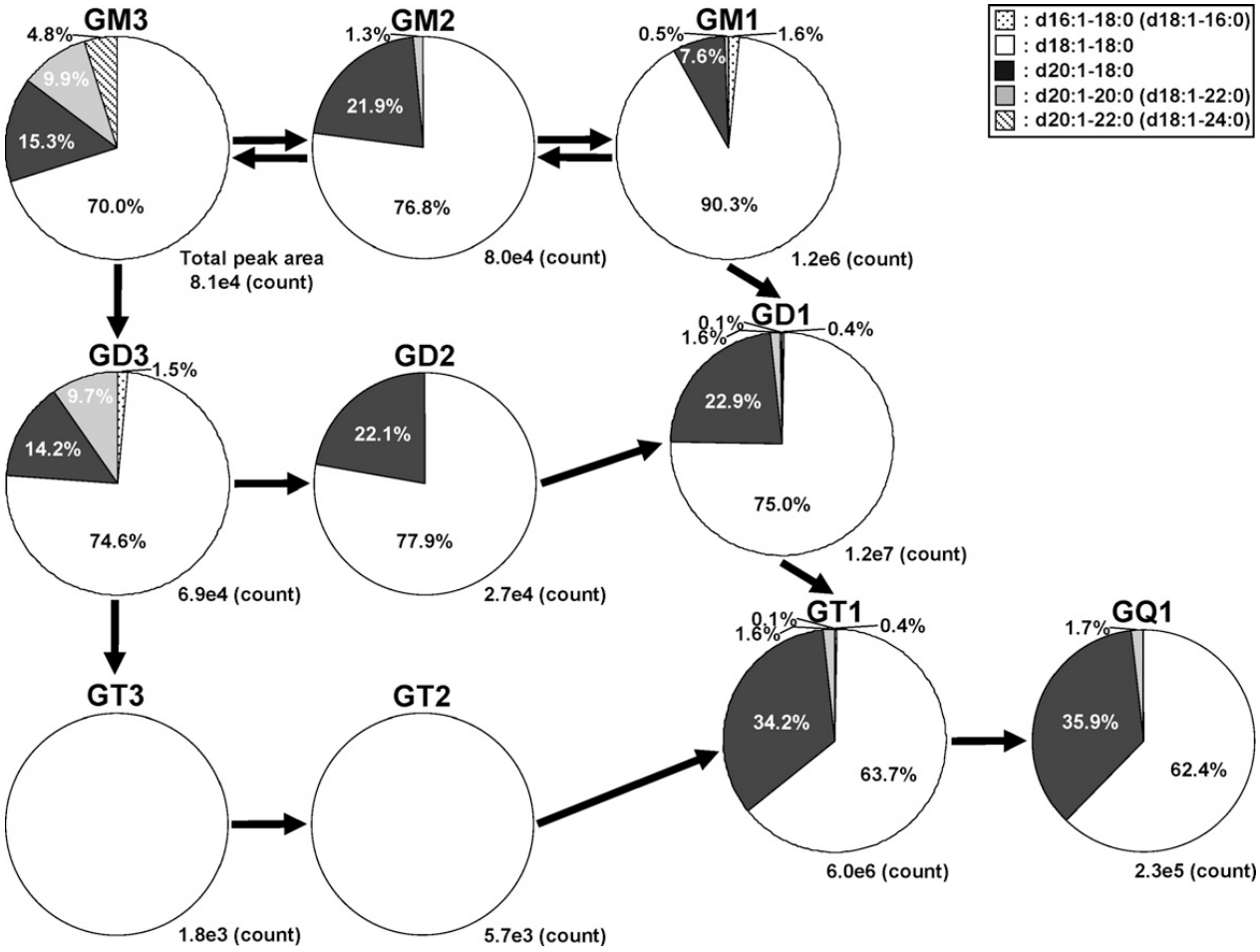

Figure 3. Ganglioside molecular species from mouse brain identified by RPLC/ESI-MS/MS and MRM detection. The percentage of each ganglioside molecular species has been calculated by the ratio of individual peak areas of individual ganglioside molecules to the total peak area. Figure was adapted from (Ikeda et al., 2008).

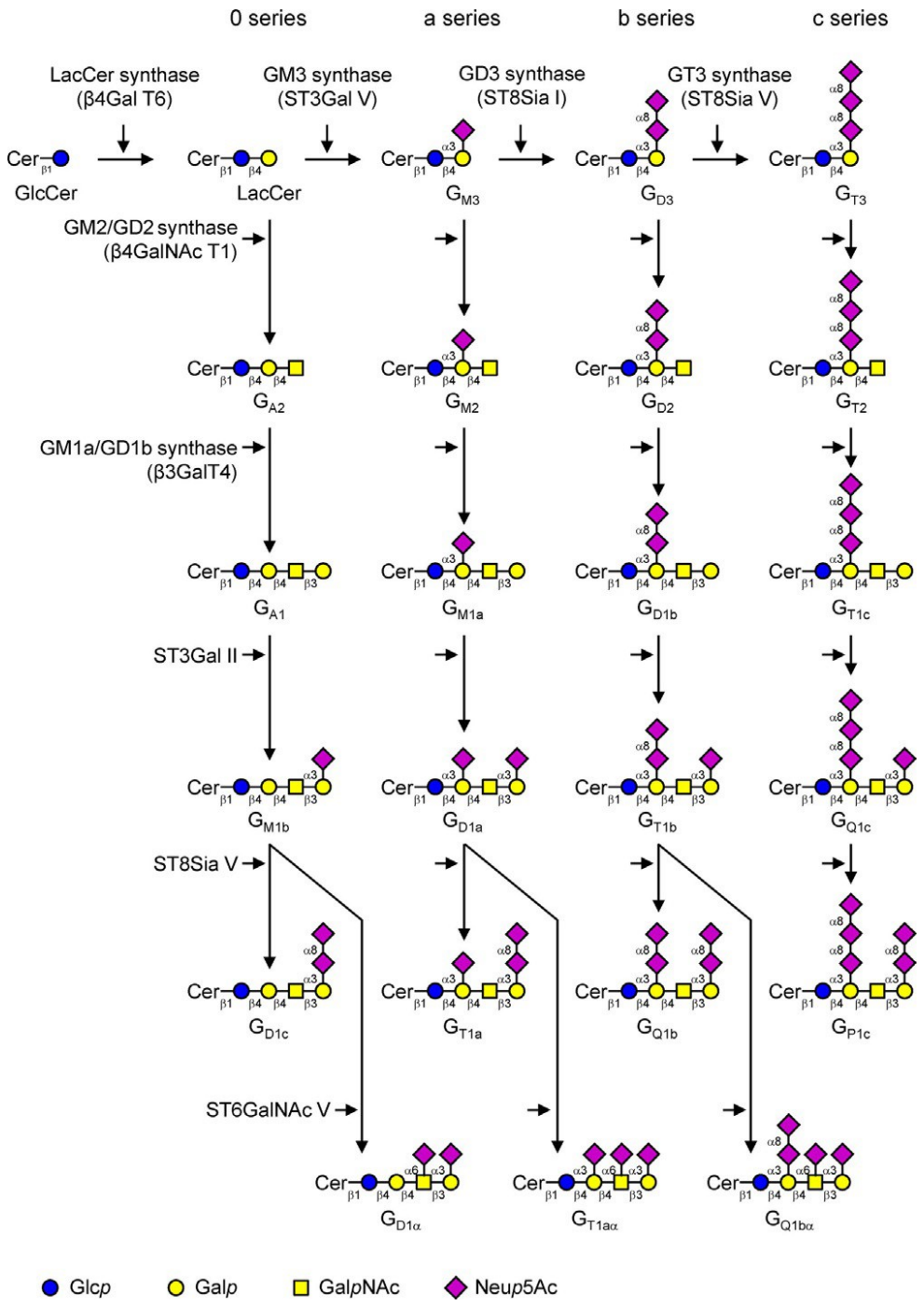

Figure 4. Biosynthesis pathways of gangliosides. Gangliosides are synthesized by stepwise addition of monosaccharides to ceramide (Cer). Gangliosides are categorized into 4 groups called 0-, a-, b-, and c-series. The categorization depends on the amount neuraminic acid added to the lactosylceramide (LacCer) before the addition of GalpNAc by GM2/GD2 synthase occurs. The ganglioside biosynthesis pathway is continued after LacCer with the sequential work of the enzymes β4GalNAc T, β3Gal T4 (also called GM1a/GD1b synthase), and the sialyltransferases ST3Gal II and ST8Sia V. Figure adapted from (Groux-Degroote et al., 2015)

1.4. Function

1.4.1. Membrane Microdomains and Lipid Rafts

For a long time, the working hypothesis was that cellular membranes consist out of a homogenous liquid or fluid phase formed by the lipid bilayer (Singer and Nicolson, 1972). It was first in the 1970s when it became clear that lipids and proteins can move laterally in the lipid bilayer, i.e. that cell membranes are fluids. Gradually accumulating evidence suggested, that plasma membranes can sub-compartmentalize. This is based on the weak affinity between sphingolipids and cholesterol, which organize dynamic assemblies that can form functional platforms in the membrane. Such compartmentalization principle is based on 2-dimensional phase separation. Simple model systems consisting out of sphingomyelin, unsaturated phospholipids and cholesterol can form two liquid phases, the liquid-disordered (L_d) and liquid-ordered phase (L_o) (Simons and Ikonen, 1997). The L_d-phase is characterized by high lateral mobility and consists of disordered acyl chains with conformational low order in the unsaturated phospholipids (Hancock, 2006). The (L_o)-phase on the other hand is more ordered (liquid-ordered) and the hydrophobic moieties are saturated. This segregation depends on cholesterol due to its rigid sterol ring favoring interactions with straighter, stiffer hydrocarbon chains of saturated lipids and hence, disfavors interaction with the more flexible unsaturated lipid species, resulting in lateral segregation (Lingwood and Simons, 2010). Thus, cholesterol induces a liquid-liquid phase separation into a unique L_o phase and the L_d phase. Plasma membranes can also phase separate into liquid-ordered and –disordered phases. Especially glycosphingolipids form ordered domains in the phospholipid bilayer, due to the affinity of sphingolipids to form hydrogen bonds and their affinity to cholesterol (Abrahamsson et al., 1977; Thompson and Tillack, 1985). This has been shown microscopically in giant plasma membrane vesicles (GPMVs) (Sezgin et al., 2012). The fact that biological membranes are not as homogenous as previously thought was also observed by the aggregation of sphingolipids (Thompson and Tillack, 1985) and resulted in the suggestion that sphingolipid microdomains may be the reason for differences in the lipid composition of the apical and basolateral plasma membrane of epithelial cells (Simons and van Meer, 1988). Simons and van Meer suggested, that sphingolipid microdomains can influence the apical lipid sorting process in the trans-Golgi network and this hypothesis has been supported when an apically sorted protein was shown to be associated with sphingolipids, enriched in detergent-resistant membranes (DRMs) insoluble to the detergent Triton X-100 at 4°C (Brown and Rose, 1992). All these studies prompted Simons and Ikonen to postulate their lipid raft concept, in which they propose the

existence of sphingolipid- and cholesterol enriched membrane microdomains with a higher fatty acid chain order that contribute to various cellular processes, such as assembly of signal platforms and the formation of vesicular carriers in membrane trafficking (Simons and Ikonen, 1997). These lipid rafts are defined as small lipid or membrane rafts (10-200 nm), heterogenous, highly dynamic, sterol- and sphingolipid-enriched membrane domains that compartmentalize cellular processes (Simons and Ikonen, 1997). In the resting state, the raft lipids and proteins form fluctuating nano-assemblies which can be clustered to form larger and more stable platforms that are key to their biological function. Using stimulated emission depletion (STED) microscopy it was possible to show the existence of small membrane areas (< 20 nm), where glycosylphosphatidylinositol (GPI)-anchored proteins where enclosed by lipid rafts lipids, i.o. sphingomyelin (SM), GM1 and cholesterol, for an average lifespan of 10-20 ms and thus, forming transient and dynamic molecular complexes (Eggeling et al., 2009a, 2009b). Because glycosphingolipids and gangliosides can form such dynamic structures, the lipid raft principle will be an important element in elucidating ganglioside function. So far most of this work remains to be done. The capability to form functional larger platforms (Pike, 2006) in a sterol-dependent manner (Sharma et al., 2004; Eggeling et al., 2009b) may be essential for the biological role that gangliosides play, for instance in cell-cell interactions (Baumgart et al., 2007; Lingwood et al., 2008).

1.4.2. Microdomains in the brain

The compartmentalization of cellular membranes and existence of membrane microdomains is probably more evident in the brain than in any other tissue. Cells of the central nervous system (CNS), but also in the peripheral nervous system (PNS), are highly specialized, which is also reflected in their morphology (Zhang and Cui, 2014, p. 2). Neurons, oligodendrocytes, Schwann cells (in the PNS) and to a lesser extent astrocytes are highly polar cells, hence compartmentalization of signaling events is required in order to maintain normal neuronal physiology, including neuronal differentiation, polarization, synapse formation, synaptic transmission and glial-neural interactions (Marin et al., 2013). This is achieved by the polarization of the neuronal plasma membrane into somatodendritic, axonal and synaptic membrane macrodomains, while myelinating cells have a multi-layered myelin-sheath and nodal domains (Poliak and Peles, 2003). Although neuronal membrane regions lack morphologically distinguishable cell junctions such as tight junctions in epithelial cells, lateral diffusion is hindered between the plasma membrane domains, isolating these membrane compartments from each other (Jacobson et al., 1995). The role of lipid rafts in the brain has

been analyzed over the years and particular lipids, and specific subsets of membrane proteins have been identified to be necessary for the function of neuronal lipid membrane domains (see Table 1 in review (Sonnino et al., 2014)). These reports were also supported by a growing number of proteomics studies (Cayrol et al., 2011; Hashimoto et al., 2012; Shah et al., 2015). Membrane receptors are most prominent proteins in neuronal cells, whose function often depends on integration into specific lipid membrane domains. Among these receptors tyrosine kinases (Trks) are probably the most important ones, since they are crucial in the mediation of cell-cell interactions.

During the maturation processes in the brain, i.e. after birth and during the aging processes, the lipid homeostasis in the nervous system is changing and various neurodegenerative diseases cause alterations in the homeostasis, ultimately affecting the organization of lipid rafts. Understanding these processes better can facilitate the development of improved therapies for neurodegenerative disease treatment. This topic is addressed in section 1.6.

1.5. Localization and quantities of gangliosides in the mammalian brain

The expression, sorting and turnover of constituents of the membrane is a tightly regulated process which continues along with the development of cells and tissues. Each cell type has its own individuality. Of all the different cell membrane lipids, the highest structural complexity is seen for glycosphingolipids (GSLs), as already described before in section 1.2 Structure and biosynthesis of glycolipids The expression of a developmentally regulated cell-specific lipid pattern, for example the GSLs in the nervous tissue, requires a complex set of biosynthetic and catabolic enzymes (Yu et al., 2009; Aureli et al., 2011) and an extremely complex trafficking and sorting machinery (van Meer and Hoetzl, 2010; Tidhar and Futerman, 2013; Sonnino et al., 2014). Glycolipids are present on probably all eukaryotic cells and account overall for 5% of all lipid molecules in the outer monolayer of the plasma membrane bilayer (Kraĉun et al., 1984). Internal cell membranes also contain glycolipids, but mostly in the post-Golgi organelles (Möbius et al., 1999). Sialic acid containing glycolipids, the gangliosides, are in general only marginally expressed in most eukaryotic cells and only nerve cells show a significant expression accounting for 5-10% of the total lipid mass (Schnaar et al., 2014). Gangliosides occur primarily on the plasma membrane, with the ceramide compartment anchored in the membrane together with most of the first sugar moiety (commonly glucose,see Figure 4) engaged with the lipid leaflet, while the remaining glycan part reaches into the ECM (DeMarco and Woods, 2009). The quantity as well as the complexity of gangliosides are subject to a

continuous change in living organisms. These changes vary for different organs and are also age dependent. Clues about the function of glycolipids can be drawn from their localization. For example, glycolipids are confined to the apical surface of the plasma membrane of epithelial cells, where they are involved in protecting the membrane against extracellular noxious conditions, for instance low pH-values and high concentrations of degrading enzymes in the stomach (Sato et al., 2005, p. 200). The sialic acid that gangliosides are carrying adds a net negative charge to them. This electrical effect is of importance, since the presence of gangliosides changes the electrical field across the membrane and thus the concentration of ions, especially Ca^{2+}, at the membrane surface (Schnaar et al., 2014). It is also well established that glycolipids function in cell-recognition processes, were the sugar groups on glycolipids and glycoproteins serve as binding partners for membrane-bound carbohydrate-binding proteins, called lectins, during cell-adhesion. Mice with induced gene deficiencies for the biosynthesis of complex gangliosides, i.o. GD1a, GD1b, GT1b, GQ1b, showed abnormalities in the central nervous system, including axonal degeneration and reduced myelination (Norton and Poduslo, 1973).

In all mammals the composition of glycoconjugates, including glycolipids, glycoproteins, and proteoglycans are constantly changing during neural development (Yu et al., 1988; Ngamukote et al., 2007; Yanagisawa and Yu, 2007). Changes in the expression of glycolipids, in particular gangliosides, correlate with neurodevelopmental events (Yu et al., 2009; Xu et al., 2010; Yu and Itokazu, 2014; Itokazu et al., 2017). For instance, in mice the fertilized egg itself strongly expresses the *globo*-series of glycolipids (see Table 1), e.g., the stage-specific embryonic antigen, SSEA-3/SSEA-4. As the fertilized egg continues to proliferate, the *lacto*-series becomes predominantly expressed around embryonic day (E)1.5, which is later followed by the *ganglio*-series GSLs in the developing brain of the embryo at E7 (Xu et al., 2010). As mentioned before, the lipid moiety of gangliosides, ceramide, is in turn synthesized from a sphingosine base and a fatty acid residue in the endoplasmic reticulum (ER). From there, ceramide is transferred to the Golgi apparatus and glycosylated to glucosylceramide (GlcCer) (see Figure 4) at the cytosolic leaflet of the *cis*-Golgi, which is abundant in early embryonic mouse brain from E16 (Ngamukote et al., 2007). In the next step, GlcCer is transported to the *trans*-Golgi by the phosphoinositol 4-phosphate adaptor protein 2 (FAPP2) and *trans*-located to the luminal side of the Golgi vesicle (D'Angelo et al., 2007, 2013). FAPP2 is also a mediator for GlcCer transportation from the *cis*-Golgi back to the ER (Halter et al., 2007). There, GlcCer gets flip-flopped back into the lumen of the ER and is then shuttled by the vesicular transport towards the lumen of the Golgi (Chalat et al., 2012). This is the location where GlcCer gets converted

to lactosylceramide (LacCer) (see Figure 4). At this stage the carbohydrate moieties of the gangliosides can be elongated via catalyzation by sialyltransferases (GM3 of the a-series) and galactosyltransferase (GA2 of the asialo-series). The biosynthesis proceeds as shown in Figure 4.

GM3 and GD3 are expressed in large quantities in early embryonic rodent brains, as more simple gangliosides are commonly expressed at the beginning of brain development. Upon later developmental stages the ratio shifts more towards the already mentioned complex gangliosides, GM1, GD1a, GD1b, and GT1b, that will also remain throughout the adult life the dominant brain gangliosides (Yu et al., 1988; Ngamukote et al., 2007). However, the ratio between them will continue to shift with progressing age (O'Brien and Sampson, 1965; Norton and Poduslo, 1973; Sastry, 1985).

On one side the constant change of ganglioside expression with progressing brain development and age, on the other the different technical and analytical approaches that have been used to quantify brain gangliosides, make it difficult to state robust numbers for their quantity. For example, in several studies the gangliosides present in the brain of Alzheimer's disease were investigated, but the reported results are not consistent, because in each study the peak area taken from the chromatogram to calculate the concentration was selected manually and hence, not reproducibly (Crino et al., 1989; Kracun et al., 1990, 1991; Svennerholm, 1994).

Nevertheless, overall basic trends could and have been identified; as mentioned before, gangliosides can make up to 5-10% of the total lipid mass in nervous cells (Wang and Brand-Miller, 2003). In the brain, grey matter and neurons are highly enriched with gangliosides, while the sphingolipid species sphingomyelin (SM), galactosylceramide (GalCer) and sulfatide are enriched in oligodendrocytes and myelin (O'Brien and Sampson, 1965; Aureli et al., 2015). The brain grey matter contains four to five-fold more ganglioside content per mg of protein than the brain white matter (Kracun et al., 2002). The development of a method that more precisely quantifies the major ganglioside classes within the mammalian brains will boost the understanding of the role and function of this lipid class in health as well as in disease.

1.6. Diseases

The expanding knowledge about cellular lipidomes gives rise to new ideas and hypotheses, which are brought forward and illuminate how the membrane composition of different cells

impacts the function as well as dysfunction of cells and whole organs, eventually resulting in disease. Most prominent, with regard to gangliosides, are the glycosphingolipidoses (Sandhoff and Kolter, 2003), a prototypical family of lysosomal storage diseases (LSDs). LSDs are characterized by defects in the catabolism of GSLs and share some features with other lysosomal disorders (Vitner et al., 2010). These disorders only occur at a low rate of 1 in 5,000 live birth in humans and lead to a severe monogenic disease, typically inherited as autosomal recessive traits (Platt, 2014). For a long time, it was presumed that diseases related to GSL biosynthesis are nonexistent due to the *in utero* lethality. Indeed, experiments in mice showed that a loss of function mutation for the very first enzyme GlcCer synthase (See Figure 4) catalyzing the GSL biosynthesis leads to embryonic lethality due to the inability of the embryo to develop past gastrulation (Yamashita et al., 1999). However, loss of function in genes encoding for enzymes more downstream of the GSL biosynthesis are viable (Proia, 2003). By achieving double knockouts for the enzymes GalNAcT and GD3S, the biosynthesis for all a- and b-series gangliosides (see Figure 4) could be inhibited in mice (Kawai et al., 2001; Inoue et al., 2002). While it was possible to obtain viable mice with these knockouts, severe phenotypes could be observed such as spontaneous adult lethality. Shortly after weaning was stopped the double mutant mice began to die. At 13 weeks of age more than 50% of the mice had died of unknown cause, with the mortality rising to 92% at 36 weeks of age (Kawai et al., 2001). Interestingly, the cause of death seems to differ between the two independent studies. The mice from Kawai *et al.* 2001 seemed to be very sensitive to sound-induced seizures; nearly 100% of the animals could be induced to have a lethal seizure by just jangling a standard set of house keys (Kawai et al., 2001), however the mice of Inoue *et al.* 2002 did not have such a susceptibility to sound induces seizures (Inoue et al., 2002). Inoue *et al.* suggested possible modifier background loci as a reason for this different phenotype, yet his mouse line showed propensity for skin injury. A likely reason for such a phenotype could be a peripheral nerve degeneration leading to reduced sensory function and inadvertent injury to the skin (Proia, 2003).

Altogether, it could be shown that the complex ganglioside structures (a- and b-series gangliosides) are not necessary for the development of the mammal nervous system. Nonetheless, due to the essential role of complex gangliosides in myelin stability and axonal glia signaling they are a necessity for a functioning nervous system after birth.

There is only a small number of genetically confirmed disorders in humans for ganglioside biosynthesis, namely the deficiency of GM3-synthase (Simpson et al., 2004) and GM2-

synthase (Boukhris et al., 2013; Harlalka et al., 2013) (see Figure 4). While the GM3-synthase deficiency resulted in a severe epilepsy syndrome, the clinical picture for the GM2-synthase deficiency resulted in a spastic paraplegia, characterized by lower limb weakness and spasticity. Measurements of blood plasma levels of GSLs in the patients verified the predicted deficiencies in GM2 or GM3, respectively and their downstream derivatives. The precursors of GM2 or GM3 were elevated due to the block in the biosynthesis pathway of gangliosides (Simpson et al., 2004; Harlalka et al., 2013). Remarkable was the discovery of minor amounts of a previously unknown GSL structure called sialylated Gb3 in GM2-synthase deficient patients (Harlalka et al., 2013). Whether the disease is caused by the loss of a specific ganglioside species, by the elevation of the precursor molecules or by an imbalance in the charge/neutral GSL ratios, is yet to be determined (Proia, 2004). While these are the first two disorders within human populations known to originate from the inability to synthesize complex gangliosides, it is possible that in the future more deficiencies will be identified regarding other enzymes that are part of the ganglioside biosynthesis pathways (see Figure 4).

Whereas disorders in GSL anabolism are rare, this is not true for GSL catabolism defects (Schultz et al., 2011). The latter form an important subgroup of a larger family of more than 70 LSDs. The clinical picture of many LSDs is of progressive neurodegenerative nature, that often starts already in infancy or during the childhood (Platt and Walkley, 2004). With that being said, symptoms and progression of LSDs have also been reported to start at any other stage of life, but with a lower probability (Sedel, 2007; van der Beek et al., 2012). The understanding of the working mechanisms of LSDs was propelled forward considerably, when more and more animal models became available for these disorders; ranging from genetically engineered mice (Platt and Lachmann, 2009) to spontaneous mutants found in species such as cats, dogs, sheep, cattle (Hemsley and Hopwood, 2010) and even a flamingo with Tay-Sachs disease (Zeng et al., 2008). These spontaneous mutations include GM1-gangliosidosis (Sandhoff and Harzer, 2013), caused by defects in the lysosomal degradation of gangliosides, certain forms of Gaucher's disease (GD) (Vitner and Futerman, 2013), caused by defects in lysosomal glucosylceramides activity, as well as Niemann-Pick disease type A (Ledesma et al., 2011) that originates from a lack of acidic sphingomyelinase. The common factor of these pathologies is accumulation of undegraded sphingolipids, because of the enzymatic defects. Examples are different gangliosides in gangliosidosis, glucosylceramide in the case of GD, and sphingomyelin in the case of Niemann-Pick disease type A. It appears, however, that trafficking from the lysosomal membranes with abnormal SL composition to the plasma membrane (Reddy et al., 2001) causes notable changes in the plasma membrane lipid composition

(Scandroglio et al., 2008; Buccinnà et al., 2009; Ledesma et al., 2011). The study of the progression of these disorders with such a variety of accumulating lipid species, has led to the increased understanding of these disorders, culminating in the development of therapies for different LSDs (Brady et al., 2001; Ioannou et al., 2001; Zervas et al., 2001; Patterson et al., 2007). This success stands in contrast to the much more wide spread sporadic neurodegenerative diseases, such as Alzheimer's disease, where the shortage of authentic animal models contributes to a lack of potential treatment options available (Laurijssens et al., 2013).

Alzheimer's disease (AD) is the most common form of dementia and is characterized by loss of neurons in the cerebral cortex and subcortical regions, atrophy and degeneration in the temporal lobe and parietal lobe as well as in parts of the frontal cortex and cingulate gyrus (Ariga et al., 2008). The cause of the development of AD is still not completely understood, but the deposition of amyloid β-protein (Aβ), which is a cleaved product of its precursor protein, amyloid precursor protein, APP, in the brains of patients affected with AD is clear. A better understanding of the assembly of soluble Aβ unto amyloid fibrils would not only promote our knowledge of AD but also of other human amyloidosis, such as prion disease and pancreatic islet amyloidosis, in which non-toxic proteins are assembled into their pathological, toxic forms. Yanagisawa *et al.* discovered already in 1995 a unique ganglioside-bound form of Aβ (GAβ) in membrane fraction prepared from brains that exhibited early pathological changes of AD (Yanagisawa et al., 1995). In fact, GAβ was characterized by its binding to GM1 and based on this molecular characterization it was hypothesized that GM1-bound Aβ acts as a seed for Aβ assembly in the AD brain, because it shows a strong tendency to form large Aβ assemblies and has altered immunoreactivity (Yanagisawa et al., 1997). This hypothesis was later confirmed by several *in vitro* studies (McLaurin et al., 1998; Matsuzaki and Horikiri, 1999; Ariga et al., 2001; Kakio et al., 2001), particularly Matsuzaki *et al*. reported that binding of Aβ to GM1 is facilitated in cholesterol-rich environment, and it is dependent on cholesterol-induced GM1 clustering in rafts in the host membranes (Matsuzaki and Horikiri, 1999; Kakio et al., 2001). Strikingly, there are several familial inheritable types of AD caused by several mutations within the Aβ sequence that induces Aβ assembly and deposition, which preferentially occur in specific but different areas in the brain, where Aβ interacts with specific gangliosides. The Dutch-, Italian- and Iowa-type mutations induce Aβ depositions particularly in cerebral blood vessel walls, while the Arctic-type mutation induces predominant Aβ deposition in the parenchyma of the cerebral cortex and are all mutations of APP (Tsubuki et al., 2003). Finally,

there is also a Flemish-type mutation that induces Aβ deposition starting from the outer surface of cerebral blood vessels (Tsubuki et al., 2003).

Aβ protein can also be enzymatically cleaved into two peptides, Aβ40 and Aβ42. It has been suggested that, due to their different effects on cell function, the Aβ40 and Aβ42 peptides initially disrupt the membrane lipid environment, thus impairing the activity of various proteins involved in signal transduction and ion fluxes (Roth et al., 1995). Aβ peptides may alter the neuronal membrane lipid environment by inducing lipid peroxidation and/or changing lipid fluidity. It has also been shown that Aβ40 increased both annular and bulk fluidity of synaptic plasma membranes (Avdulov et al., 1997). On the other hand, in lymphocyte membranes as well as in membranes isolated from cortex, hippocampus, striatum, and cerebellum, it was shown that Aβ40 decreases the bulk fluidity (Müller et al., 1995). Most likely, the different cellular lipid composition is the reason for this disparity. Also, both Aβ peptides seem to have different binding preferences regarding gangliosides. Aβ40 as well as Aβ42 were reported to form a stable and specific complex with GM1, but to a lesser extent with more complex gangliosides such as GD1b and GT1a (McLaurin et al., 1998; Evangelisti et al., 2013). The interaction of Aβ with gangliosides in the neuronal membrane may be only one of several mechanisms by which the membrane fluidity and/or membrane integrity could be disrupted by Aβ and a possible explanation for the increased permeability to ions and dysregulation of signal transduction systems seen in the presence of Aβ (Roth et al., 1995).

Besides of their role in neuronal disorder, gangliosides, especially GD2, have recently gained a lot of attention in cancer research. Gangliosides GM2, GD2 and GD3 are highly expressed in human tumors of neuro-ectodermal origin, such as melanomas, gliomas, and neuroblastomas, but in contrast, they are mostly absent or very low expressed in healthy tissues (Lloyd and Old, 1989; Hakomori, 1996). The exception is GD2, which is also highly expressed on bone marrow-derived mesenchymal stem/stromal cells (MSCs) and serves as a marker for them during prospective isolation (Martinez et al., 2007). Intriguingly, over the last years GD2 was established as a marker and a possible therapeutical target among pediatric and adult solid tumors, including neuroblastoma, glioma, retinoblastoma, Ewing's family of tumors, rhabdomyosarcoma, osteosarcoma, leiomyosarcoma, liposarcoma, fibrosarcoma, small cell lung cancer, melanoma and breast cancer (Mennel et al., 1992; Martinez et al., 2007; Jin et al., 2010; Yanagisawa et al., 2011; Battula et al., 2012; Kailayangiri et al., 2012; Liang et al., 2013; Ahmed and Cheung, 2014). What makes GD2 especially appealing for targeted immunotherapy is its high concentration in tumor cells and restricted expression in healthy

tissue (Wu et al., 1986; Cheung et al., 1987; Tsuchida et al., 1989; Chang et al., 1992; Lammie et al., 1993; Modak et al., 2002). The National Cancer Institute pilot program for the prioritization of cancer antigens ranked GD2 as the 12th most important cancer antigen out of 75 potential targets, thus highlighting its potential in cancer therapies (Cheever et al., 2009).

It was demonstrated that GD2 can be a marker for breast cancer stem cell (Battula et al., 2012). GD2^{+} cells identify a small fraction of cells in human breast cancer cell lines that not only show similar gene expression patterns as CD44^{hi}CD24^{lo}, but can also form mammospheres in cell culture and induce tumors in NOD/SCID mice upon injection of as few as 10 GD2^{+} cells (Battula et al., 2012). What function GD2 fulfills in cancer stem cells is yet not understood, but it is recognized that gangliosides for instance facilitate cell-cell communication between immune cells and that gangliosides are widely expressed on tumor cells (Hakomori, 1996, 2001). Thus, a hypothesis has been proposed that gangliosides help tumor cells escape immune clearance within the tumor microenvironment (Potapenko et al., 2007). This seems to be the case not only for GD2, but also for GD1a, GD1b, GD3, and GM3 (Ravindranath et al., 2005; Potapenko et al., 2007; Mukherjee et al., 2008). Additionally, it has been reported that gangliosides can induce apoptosis in immune cells important for fighting tumor cells, such as T- and NK cells (Biswas et al., 2006; Sa et al., 2009).

In summary, gangliosides are involved in many cellular processes and their dysregulation seems to be involved in a variety of severe disorders, ranging from lipid storage diseases over neurodegenerative diseases to cancer and possibly other diseases involving either a lack or overreaction of the immune system.

1.7. Analytical methods for lipidomics

Key to progress in the lipidomic field has been the development of diverse analytical methods, which have progressed over time owing to technological improvement. Most importantly were the advances in mass spectrometers, resulting in increased sensitivity, higher mass accuracy, higher scan speeds, and the ability to acquire in both positive and negative mode in one run. Overall that lead to an increased popularity of MS as a detection technique for biomolecules in recent years (Ivanova et al., 2009; Surma et al., 2015; Zhang et al., 2015). In this chapter an overview regarding the most important techniques will be given. Independently of the subsequently used analysis method, the first and one of the most important steps is lipid extraction. This probably trivial sounding procedure is actually a very important point due to the different characteristics of lipids, many of which are non-polar and hydrophobic, while some

polar and hydrophilic. Furthermore, lipids are frequently associated with other biological compounds in the sample and cannot be extracted so easily. An overview of the most common methods used is provided in the following.

1.7.1. Lipid extractions

A multitude of lipid extraction methods exist, reflecting the diverse nature of individual lipid classes and membrane complexity, as well as the source material (e.g. liquid or solid). Generally, the different methods can be distinguished by several main categories. Most widespread is the use of organic solvents (Folch et al., 1957; Bligh and Dyer, 1959; Svennerholm and Fredman, 1980; Ladisch and Gillard, 1985), such as chloroform-methanol-water mixtures, or silica extractions (Neoh et al., 1986) which are also common extractions methods. Nowadays, in lipidomic studies most widely employed are mixtures of organic solvents, in particular, a chloroform-methanol mixture based on Bligh and Dyer from 1959, that uses an additional water phase to extract the lipids from biological materials (Bligh and Dyer, 1959). Despite the age of this method, most variations are only concerning the reduction of organic solvents employed in it. For the extraction of gangliosides, a protocol developed by Svennerholm and Fredman (Svennerholm and Fredman, 1980) combined with a method developed by Ladisch and Gillard (Ladisch and Gillard, 1985) are frequently used.

The most suitable extraction method needs to be chosen considering the physicochemical features of the lipids of interest, e.g. amphiphilicity or chemical structure, and which parts of the membranes are supposed to be investigated. For biological samples, e.g. tissues, cells and body fluids, an optimization or modification of existing techniques is often necessary. Two of the major challenges to overcome are the extraction efficiency and a complete removal of the nonlipid content. Additionally, the sample throughput and reproducibility are important factors that need to be optimized. Polar lipids that contain hydrophilic as well as hydrophobic groups are commonly extracted with a mixture of chloroform and methanol (Pati et al., 2016). For non-polar lipids, that lack hydrophilic groups, alkane solvents are better suited for the extraction (Efthymiopoulos et al., 2018). The non-polar lipids include triglycerides, diglycerides, monoglycerides and sterols, while polar compounds are phospholipids, free fatty acids and sphingolipids.

Lipids can bind to proteins and carbohydrates, resulting in the formation of glycolipids and lipoproteins. Such formations influence the solubility of the lipids and may alter the requirements for suitable solvents to extract them. Depending on the nature of the lipids of

interest, a variety of solvent mixtures and methods can be utilized to solubilize these lipid classes. The improved understanding of lipidomics has paved the way for the distinction between “total lipid extracts” and “extractable lipids” (Jahnke et al., 2015).

For the purpose of this project, the most important method to start with was a modified Svennerholm (Svennerholm and Fredman, 1980) and Ladisch (Ladisch and Gillard, 1985) method for ganglioside extraction.

1.7.2. Thin layer chromatography (TLC)

Thin layer chromatography (TLC) is the classic way to analyze lipids and it set the field moving decades ago. Even William Christie, one of the most well-known experts for lipid analysis, asked himself already in 1990 if “TLC had its day?” (Christie, 1990). About 30 years later, TLC is still around and one of the most important methods to analyze lipid samples and their content. The reasons for the longevity of TLC are many, but one of the most important ones were the increasing commercial availability of pre-coated TLC plates that improved the possible inter-site reproducibility, since it could be implemented in different laboratories without compromising reproducibility anymore compared to the home-made TLC plates which were used before. This development was also accompanied by a vast increase in the possible absorbent materials with which the plates can be coated; most prominently, high-performing silica, bonded phases and impregnated layers have helped to boost the versatility of high-performance TLC (HPTLC) and made them an indispensable tool of modern analytical chemistry (Peterson and Cummings, 2006). The main difference between TLC and HPTLC lays in the different particle sizes of the stationary phases and the care that is used to apply the samples and to process obtained data (“The Evolution of Thin-Layer Chromatography,” 2008). Despite its limitations and concerns for the wider use of TLC, e.g. due to the lower chromatographic resolution in comparison to high-performance liquid chromatography (HPLC) as well as the potential oxidation of the analyte caused by its exposure to atmospheric oxygen, the benefits of HPTLC make it still a useful and competitive method compared to other modern methods (Fuchs et al., 2008).

To name just a few of the advantages of HPTLC; the application of commercially available ready-made TLC plates allows even the less experienced users perform good separations and, additionally, makes the technique convenient and simple. Compared to other techniques, such as HPLC-MS, the needed equipment for HPTLC is inexpensive and therefore can be afforded by more labs, without the need to specialize to a high degree to perform experiments. On the

same note, also the solvents used for a HPLC-MS set up are of much higher quality than for HPTLC, which increases the running costs. While HPLC columns can have a “memory” effect for previous analytes, TLC uses always a fresh stationary phase and hence does not face the problem of contaminated molecules from previous runs. It is also possible to apply several samples simultaneously on a HPTLC, while a HPLC can only process one sample at a time.

In lipid analysis TLC is still a benchmark and classically used for routine separations, identification of lipids and their rough quantification in the sample. A lasting limitation of stand-alone TLC is and will be the non-existing ability to provide information on the molecular lipid composition of a sample and not only a guess about the quantities of the class levels. But with the technological progress in this field, automated multiple development (AMD) machines have become available, enabling a more productive and less labor-intensive way to mix the solvents and perform the development and drying process (Zellmer and Lasch, 1997).

1.7.3. Immunoassays

Immunoassays encompass any use of an antibody-based method to detect a specific protein or lipid in a sample. Usually they are not stand-alone, meaning they are coupled with another analysis method, e.g. fluorescence-activated cell sorting (FACS) in flow cytometry, enzyme-linked immunosorbent assay (ELISA) and immunohistochemistry, to name some of the most prominent representatives of this category. The common denominator for all assays is antibody binding. Undoubtedly, one of the biggest strength of immunoassays is their analytical sensitivity and their overall robustness, but there is a string of problems that can be associated with immunoassays, leading to occasional analytical errors. One is the possible lack of adequate specificity and accuracy. Many factors can influence the ability of an antibody to find and bind its epitope, compounds or patient conditions can interfere with clinical immunoassay measurements. Generally, these factors are divided in two categories:(1) exogenous errors, arising from wrong sample preparation, and (2) endogenous interferences, when endogenous antibodies bind to, bridge, or block the binding sites of the signal antibodies, leading to false negative or false positive results of the assay.

Endogenous interferences can be very difficult to be spotted. Exogenous errors, on the other hand, can occur randomly, e.g. due to variability in sample pipetting, or systemically, e.g. due to calibration errors. They can be prevented by good internal quality control (Zarbo et al., 2002) and sporadic external quality assessments (Sturgeon and Viljoen, 2011). A useful parameter to assess the robustness of immunoassays can be to study the outlier rate (Ungerer et al.,

2010). But there can also be many more basic problems existing, which are easier to spot, such as degradation of the molecule of interest bearing the target epitope by wrong sample handling.

The biggest limitation of immunoassays for ganglioside determination is the lack of high-quality antibodies. It is still very difficult to produce specific antibodies against lipids including glycosphingolipids. Therefore, these assays have limited use in this field.

1.7.4. Mass Spectrometry (MS) Technologies

Due to the advancement in computational technologies, mass spectrometry has evolved over the last decade rapidly and enabled MS methods to revolutionize lipid science, helping lipidomics to emerge as one of the most promising research fields (Yang and Han, 2016). The two major MS methods are the high-performance liquid chromatography (HPLC) coupled with mass spectrometry (MS), which is the most widespread method to analyze lipidomes and glycosphingolipids, and the shotgun-MS, also called direct infusion MS (DIMS), where the sample gets directly injected into the MS machine without the necessity to perform any separation/purification steps prior to the injection. Both techniques have their specific advantages, disadvantages and similarities. In most mass spectrometers used nowadays for lipid analysis the ionization technique of choice is the electrospray ionization (ESI), which can be run in positive- and negative-ion modes. Both techniques provide detailed quantitative information about hundreds of lipid species per measurement, what has opened new possibilities and provided new insights into lipid biology. MS helped to pave the way to a better understanding of the vital role of different lipid species as membrane building blocks, as well as of their bioactive functions. The promise that lipidomics hold is that, due to the involvement of lipids in many crucial (in particular metabolic) pathways, a better understanding as well as faster and cheaper analysis of the lipidome could and would lead to the discovery of potential new biomarkers to monitor human health and disease (Surma et al., 2015; Sales et al., 2016, p. 201).

Both MS methods begin with the lipid extraction from the biological sample. LC-MS involves LC separation either based on the lipid class, e.g. normal-phase LC (NPLC), or lipid species, e.g. reversed-phase LC (RPLC). Once the partitioned lipid molecules are separated, they are injected into the MS, where they get directly evaporated and ionized in the ion source. Subsequently, the generated ions are sorted in an electric field with changing polarities. A widespread method currently used involves quadrupoles - sets of four parallel electrically

connected metal rods. Therein, radio frequency voltage is applied with a slightly offset direct current in a way that the opposing metal rods have the same frequency. Hence, ions that are travelling alongside the quadrupoles are separated depending on their mass-to-charge ratio (m/z). Depending on the used MS, there can be one or several quadrupoles in series. Eventually the ion masses are being detected. which, again, can be performed in several possible ways. One option is to measure the time-of-flight (TOF). In this approach ions are accelerated in one constant electric field, resulting on all the ions having the same potential. Next, the time needed by the ions to reach the detector is measured. Lighter ions have less tendency for a curved trajectory and therefore reach the detector faster than heavier ions, given that all the ions have the same charge.

Another commonly used mass detector comprises so called ion traps, where ions are captured and sequentially ejected. To do so, the ion trap mass analyzers use a combination of electric and magnetic fields to capture the ions. Again, several variants of ion traps exist, e.g. 3D and linear ion traps. The advantage of MS machines that possess an ion trap is that the ions can be stored and multiple gas-phase fragmentation (MS/MS) experiments can be performed on the same specimen. Fragmentation is an important tool to gather additional structural information by computationally assembling the acquired fragments into mass spectral trees.

The reasons why the majority of laboratories prefer LC-MS over the direct infusion shotgun-MS are the more reliable identification of individual lipid species, including the ones with low quantity levels, the possibility to separate between isomers and isobars, as well as the reduced ion suppression effects. With newer generations of LC instruments also the chromatographic separation became more efficient by reduction of analysis time and solvent consumption (Li et al., 2011).

The most important strength of shotgun-MS simultaneously poses its biggest challenge - the injection of crude lipid extracts. It is the injection of the total lipid extract that makes this method so versatile and suitable for high throughput measurements, however, at the same time, it hampers the identification of the lipids of interest. Depending on the specific ionization and the resulting adduct formation properties, separation can be achieved in-source (Han et al., 2004; Schwudke et al., 2007). However, the development of the Orbitrap Thermo Fischer shotgun mass spectrometers has overcome the separation problem owing to their superior resolution. Using these machines shotgun lipidomics have emerged as the method of choice for high throughput analysis. With the shotgun approach a large amount of lipidomic data for various tissues (Han et al., 2006; Sewell et al., 2012) and organisms, such as yeast (Ejsing et al., 2009;

Klose and Tarasov, 2016) and *Drosophila* (Carvalho et al., 2012), has already been provided. Due to the direct injection of the total lipid extract and the lack of pre-separation, the low abundant lipid species can be missed as a result of their suppression by predominant lipid classes. Hence, ion suppression and ion enhancement effects are a major challenge for all electrospray based ionization methods (Yang and Han, 2011).

1.7.5. Characteristics and disadvantages of Shotgun-MS versus LC-MS

When comparing with LC-MS, the injection of crude/total lipid extracts into the shotgun-MS results in higher background during the acquisition, arguably resulting in lower sensitivity for the direct infusion. A separation of isomeric lipid species is not possible with shotgun-MS alone, while it is possible with LC-MS. If not provided with a solid know-how and a software like LipidXplorer (Herzog et al., 2012),an in-depth characterization of lipid species in crude lipid extracts may be more complicated than with LC-MS, where, for example, retention times can help with identification of acquired peaks. Both methods typically use tandem mass spectrometry (MS/MS) to analyze low abundant lipid mediator species. It can occur that one precursor ion produces different fragments, indicating that there are possibly several molecules, in which case a deconvolution may help to distinguish which fragments originated from which precursor molecule group.

However, for shotgun mass spectrometry suppression is the same for all lipids and therefore can be corrected by suitable standards more conveniently than in LC-MS, where each injected fraction has a different matrix and thus different suppression.

To be able to normalize the intensity output from MS data, it is necessary to use internal standards that are added to the sample before any extraction or separation procedure is performed. Consequently, the analytes and the internal standards are present in the same sample matrix and undergo the same ion suppression and matrix effects. Finding suitable internal standards (IS) can prove to be difficult, since the IS must mirror both the chemical and the physical behavior of its analyte as close as possible, while being a unique entity itself in terms of its sum composition and molecular weight. In the lipidomic field opinions still vary how many and under which aspects internal standards have to be used and reporting criteria have been put out for discussion (Liebisch et al., 2017).

1.8. The goal of this thesis

The goal of this project was to explore whether the direct infusion shotgun mass spectrometry can be employed for ganglioside analysis. Previously reported extractions and analytical methods have either been too complicated, time consuming, or required too much sample material and are therefore limited in their application. Hence, there is still the need for improved ganglioside analysis tools, which could contribute towards a better molecular understanding of their roles in neuronal microdomains and their impact on such essential processes as brain development, differentiation of neuronal cells, cell-cell interactions, signal transduction and synapse formation. Deciphering not only the ganglioside distribution but the overall membrane composition during these cellular events may provide answers to some of the most fundamental questions. The goal of this thesis is to add such a novel analytical method, that is capable to quantify individual ganglioside species and is sensitive enough to detect also the fine differences in the lipid composition of the membranes, while at the same time being able to put the findings in the bigger picture provided by the measurement of the remaining lipidome.

The following imperative will be to integrate the new method as smoothly as possible into the preexisting high-throughput shotgun mass spectrometry workflow and, eventually, make it and inherent part of it (Surma et al., 2015). To reach this goal, certain criteria must be met, e.g. the reproducibility needs to be on the same level as the rest of the measured lipidomic data the same applying to the number of samples that can be processed simultaneously. But most importantly, the new method needs to be able to work with the water phase in which the gangliosides reside and which is left after the lipids that partition into the organic solvent phase have been extracted. This limitation can be overcome owing to the polar nature of the sugar moieties from the gangliosides, but with the downstroke of losing sensitivity.

2. Materials and Methods

All the standard chemicals and reagents were purchased from Sigma Aldrich and Fisher Scientific. The lipid standards were purchased either from Avanti Lipids Inc. or Sigma Aldrich.

Importantly, it must be acknowledged, that all plasticware used in this protocol cannot be made from polystyrene, due to the extraction of organic plasticizers and stabilizers such as phthalates and butylated hydroxytoluene (BHT) by the used organic solvent, namely chloroform. For this reason, all plasticware needs to be made from polypropylene (PP) or polyethylene (PE). Therefore, for all done extraction solely products from Eppendorf™ (PP) were used. Nevertheless, PP and PE only have a higher resistance to chloroform, hence it is recommended to minimize the exposure to chloroform as much as possible.

A special acknowledgement goes to Ludger Johannes from the Institute Curie in Paris, France. The collaboration with him made it possible to get ganglioside class specific standards for most ganglioside classes of interest, namely GM1, GD1 and GT1.

2.1. Materials

2.1.1. Chemicals and consumables

Chemicals, materials and consumables were obtained from the companies and with the catalogue numbers, shown in Table 2, Table 3 and Table 4.

Chemical	Company	Cat #
Acetone (HiPerSolv)	VWR GmbH, Darmstadt, Germany	20067-320
Ammonium bicarbonate (ABC)	Sigma Aldrich, St. Louis, USA	11213-1KG-R
Di-isopropyl ether	Sigma Aldrich, St. Louis, USA	38270-1L-F
Chloroform CHROMASOL® for HPLC	VWR GmbH, Darmstadt, Germany	83627-290
Chloroform (HiPerSolv)	VWR GmbH, Darmstadt, Germany	18G054007
1-Butanol	Sigma Aldrich, St. Louis, USA	33065-1L-R
2-Propanol	Fisher Scientific, Geel, Belgium	A461-212
Ethanol absolute	VWR GmbH, Darmstadt, Germany	20621-310
Methanol Optima® LC/MS Grade	Fisher Scientific, Loughborough, UK	1076-7665

Methylamine solution	Sigma Aldrich, St. Louis, USA	BCBK0866V
Neuaminidase (Sialidase)	Sigma Aldrich, St. Louis, USA	11585886001
Non-fat dried milk	Carnation Co., Los Angeles, USA	NA
Sodium chloride	Sigma Aldrich, St. Louis, USA	091M0095V

Table 2. Chemicals.

Material	**Company**	**Cat #**
Deep well plate 2 ml	Corning™; Sigma Aldrich, St. Louis, USA	3961
2 ml amber glas vial	Supelco / Merck KGaA, Darmstadt, Germany	29653-U
4 ml amber glas vial	Supelco / Merck KGaA, Darmstadt, Germany	27115-U
Robot tips 300 µl	Hamilton Robotics, Martinsried, Germany	235902
Robot tips 1000 µl	Hamilton Robotics, Martinsried, Germany	235904
Sealing Alu-foil	Corning™; Sigma Aldrich, St. Louis, USA	734-1774
SOLA™ SPE plates, HRP 10 mg/2 ml 96-well	Fisher Scientific, Loughborough, UK	11899163
Pierce™ C-18 Spin Columns 8 mg C-18 resin	Thermo Fisher Scientific, Waltham, USA	89873
Ultrasonic bath Sonorex	Bandelin GmbH & Co KG, Berlin, Germany	303
Vacuum Manifold VacMaster™ 96	Biotage AB, Uppsala, Sweden	121-9600

Table 3. Used materials list.

Ganglioside Class	Manufacturer/Supplier	Cat #
Mixed porcine brain gangliosides	Avanti Polar Lipids Inc.	860053P-10mg
Ovine GM1 Standard	Avanti Polar Lipids Inc.	860065P-1mg
Bovine GM1 Standard	Sigma Aldrich, St. Louis, USA	G7641
Bovine GD1a Standard	Matreya LLC, State College, USA	1062
Bovine GT1b Standard	Matreya LLC, State College, USA	1063
Bovine GT1b Standard	Sigma Aldrich, St. Louis, USA	G3767-1MG
Bovine GQ1b Standard	Matreya LLC, State College, USA	1064
C17-GM1b Standard	Ludger Johannes Lab (Curie-Institute, Paris, France)	N/A (custom made)
C17.2-GM1b Standard	Ludger Johannes Lab (Curie-Institute, Paris, France)	N/A (custom made)
C17-GD1a Standard	Ludger Johannes Lab (Curie-Institute, Paris, France)	N/A (custom made)
C17- GT1b Standard	Ludger Johannes Lab (Curie-Institute, Paris, France)	N/A (custom made)

Table 4. Used Gangliosides Standards; the bovine ganglioside standards were purchased as shown and used for evaluating the method as well as determining the LOD and LOQ in titration versus the fitting class of C17 standard; the C17 standards were custom made by the Ludger Johannes Lab and therefore do not possess a Cat #.

For the purification of gangliosides out of the total lipid extract (TLE) the Pierce™ C-18 Spin Columns from Thermo Scientific, Rockford, USA (Cat # 89870), were used. At a later stage of the project SOLA™ SPE-96 well plates, also from Thermo Fisher Scientific (Cat # 60309-001), were adapted. The advantage of these SOLA plates is the tight packing of the sorbent, preventing cavities and tunnels in it, and generally performing with a higher reproducibility. Additionally, there was no plate equivalent for the Pierce™ C-18 Spin Columns, limiting the number of samples that could be handled per run to 24, thus preventing a high-throughput approach and resulting, combined with the improved reproducibility, in the switch to SOLA™ plates after they became commercially available.

2.1.2. Reagent mixes

Name	Amount
Methanol	50 ml
Chloroform	10 ml
Methylamine Solution	30 µl

Table 5. Mass spectrometer injection mix methylamine.

Name	Amount
Water	1 l
Ammonium bicarbonate	11.85 g

Table 6. Ammonium Bicarbonate (ABC) solution for cell or tissue dilution.

2.2. Methods

2.2.1. Lipid extraction methods

The final version of the lipid extraction and processing protocol is described in the following. The starting protocol, how it was evaluated and the evolution to the final protocol are described in detail in the result sections 3.1 and 3.3.

In the first extraction step with the TLE, and after adding the internal standards, 750 µl of chloroform/methanol (C/M) 10:1 mixture was added to 150 µl of 150 mM ABC and shaken at 1,400 rpm for 2 h at 4°C. Then, the mixture was centrifugated at 3,000 g for 5 min at 4°C. The upper (organic) phase was subsequently transferred to a new 2 ml Eppendorf™ tube and the second extraction step was performed by adding 750 µl of C/M 2:1 mixture shaking at 1,400 rpm for 2 h at 4°C and centrifugation at 3,000 g for 5 min at 4°C. Contrary to the starting protocol (see chapter 3.1) it is not necessary anymore with the final protocol to evaporate the aquatic phase before loading it on the columns for the solid phase extraction, which allows to reduce time needed to perform the protocol from 1,5days to 10 h.

Equilibration of the SOLA™ plates was done by adding 400 µl methanol, followed by 5 min incubation and draining the plate via the vacuum manifold. Next, the plates were treated in subsequent steps with 400 µl of C/M 2:1, followed by methanol and eventually methanol/water (M/W) 1:1, each liquid with a 5 min incubation time and draining by vacuum before applying the next liquid. For the sample loading a 96 deep well plate was positioned underneath the SOLA™

plate, to catch the loaded samples while being able to load them in total 3 times with 2 min incubation steps in between. The introduction of the SOLA™ plates combined with the vacuum manifold reduced the hands-on worktime additionally, together with the direct loading of the aquatic phase onto the SPE columns. With the SOLA™ plates it was not necessary anymore to load the individual spin columns manually in and out of the centrifuge for each spinning and the required time to perform the 20 washing steps was therefore reduced considerably. For the washing in total 8 ml of H_2O per column were added and drained with the vacuum system. Afterwards, a new 96 deep well plate was positioned underneath the SOLA™ plate to catch the eluate. Elution was done by pipetting first 400 µl methanol per column followed by 5 min incubation and subsequently drainage by vacuum and repeating these steps twice with 400 µl chloroform/methanol 1:1. Eventually, the eluate was transferred into 1.5 ml Eppendorf™ tubes and evaporated. Thanks to the improved packing of the SOLA™ compared to the loose Pierce C18 resin bed, further steps to get rid of the remaining column material were not necessary anymore. After evaporation, the purified extracts could be resuspended in smaller compared to previous protocol volume of 20 µl MS-mix MA, resulting in a higher sample concentration for the injection into the mass spectrometer. After addition of the 20 µl MS-mix MA, the extracts were shaken for 10 min at 1,400 rpm, 4°C and then transferred to a 96 well plate and injected into the mass spectrometer.

2.2.2. Infusion and MS method

The machines used for the acquisitions were Q-Exactive™ from Thermo Fisher Scientific coupled with the Triversa NanoMate™ from Advion Bioscience for automated microchip Nano electrospray infusion. A sample volume of 5 µl was injected into the MS with a gas pressure of 0.8 psi (pound pressure per square inch). Applied voltage for ESI was 0.95 kV. Acquisition was done in the negative ion mode. Delivery times varied depending on the measured samples and experimental setting. The contact closure delay was set to 5 s to avoid initial spray instability.

The measured mass-to-charge ratio (*m/z*) windows were chosen to fit the individual ganglioside classes (i.o. GM1, GD1, GT1, GQ1) being double negative charged and for the two most dominant species (36:1 and 38:1) with the modified C17-ganglioside standards (35:1) (see Table 4) still laying within these m/z windows (see Table 7).

Ganglioside Class	*Ionization*	m/z of Species 35:1 (d18:1/17:0)	m/z of Species 36:1 (d18:1/18:0)	m/z of Species 38:1 (d18:1/20:0)	Used *m/z* window
GM1	$[M-2H]^{2-}$	764.92	771.93	785.95	760-795
GD1	$[M-2H]^{2-}$	910.475	917.48	931.49	905-940
GT1	$[M-2H]^{2-}$	1056.02	1063.03	1077.04	1050-1085
GQ1	$[M-2H]^{2-}$	N/A	1208.57	1222.59	1200-1235

Table 7. The m/z of individual ganglioside classes of interest, if they are double charged, and out of that resulting m/z windows for the measurements. For GQ1 no modified C17-ganglioside class standard is available and due to the generally low abundancy of GQ1 the mass window was held narrower.

Acquisition times for each measured m/z segment also varied over the course of the project but were usually within 20 s – 30 s per acquired lipid class. All individual scans in every segment are the average of 2 microscans. Automatic gain control (AGC) was set to 1×10^6 and maximum ion injection time (IT) to 500 ms. For a long time, it occasionally happened that in a few individual scans a little shoulder appeared at the peak of interest, that was closer towards the in the Molecular Fragmentation Query Language (MFQL) defined m/z and hence preferred in the final output file generated by LipidXplorer over the main peak. This artifact required laborious manual analysis of the raw files, which, unavoidably, was less reproducible than automated analysis. Solution to this problem was the combination of the common background molecules with the lock mass function (Schuhmann et al., 2012). Measured m/z windows had a width of 35 Dalton (Da), but for quality control also acquisitions with narrower windows of 5 Da around each individual species of interest were performed.

2.2.3. Analysis of Shotgun-MS lipidomic data

All data were analyzed with an in-house developed lipid identification software called LipidXplorer (Herzog et al., 2011, 2012). Tolerance for MS identification was set to 4ppm without lock mass and 2 ppm with lock mass activated. Data post-processing and normalization were performed using an in-house developed data management system. Data visualization, linear regression (linear least squares method), and correlation (two-tailed Pearson correlation) calculations were performed either manually or with the statistical analysis software “R”.

Mass spectrometry-based lipid analysis was performed by Lipotype GmbH (Dresden, Germany) as described elsewhere (Sampaio et al., 2011). Lipids were extracted using a two-

step chloroform/methanol procedure (Ejsing et al., 2009). Samples were spiked with internal lipid standard mixture containing: cardiolipin 16:1/15:0/15:0/15:0 (CL), ceramide 18:1;2/17:0 (Cer), diacylglycerol 17:0/17:0 (DAG), hexosylceramide 18:1;2/12:0 (HexCer), lyso-phosphatidate 17:0 (LPA), lyso-phosphatidylcholine 12:0 (LPC), lyso-phosphatidylethanolamine 17:1 (LPE), lyso-phosphatidylglycerol 17:1 (LPG), lyso-phosphatidylinositol 17:1 (LPI), lyso-phosphatidylserine 17:1 (LPS), phosphatidate 17:0/17:0 (PA), phosphatidylcholine 17:0/17:0 (PC), phosphatidylethanolamine 17:0/17:0 (PE), phosphatidylglycerol 17:0/17:0 (PG), phosphatidylinositol 16:0/16:0 (PI), phosphatidylserine 17:0/17:0 (PS), cholesterol ester 20:0 (CE), sphingomyelin 18:1;2/12:0;0 (SM), triacylglycerol 17:0/17:0/17:0 (TAG) and cholesterol D6 (Chol). After extraction, the organic phase was transferred to an infusion plate and dried in a speed vacuum concentrator. Dry extract was resuspended in 33% ethanol solution of methylamine in chloroform/methanol (0.003:5:1; V:V:V). All liquid handling steps were performed using Hamilton Robotics STARlet robotic platform with the Anti Droplet Control feature for organic solvents pipetting.

2.2.4. MS data acquisition

Samples were analyzed by direct infusion into the QExactive mass spectrometer (Thermo Scientific) equipped with a TriVersa NanoMate ion source (Advion Biosciences). Samples were analyzed in both positive and negative ion modes with a resolution of $R_{m/z=200}$=280000 for MS and $R_{m/z=200}$=17500 for MSMS experiments, in a single acquisition. MSMS was triggered by an inclusion list encompassing corresponding MS mass ranges scanned in 1 Da increments (Surma et al., 2015). Both MS and MSMS data were combined to monitor CE, DAG and TAG ions as ammonium adducts; PC, PC O-, as acetate adducts; and CL, PA, PE, PE O-, PG, PI and PS as deprotonated anions. MS only was used to monitor LPA, LPE, LPE O-, LPI and LPS as deprotonated anions; Cer, HexCer, SM, LPC and LPC O- as acetate adducts and cholesterol as ammonium adduct of an acetylated derivative (Liebisch et al., 2006).

2.2.5. Data analysis and post-processing

Data were analyzed with an in-house developed lipid identification software based on LipidXplorer (Herzog et al., 2011, 2012). Data post-processing and normalization were performed using an in-house developed data management system. Only lipid identifications with a signal-to-noise ratio >5, and a signal intensity 5-fold higher than in corresponding blank samples were considered for further data analysis (Surma et al., 2015).

Also, for evaluation and optimization of the initial protocol a statistical software called Optival™ from the company Quodata GmbH was used. This software helped to identify the critical working steps of the protocol and to determine the optimal conditions, e.g. salt concentrations, for these steps of the protocol (see chapter 3.2).

3. Results

The goal of this thesis was to develop a direct infusion shotgun mass spectrometry protocol for the four major mammalian brain gangliosides, that would operate within the same parameters, e.g. coefficient of variance (CV), as the previously established protocols for the Lipotype GmbH (Surma et al., 2015). Additionally, the developed protocol should also be more sensitive than the so far existing protocols for brain gangliosides, while requiring less sample material (Fong et al., 2009; Ikeda et al., 2008). One of the biggest challenges throughout this project was to obtain suitable internal standards that share close physico-chemical behavior with the analyte, while being unique, meaning they do not, or only in insignificant amount, occur naturally in the sample material. Commonly deuterated standards are used for that purpose in lipidomics, but there are no deuterated ganglioside standards commercially available. This presented a major obstacle for the project. In an attempt to circumvent it, a deuterated standard for phosphatidylethanolamine (PE) (Surma et al., 2015) was tested, but to no avail, as its physico-chemical behavior was not compatible to gangliosides.

The first parts of the results chapter are dedicated to the starting protocol and to explain how and why it has evolved over time (see chapters 3.1-3.3). Subsequent attempts to establish an alternative internal standard for quantification as long as no modified C17-ganglioside standards were available, are described in chapter 3.4. Later, the fitting ganglioside class specific standards were obtained and subsequently incorporated to the protocol, as described in chapters 3.5-3.7. The unique feature of these standards, also referred to as the modified ganglioside standards, is the lack of the fatty acid moiety which has been enzymatically removed and replaced by a 17-carbon atom long aliphatic chain, resulting in a GM1 35:1 species. Gangliosides carrying such odd-numbered fatty acids do not occur naturally, or are found in very low amounts, among the brain ganglioside species, thus have a great potential to serve as suitable internal standards. At first it was only possible to obtain a modified standard for ganglioside GM1b, C17-GM1b. While the results with the C17-GM1b standard proved far superior to any results achieved with the PE standard, further experiments with the PE standard were stopped (see chapter 3.4). A response factor for the other three ganglioside classes, namely GD1, GT1 and GQ1, was empirically established with the modified C17-GM1b standard (see chapter 3.5). Later, also modified C17-ganglioside standards for the ganglioside classes GD1a and GT1b could be procured. For ganglioside class GQ1b it was not possible to get a specific internal standard, but modified C17-GT1b proved to be the most fitting standard and was subsequently used for the quantification of GQ1b with its corresponding response factor (see chapter 3.5). Simultaneously, the limits of detection (LOD) as well as the limits of

quantification (LOQ) were determined for each of the major mammalian brain ganglioside classes were determined by titrating different concentrations of ganglioside standards versus a steady concentration of the fitting modified C17-ganglioside standard (see chapter 3.6). Eventually, the evaluated starting protocol was tested by using it to quantify different wet weight amounts of a mix of mouse brains. The measured amounts of gangliosides reflected the values described in literature (see chapter 1.5). Ultimately, chapter 3.9 presents the final test of the protocol in an applied experimental setting, that aimed at quantifying the lipid content - gangliosides as well as other lipids - in two different mouse brain regions - cerebellum and hemisphere - at mice of different age (4 days, 14 days, 21 days, 8 weeks and 18 months after birth).

3.1. The starting protocol

As a starting point for the ganglioside extraction, a slightly modified version of the extraction protocol of Ladisch *et al.* (Ladisch and Gillard, 1985) and Svennerholm & Fredman (Svennerholm and Fredman, 1980) was used with a mixture of chloroform/methanol/water (C/M/W) 4:8:3. The protocol we used, employed 150 mM of ammonium bicarbonate (ABC) solution instead of water. The first step, after thawing the samples, was always to add 50 pmol of the internal standards. Commonly all handled tissue/cell samples were frozen in 300 µl of 150 mM ABC and hence 800 µl methanol and 400 µl chloroform were added to reach C/M/W 4:8:3. Then, the extraction was done by shaking for 30 min at room temperature, followed by centrifugation for 10 min at 16,000 x g at 4°C. The supernatant was transferred to a fresh 2 ml Eppendorf™ tube and evaporated. The total lipid extract (TLE) was subsequently dissolved in 100 µl of C/M 1:1 and sonicated for 10 min, centrifuged again (10 min, 16,000 x g, 4°C) to remove insoluble material, transferred to a new 2 ml Eppendorf™ tube and evaporated.

To separate between the bulk of non-polar lipids and the polar lipids, to which gangliosides belong, the total lipid extraction needed to undergo a 2-phase partitioning process. For that, the total lipid extract (TLE) was dispersed in 400 µl of di-isopropyl ether/1-butanol 6:4, vortexed and sonicated for 10 min. Afterwards, 200 µl of 10 mM aqueous NaCl solution were added, vortexed and shaken for 10 min at 180 g (equals 1,400 rpm) and 4°C, and centrifuged for 5 min at 4,000 x g and 4°C. In the end of the procedure gangliosides were present in the lower, aqueous 10 mM NaCl phase. The organic (upper) phase was removed and disposed, while the aqueous phase was extracted another time with 400 µl of di-isopropyl ether/1-butanol 6:4 by vortexing and shaking for 10 min at 1,400 rpm and 4°C, subsequent centrifugation for 5 min at

4,000 x g and 4°C, to speed up the phase separation, and disposal of the organic phase. Eventually, the supernatant was evaporated overnight.

The next stage of the extraction was the solid phase extraction (SPE) which was done during the starting protocol stage with Pierce™ C18 resin spin columns (see chapter 2.1.1). All the steps of the SPE were performed at room temperature. First, the extract needed to be dissolved in 100 µl methanol, sonicated for 10 min, then 100 µl of MS-grade pure H_2O was added, followed by another 10 min of sonication. In parallel, the equilibration of the SPE columns was done. To do so, the SPE columns were put on top of 2 ml Eppendorf™ tubes and 400 µl of methanol were dispensed at the side wall of each column, with attention to not disturb the resin bed. The columns were left standing for 5 min and then centrifugation for 1 min at 16,000 x g. Subsequently, the above steps were repeated with 400 µl of C/M 2:1, methanol, and eventually M/W 1:1. Afterwards, the sample could be loaded on the column and let stand for 2 min before a centrifugation for 1 min at 1,500 x g was done. The sample was then loaded again two more times on the columns. After the samples were loaded, the columns were washed 20 times with 400 µl H_2O and centrifuged for 30 s at 1,500 x g. Next, the C18 spin columns were transferred to fresh 2 ml Eppendorf™ tubes. Subsequently, the glycosphingolipids were eluted first with 400 µl methanol and next, two times with 400 µl C/M 1:1, followed by incubation for 5 min and centrifugation for 30 s at 15,000 x g. Eluates were pooled in 1.5 ml Eppendorf™ tubes and the supernatant was evaporated. Eventually, the samples were resuspended in 50 µl methylamine MS-mix (see chapter 2.1.2) and shaken for 10 min at 180 x g and 4°C. To get rid of column material that could still be present in the Eppendorf tube, a final centrifugation step at 16,000 x g for 10 min at 4°C was performed and 30 µl of supernatant was transferred to a 96 well plate and analyzed by shotgun lipidomics. Injections were done with an Advion TriVersa Nanomate system. All the experiments were measured with the Thermo Scientific Q Exactive mass spectrometer.

The individual steps of this starting protocol were evaluated under the aspects of an evaluation software called Optival™ from the company Quodata.

3.2. Protocol evaluation

One of the first major phases of this project was the identification and evaluation of the protocol's working steps, that could significantly impact the outcome of each experiment and to assess the optimal conditions (see Table 8).

Salt conc. in 2-phase partitioning	No. of sample loadings on resin columns	No. of washing steps
0 mM	1	3
10 mM	3	10
50 mM	5	20

Table 8. Working steps of the protocol that could significantly impact the result needed to be evaluated for the most optimal outcome in regard to sensitivity and reproducibility. Additionally, to the three different salt concentrations in the water phase of the 2-phase partitioning, number of sample loading on SPE columns and the number of washing steps were also tested if the MS-mix volume of 30 µl or 50 µl has a significant impact.

The evaluation was done with the help of the OptiVal™ software (Quodata). This software applies statistical methods to provide the user with a detailed analysis of performed experiments, in order to maximize the sensitivity and intensity of the outcome, as well as minimize random and systemic errors. The experiment was designed to test each factor of the four variables in triplicates, resulting in a total of 162 samples. At this time, each sample had to be handled manually, with single spin columns for the lipid extract purification, meaning a maximum of 24 samples per run could be handled simultaneously. Also the initial protocol took 2 days for the performance of a single run. Thus, the OptiVal™ experiment was carried out over the course of 7 days, where on the second day of each run the first day of the next run had to be started. To provide a lipid background that is free of gangliosides, HEL-SCR cells of the human erythroleukemia cell line were used as starting material, containing 3600 pmol total lipid per sample. To that an ovine GM1 brain extract standard (Avanti Inc., see Table 4) was added in the amount of 100 pmol per sample.

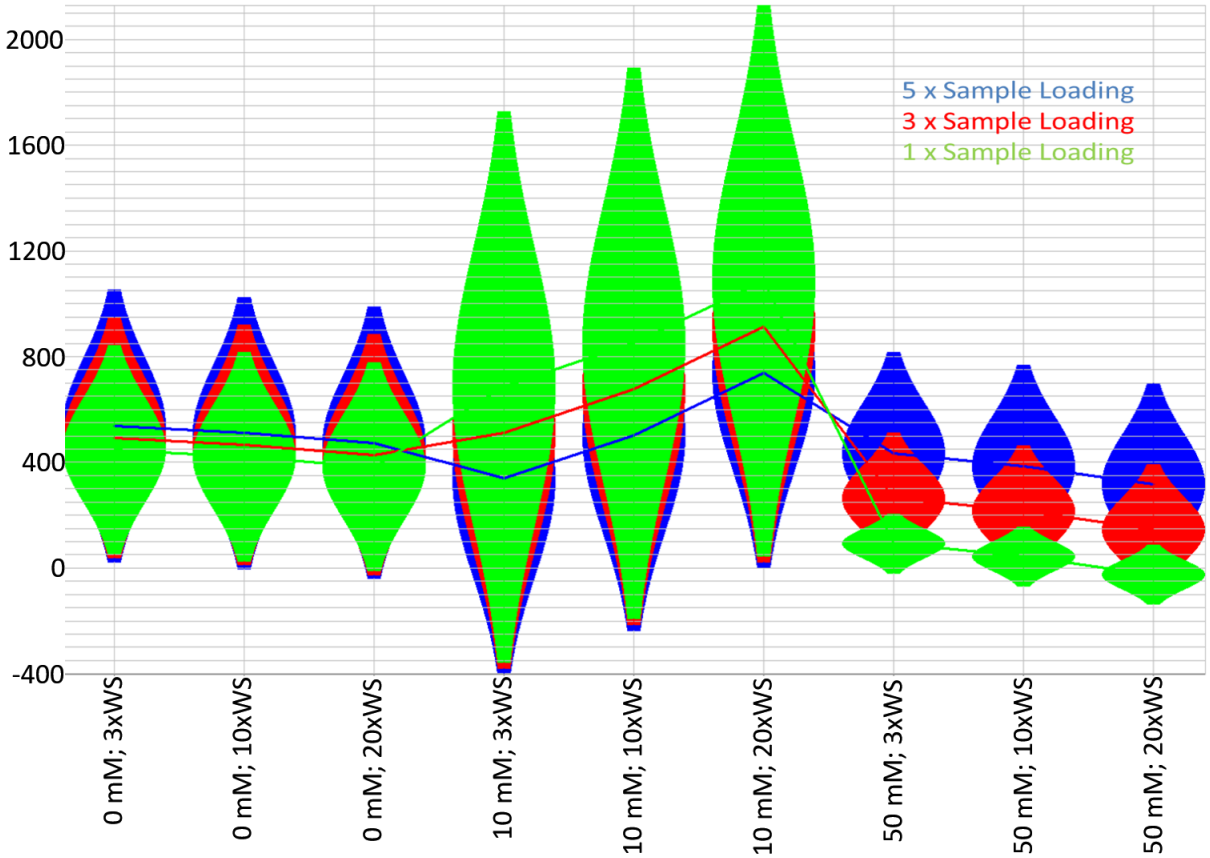

Figure 5. Dispersion plot of protocol evaluation with the number of sample loadings as portrayed influence factor. X-axis shows the tested parameters, in this case the varying salt concentrations for the aqueous. phase during the 2-phase partitioning and the number of washing steps per SPE column during the total lipid extract purification. Y-Axis: With the signal-to-noise (S/N) ratio of the used GM1 standards in the evaluation experiment, the OptiVal™ software calculated a response factor (Y-axis values) for each evaluation point to quantify the corresponding uncertainty associated with each influence factor. The higher the score the better the setting is in terms of reproducibility and sensitivity.

The outcome of the experiment is shown in Figure 5 and Figure 6. Each of the individual evaluation points (see X-axis) in the dispersion plot shown in Figure 5 illustrates either a different salt concentration in the aqueous phase during the 2-phase partitioning or a different amount of washing steps of the resin columns. Based on the measured signal to noise (S/N) ratios, the OptiVal™ software calculated for each point a response value. The higher the response value the better it is in regard to its impact on the sensitivity. With the replicates the reproducibility for each point was calculated and is pictured here as a spread shape. The first three, middle three and the last three points have the same salt concentration but differ in the

number of performed washing steps (see Figure 5). The tested numbers of sample loadings are represented with different colors: green, red and blue for respectively 1, 3 and 5 sample loadings. Salt concentration of 10 mM for the 2-phase partitioning shows the biggest spread, but also the highest calculated response, reflecting the achieved sensitivity. The condition with 10 mM salt and 20 washing steps had its lowest response equal to or higher than the other conditions, but it outperformed them at the top response value, while showing not much variation about the number of sample loadings.

For a more detailed illustration, Figure 6 shows a multivariant analysis of the 10 mM salt concentration condition only. The highest signal intensity, which directly translated to the protocol sensitivity, was obtained with triple sample loading and 20 washing steps. Hence, these conditions along with 10 mM salt concentration for the aquatic phase in the 2-phase partitioning were identified as the most optimal and adapted in future ganglioside extraction experiments.

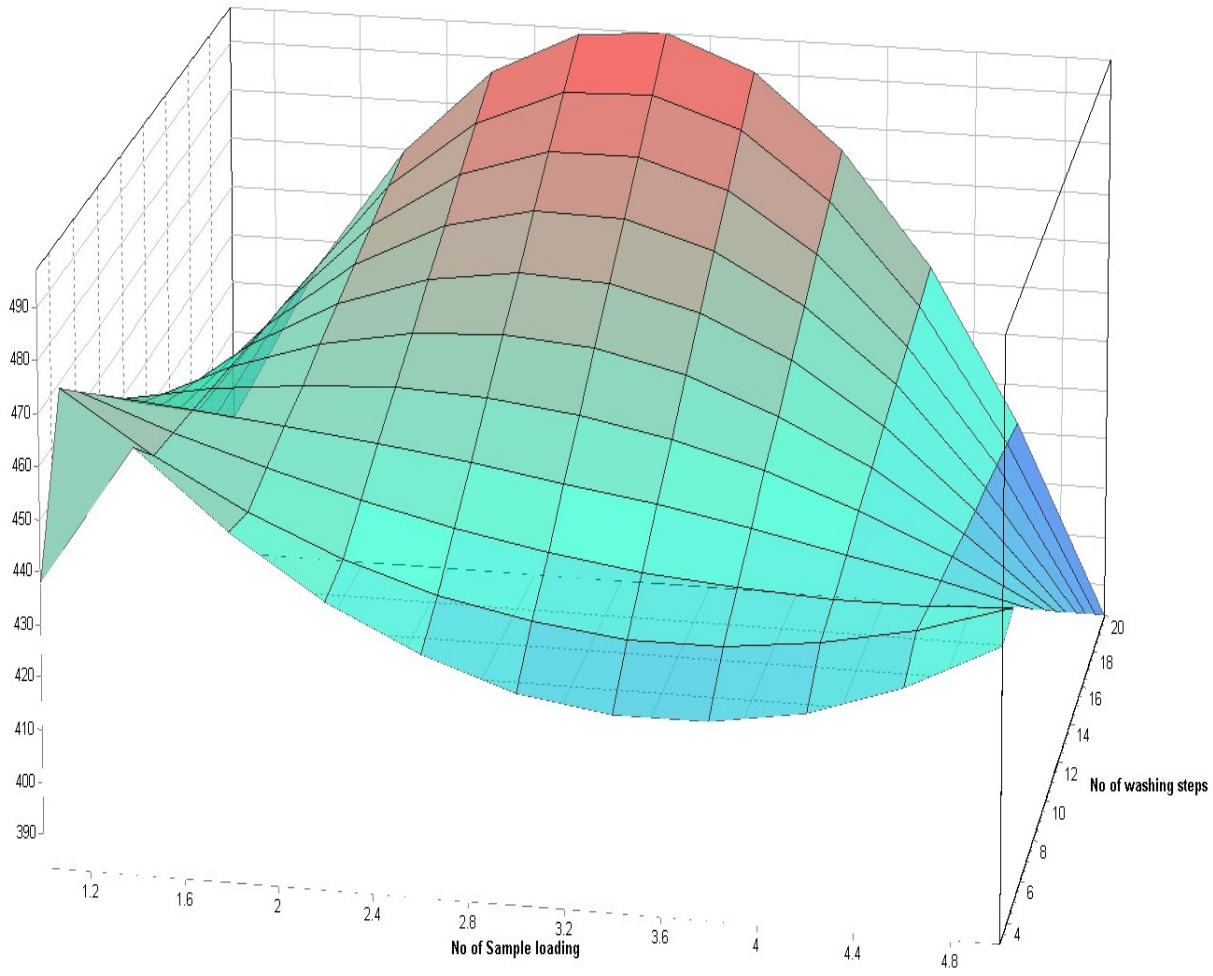

Figure 6. Multivariant analysis showing the impact of a 10 mM salt concentration during the 2-phase partitioning step in context with a varying number of sample loadings and washing steps. Intermediate values, that were not included in the experiment itself, e.g. “number of sample loading 2.4” were automatically calculated by the software. It is clear to see, that the conditions with the most optimal output are 3 sample loadings, 20 washing steps and with a salt concentration of 10 mM for the aquatic phase in the 2-phase partitioning.

3.3. Final protocol

The following section presents the final version of the extraction and analysis protocol for the major brain gangliosides of mammals. The starting protocol and its improvement over time are described in the previous result sections. While spin column ganglioside extraction offered good results in terms of sensitivity, the reproducibility could still be improved. Additionally, a major bottleneck of spin column approach was the maximum handling capacity of only 24 samples per run, which made it impossible to measure bigger sample sets together and required splitting the samples into several separate MS measurements. This posed a serious problem, since MS machines always show a slight signal drift or instability over time, and the more time passes between two measurements the stronger it becomes, adding an unnecessary variation to the final outcome. The signal drift may occur due to sample adsorption, degradation, or insulating deposits on the hot stainless steel surface of the ion source (D'Autry et al., 2010), but also different humidity and air pressure may contribute to it. It is possible to address the signal shifting problem with the help of reference samples, but it is still preferable to measure all samples subsequently in one experiment. This was the reason for switching from spin columns to SOLA™ plates once they became commercially available. Apart from enabling to process more samples at a time, the SOLA™ plates had other advantages. For example, the resin packaging methods were improved, leading to less tunnels and cavities in the resin bed of the SOLA™ plates compared to the loose bed of spin column resin. This alone increased the reproducibility of ganglioside extraction ("Thermo Scientific SOLA SPE cartridges and plates Technical Guide," n.d.).

The introduction of SOLA™ plates was also accompanied with some other changes in the extraction protocol, required to better fit into the workflow of other protocols, e.g. the general lipidomic analysis. Hence, as a first extraction step with the TLE and after adding the internal standards, 750 µl chloroform/methanol 10:1 were added to 150 µl of 150 mM ABC, shaken for 2 h at 1,400 rpm and 4°C and centrifuged at 3,000 x g for 5 min at 4°C. The upper (organic) phase was subsequently transferred to a new 2 ml Eppendorf™ tube and the second extraction step was performed by adding 750 µl of chloroform/methanol 2:1, again followed by shaking for 2 h at 1,400 rpm, 4°C and centrifugation at 3,000 x g for 5 min at 4°C. Here, it was not necessary anymore to evaporate the aquatic phase and resuspend it in 200 µl of M/W 1:1, before loading the samples on the columns for the solid phase extraction, helping to reduce the time needed for the protocol 1.5 days to 10 h.

The rest of the final protocol was already described in chapter 2.2.1 Lipid extraction methods and can be found there.

3.4. Alternative internal standards

To be able to quantify the measured gangliosides in samples, before the modified C17-ganglioside standards were obtained, experiments were performed with a deuterated PE standard. Since the deuterated PE standard would not bind to the resin columns it could not be applied at the beginning of the extraction and undergo the exact same process as the endogenous gangliosides. Therefore, standard could only be added to the final mixture that is injected into the mass spectrometer and hence could not account for the material loss that naturally occurs during the extraction process. This would result in the measured ganglioside concentration being lower than their actual concentration in the sample. Furthermore, due to the direct addition of the deuterated PE standard to the MS-injection mixture it was difficult to spike the right amount. Usually ending up with a to high concentrated standard in the injected mixture and therefor overloading the ion trap during the acquisition, even further miss representing what is measured from the original sample concentration (see Figure 7). Overall, it was not feasible to continue without a better fitting standard.

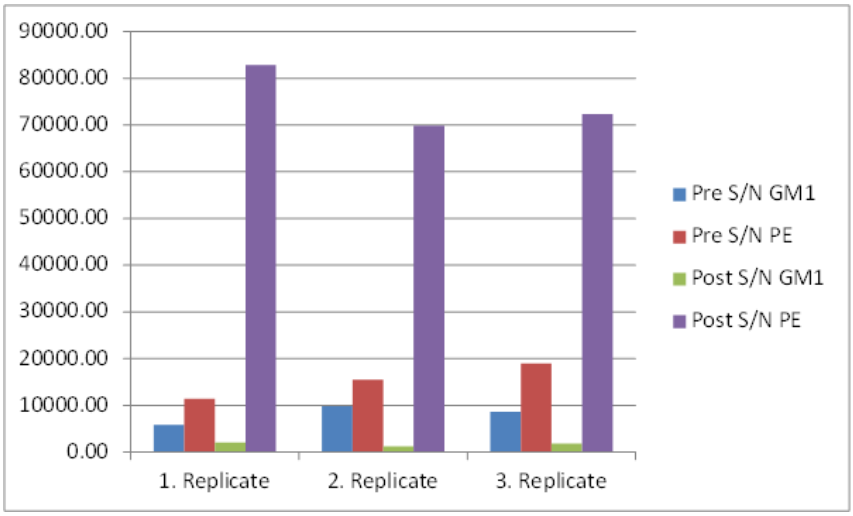

Figure 7. Alternative internal standard test. y-Axis shows the measured Signal to Noise (S/N) ratio. Pre S/N = GM1- and deuterated PE standard were added equimolar and directly injected into MS; Post S/N = GM1 standard was processed with evaluated protocol, deuterated PE standard added “equimolar” to the beginning concentration of GM1 standard before injection into MS. Since the deuterated PE standard cannot bind to the SPE columns and therefore can only be added post extraction to the MS-mix before injection in the MS. Thus, the deuterated PE standard cannot account for all the losses that may occur during the extraction and suppressing the ions of interest in the ion-trap by being overrepresented.

3.5. Response Factors of modified GM1 standard for naturally occurring GD1, GT1 and GQ1

Due to the lack of fitting internal standards for each ganglioside class of interest it was necessary to empirically determine response factors (RF) for the classes. A response factor addresses the differences in the way molecules ionize and other physico-chemical differences during sample handling, e.g. one ganglioside class could be more polar than another and hence more prone to go to the aquatic phase or bind more specifically to the C18 resin columns during the 2-phase extraction. Thus, over several experiments the RF for each ganglioside class were determined empirically and calculated with the following formula:

$$RF = \frac{Int_{wt(36:1)}}{Int_{Mod.Standard}}$$

Subsequently the RF values were averaged. With these RFs the mouse brain titration with only modified C17-GM1b as an internal standard was done (See Table 9). Nevertheless, a response factor will always be only an approximation and can never replace a suitable standard from the same lipid class.

Ganglioside Class	Response Factors (RFs)	Variation of RFs
GD1	2.682	1.48 - 4.74
GT1	0.258	0.085 - 0.412
GQ1	0.0048	0.0028 - 0.074

Table 9. Empirically determined response factors (RFs) of modified C17-GM1 standard for the other ganglioside classes.

3.6. Limit of detection (LOD) and limit of quantification (LOQ) for each ganglioside class

As mentioned before, for the determination of the limit of detection (LOD) as well as the limit of quantification (LOQ) a titration of bovine ganglioside standards was done, measured and compared to a constant concentration of the modified C17-GM1 standard. A known and stable concentration of the modified C17 standard was added to ganglioside-free human erythroleukemia cell line HEL-SCR, to provide a lipid background, and the ganglioside class to be assessed (for used ganglioside standards see Table 4). The physico-chemical behavior of endogenous GM1 should mirror the behavior of the used standard and therefore a comparison

of the measured intensities is a valid way to describe the concentration proportions in the sample. For gangliosides other than GM1, a response factor was empirically allocated by measuring samples containing the same concentration of, for example, the GD1 standard and the C17-GM1 standard. The measured intensity deviation for the same standard concentration made it possible to calculate the response factor. This was repeated for different concentrations and on several days using two mass spectrometers, to get robust data for the response factors (see Table 9).

After assessment of the response factors for modified C17-GM1b towards the other ganglioside classes, the LOD and LOQ could be calculated via a linear regression based on a linear calibration curve (see Figures 8-13). The calculation was done by titrating a constant concentration of 50 pmol of C17-GM1b standard versus a range of non-modified ganglioside standards concentrations ranging from 1600 pmol to 0.73 pmol in 1:3 dilution steps. For the linear regression to work it is assumed that the instrument response *y* is linearly related to the standard concentration *x* for a limited range of concentration:

$$y = a + xb$$

This model can then be used to calculate the sensitivity *b* together with the LOD and LOQ:

$$LOD = 3\frac{S_D}{m}$$

$$LOQ = 10\frac{S_D}{m}$$

where S_D stands for the standard deviation and *m* for the slope of the calibration curve.

LOD describes the ability to measure the existence of a signal reliably and LOQ is the minimal concentration that must be present in a sample in order to be able to measure the concentration reliably. The results stated in Table 10 are the LOD and LOQ for the evaluated starting protocol.

Class (Evaluated Protocol)	LOD (pmol)	LOQ (pmol)
GM1	3.86	15.73
GD1	8.97	12.25
GT1	15.94	44.16
GQ1	34.63	47.37

Table 10. Limit of detection (LOD) and limit of quantification (LOQ) in pmol values for each ganglioside class of interest obtained with the evaluated (=old) protocol. Notably, for these values only the modified C17-GM1 standard was available for the measurements, which is also reflected in the higher LODs and LOQs for the other classes.

At a later stage of the project also modified C17-ganglioside standards for the classes GD1a and GT1b had been kindly provided by Ludger Johannes (Curie-Institute, Paris, France) and could be used for measuring these classes with them. By not having to use the approximating RFs for these classes anymore the LOD and LOQ could be improved compared to before, where the modified C17-GM1 had to be used for all ganglioside classes of interest. Additionally, GT1b as a molecule is more like GQ1b, compared to GM1b, and assessing the LOD as well as LOQ of GQ1b via the modified C17-GT1b standard helped to improve these values.

In Table 11 a significant improvement of LOD and LOQ for each ganglioside class can be seen, which can be attributed to two reasons: firstly, the use of fitting class standards for GD1 and GT1 as well as the use of modified C17-GT1b as the new reference standard for GQ1b; secondly, changes on the protocol to increase its performance and integrate it better into the workflow for non-ganglioside lipidomic acquisition. As stated before, these changes included the switch to SOLA™ plates accompanied with usage of a vacuum manifold and streamlining of the extraction process as described in the final protocol (see Section 3.3).

Class (Final Protocol)	LOD (pmol)	LOQ (pmol)
GM1 (36:1)	0.393	1.19
GM1 (38:1)	0.644	1.95
GD1 (36:1)	0.243	0.74
GD1 (38:1)	0.3	0.911
GT1 (36:1)	0.658	1.99
GT1 (38:1)	0.796	2.413
GQ1 (36:1)	1.683	5.10
GQ1 (38:1)	4.1	12.432

Table 11. Limit of detection (LOD) and limit of quantification (LOQ) values obtained with the final protocol, using the three modified C17-ganglioside standards for the classes GM1b, GD1a, GT1b and SOLA™ plates. Even though the LOD and LOQ for GQ1 improved significantly when it was assessed via modified C17-GT1b compared to the assessment via modified C17-GM1b, with a modified GQ1 standard the values would most likely be further reduced and resemble more the values of the other ganglioside classes.

A mass range window of 30 Da was used during each acquisition. Within this 30 Da window all the mass over charge (M/Z) peaks of interest are located: Namely, the 36:1 and 38:1 peaks (the two most abundant naturally occurring ganglioside species (see 1.3), when double negatively charged), as well as the 35:1 peak of the modified C17-standards. In Figure 8 the titration curve for non-modified (=wildtype) GM1b versus a constant concentration of the modified C17-GM1b standard is shown. The calculated LOD lies at 3.86 pmol and the LOQ at 15.73 pmol. On the y-axis the responsive behavior of the constant internal standard to the changing GM1b standard is indicated. To provide a ganglioside-free lipid background per sample circa 80,000 human erythrocyte leukemic cells were used, that should equal a total lipid amount of 4000 pmol. All the following assessment experiments were performed in a similar fashion.

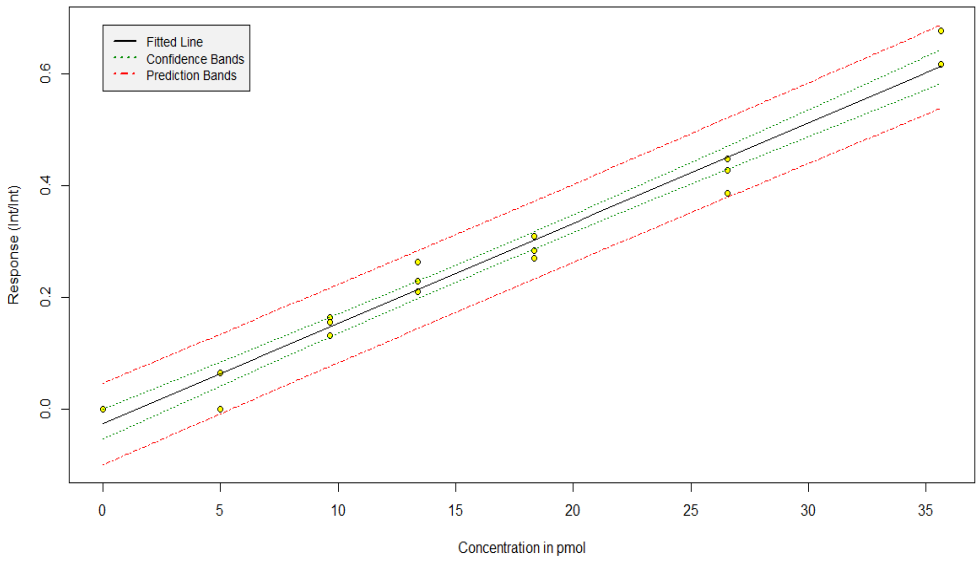

Figure 8. GM1b standard titration with HEL cells and the evaluated (=older) protocol, to provide lipid background, normalized to modified GM1; Acquired Mass Range: 30 Da.

Figure 9 shows the results for GD1 under the same conditions of acquisition as previously stated for the GM1 class, the used internal standard was still the modified C17-GM1b standard. The calculated LOD lies at 8.97 pmol and the LOQ at 12.25 pmol for GD1, when normalized to C17-GM1b.

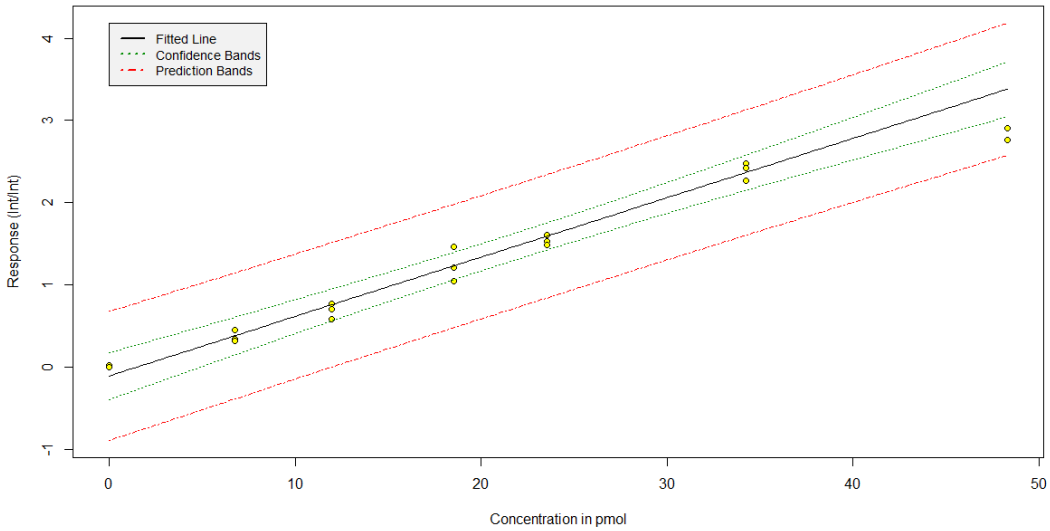

Figure 9. GD1a standard titration with HEL cells and the evaluated (=older) protocol, to provide lipid background, normalized to modified C17-GM1; Acquired Mass Range: 30 Da; LOD: 8.97 pmol; LOQ: 12.25 pmol.

For the GT1b standard titration, done with the evaluated starting protocol under the same conditions as previously stated and normalized to C17-GM1b, the LOD was 15.94 pmol and the LOQ 44.16 pmol (see Figure 10).

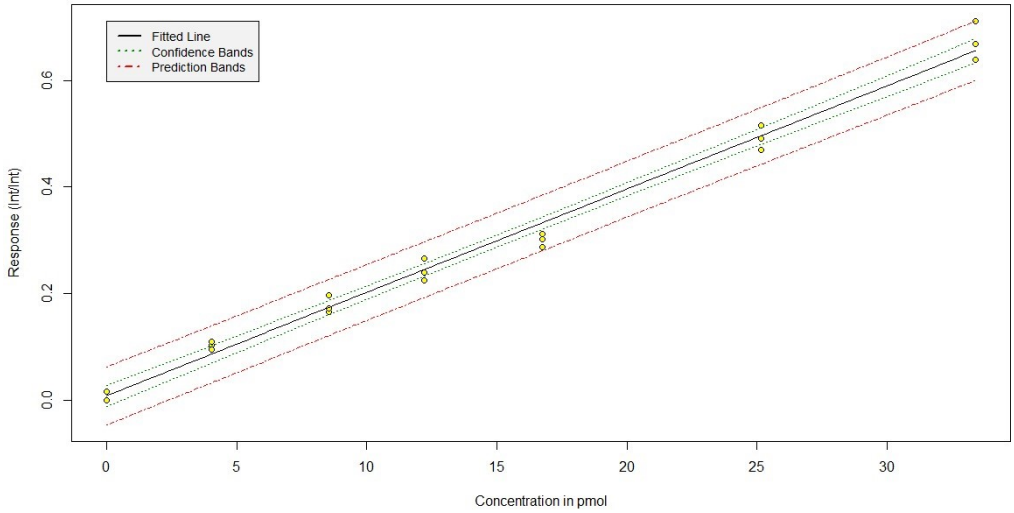

Figure 10. GT1b standard titration with HEL cells and the evaluated (=older) protocol, to provide lipid background, normalized to modified GM1; Acquired Mass Range: 30 Da; LOD: 15.94 pmol; LOQ: 44.16 pmol.

For GQ1b standard titration, same settings and evaluated protocol, the LOD was 34.63 pmol and LOQ 47.37 pmol (see Figure 11). Noticeably, LOD and LOQ diminish with increasing complexity of the measured ganglioside and the subsequent gap between measured ganglioside class and the C17-GM1b standard. Due to the lack of availability of a more fitting GQ1b standard, this was the best approximation possible at that time. To give a comparison, publications regarding the quantification of gangliosides by mass spectrometry alone are scarce, quantification was either done with calculation by the ratios of individual peak areas of ganglioside molecular species to the total peak area (Ikeda et al., 2008) or by calculation of signal to noise (S/N) ratios (Fong et al., 2009). There, the LOD was estimated by loading decreasing amounts of ganglioside standard on to the HPLC–MS system until the peak was three times the noise level, while the LOQ was estimated to be as three times the LOD. These data were obtained with LC-MS, and, to the best of our knowledge, there has been no publication quantifying gangliosides via Shotgun mass spectrometry so far.

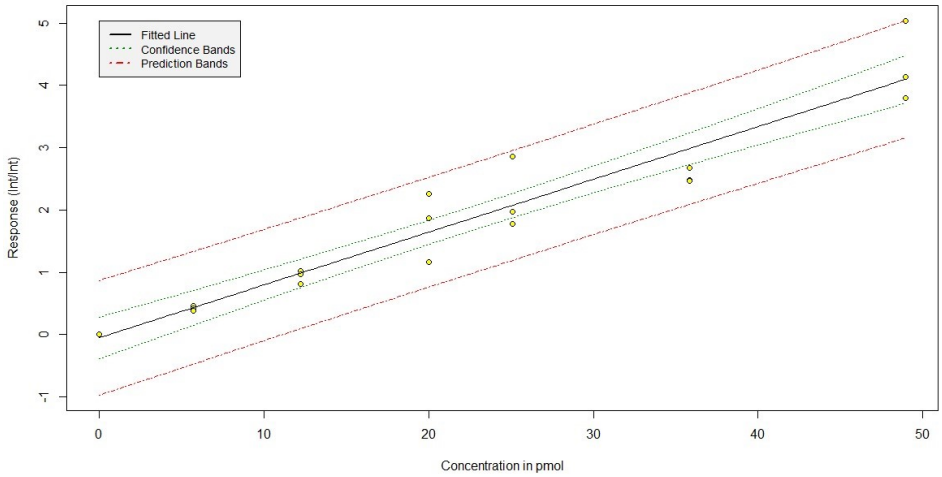

Figure 11. GQ1b standard titration with HEL cells and the evaluated (=older) protocol, to provide lipid background, normalized to modified GM1; Acquired Mass Range: 30 Dalton; LOD: 34.63 pmol; LOQ: 47.37 pmol.

The results presented in Figures 8-11 were obtained with the evaluated (=older) protocol and normalized towards the C17-GM1b standard. Upon arrival of the modified GD1a and GT1b the LOD and LOQ needed to be reassessed. Hence, the previous experiments were repeated with a standard titration from 1.5 pmol to 1000 pmol with the set of non-modified bovine standards (see Table 4), while the modified C17-standards remained at 100 pmol. The new standard

titration was also done with the improved final protocol and the LOD as well as the LOQ have already been stated in Table 11. The standard titration curve for species 36:1 can be seen in Figure 12 and for species 38:1 in Figure 13.

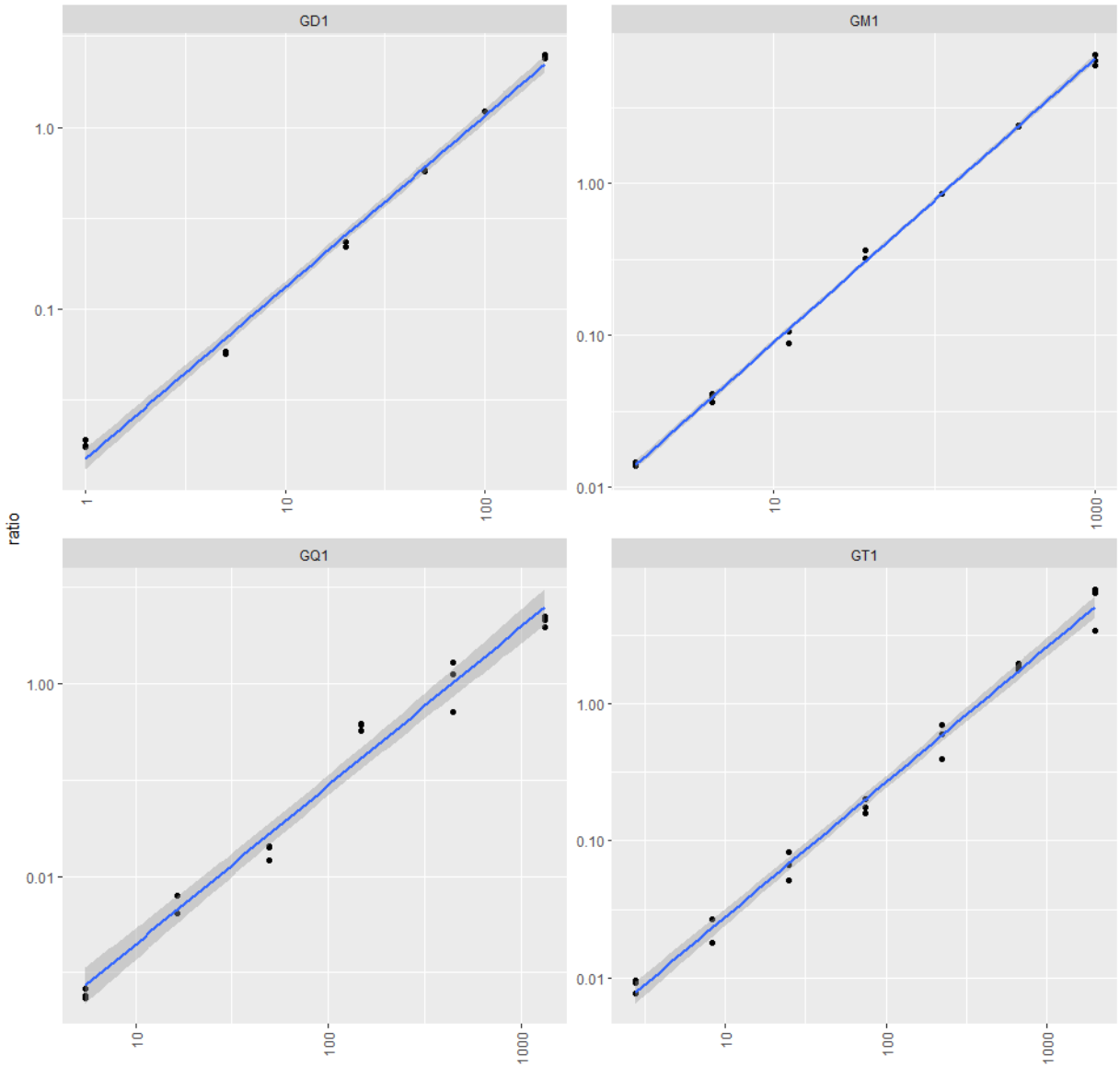

Figure 12. The standard titration curves for all ganglioside species 36:1 to determine the LOD & LOQ via all three modified C17 standards (GM1b, GD1a, GT1b) and final protocol. Wildtype ganglioside standard titration versus a steady concentration of matching modified C17-ganglioside standards with the final protocol, using SOLA™ plates and vacuum manifold. The individual graphs show intensity ratios of the standards (Wildtype vs. Modified) towards each other; GQ1 shows more outliers due to the lack of a class specific modified C17-standard. Modified C17-GT1b standard was used for the normalization of class GQ1.

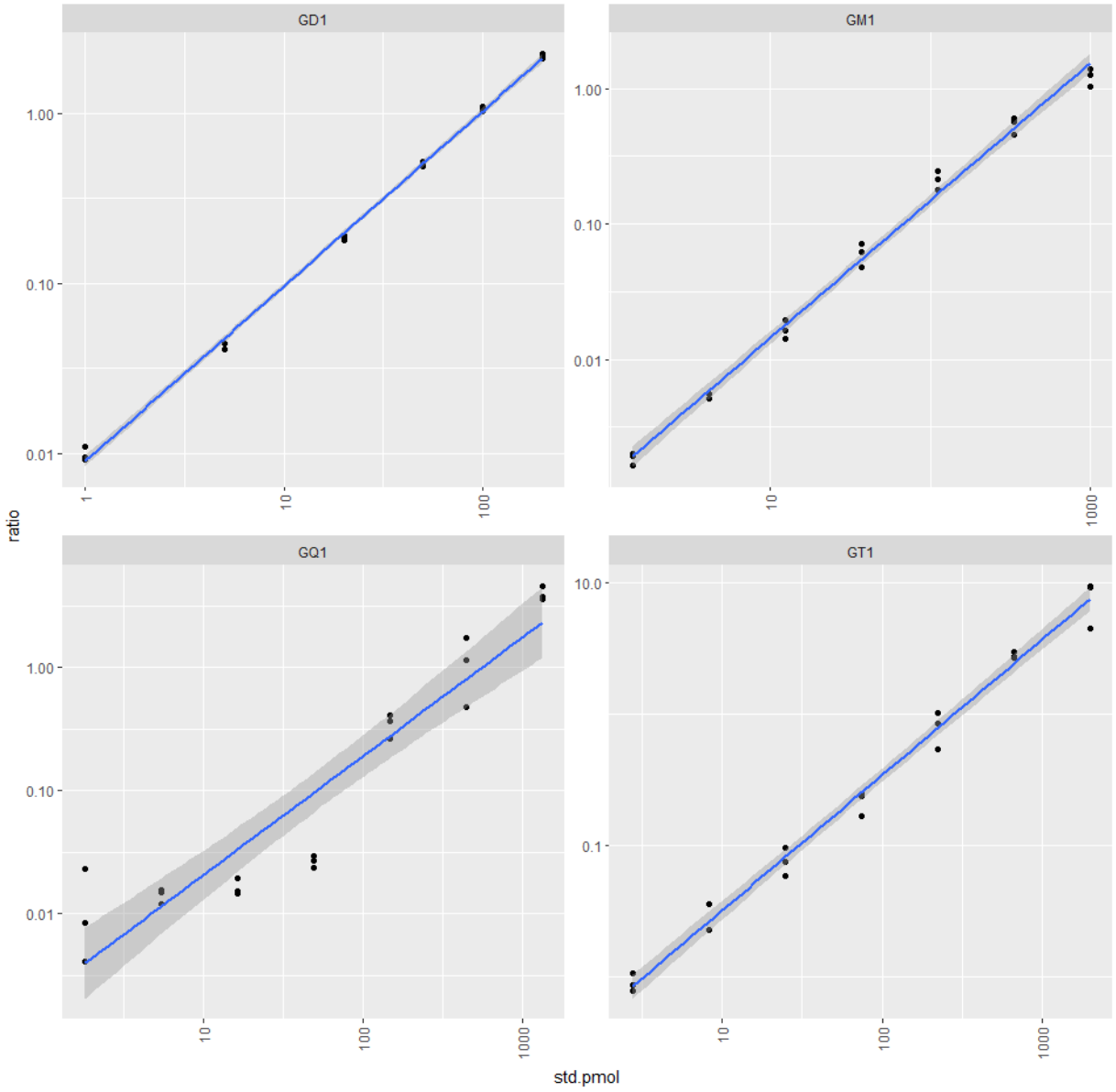

Figure 13. The standard titration curves for ganglioside species 38:1. to determine the LOD & LOQ via all three modified C17 standards (GM1b, GD1a, GT1b) and final protocol. Wildtype ganglioside standard titration versus a steady concentration of matching modified C17-ganglioside standards with the final protocol, using SOLA™ plates and vacuum manifold. The individual graphs show intensity ratios of the standards (Wildtype vs. Modified) towards each other; GQ1 shows more outliers due to the lack of a class specific modified C17-standard. Modified C17-GT1b standard was used for the normalization of class GQ1.

For both species the results for GQ1b are not as good as for the other ganglioside classes, this problem could most likely be addressed with a fitting class standard. After normalizing GQ1b to the three modified C17-standards individually, modified C17-GT1b showed the results closest to the expected outcome and was used from then on for normalization of GQ1b.

3.7. Technical variation

To assess the reproducibility of a method, the technical variation between biological replicates, the coefficient of variance (CV) are determined. The CV is calculated with the following formula:

$$Coefficient\ of\ Variance = \frac{Standard\ Deviation}{Mean} * 100$$

Six samples with an equimolar concentration of 100 pmol of non-modified bovine ganglioside standards as well as the modified C17-standards were measured subsequently. The results for the evaluated protocol with all three modified standards are shown in Table 12.

Ganglioside	**CV-average**
GM1a	8.13
GD1a/b	11.86
GT1b	7.7
GQ1b	30.79

Table 12. Average Coefficient of Variance (CV) for the different Ganglioside classes with **evaluated** (=older) protocol and all three modified C17-ganglioside standards.

For the same experimental set-up with the final protocol the CV values can be found in Table 13.

Ganglioside	**CV-average**
GM1a	5.64
GD1a/b	2.81
GT1b	5.13
GQ1b	18.43

Table 13. Average Coefficient of Variance (CV) for the different Ganglioside classes with the **final** protocol and all three modified C17-ganglioside standards.

3.8. Testing under biological conditions: brain tissue titrations

As a proof of principal experiment and to determine the performance under biological conditions a titration of various amounts of mouse brain tissue was done. In this experiment the two most abundant ganglioside species with regard to their ceramide headgroup, 36:1 and 38:1 of the four major ganglioside classes in mammal brains were of interest, as explained in 1.3 Structure and biosynthesis of glycolipids. The experimental setting for the results shown in Figure 14, was to process triplicates of 150 µg, 300 µg and 600 µg of wet weight mouse brain tissue together with 100 pmol of modified C17-GM1 standard with the evaluated protocol. In the used mouse brain 100 µg of wet weight tissue should equal a total lipid concentration of about 4600 pmol. This experiment was done at an earlier stage of the project, after the arrival and establishment of only the modified C17-GM1b standard, which was also before the other changes were applied to the protocol (e.g. SOLA™ plates and vacuum manifold). Therefore, comparing these results with the data obtained after repeating the experiment with the final protocol and all three modified C17-ganglioside standards later, allows to illustrate the overall enhancement of the method's performance.

After the acquisition the intensity values were extracted from the raw files with the help of LipotypeXplorer, subsequently normalized with regard to the modified GM1b standard and quantified with the response factors listed in Table 9.

The results were within expected parameters (see Figure 14). The only exception were the results obtained for GT1b: first, the measured concentration of 36:1 and 38:1 GT1b at 300 µg of tissue was lower than the concentration at 150 µg of the same tissue. Secondly, also the measured increase from 150 µg to 600 µg was lower than expected. By increasing the amount of tissue 4-fold one would expect a proportional increase in the measured ganglioside concentration. The measured values were, however, much lower and not even a 2-fold increase was observed between 150 µg and 600 µg input samples. This observation cannot be explained only by matrix effects. Possible reasons for this are a non-homogenous sample material distribution during pipetting or ion suppression in the ion trap due to too high GD1 amount.

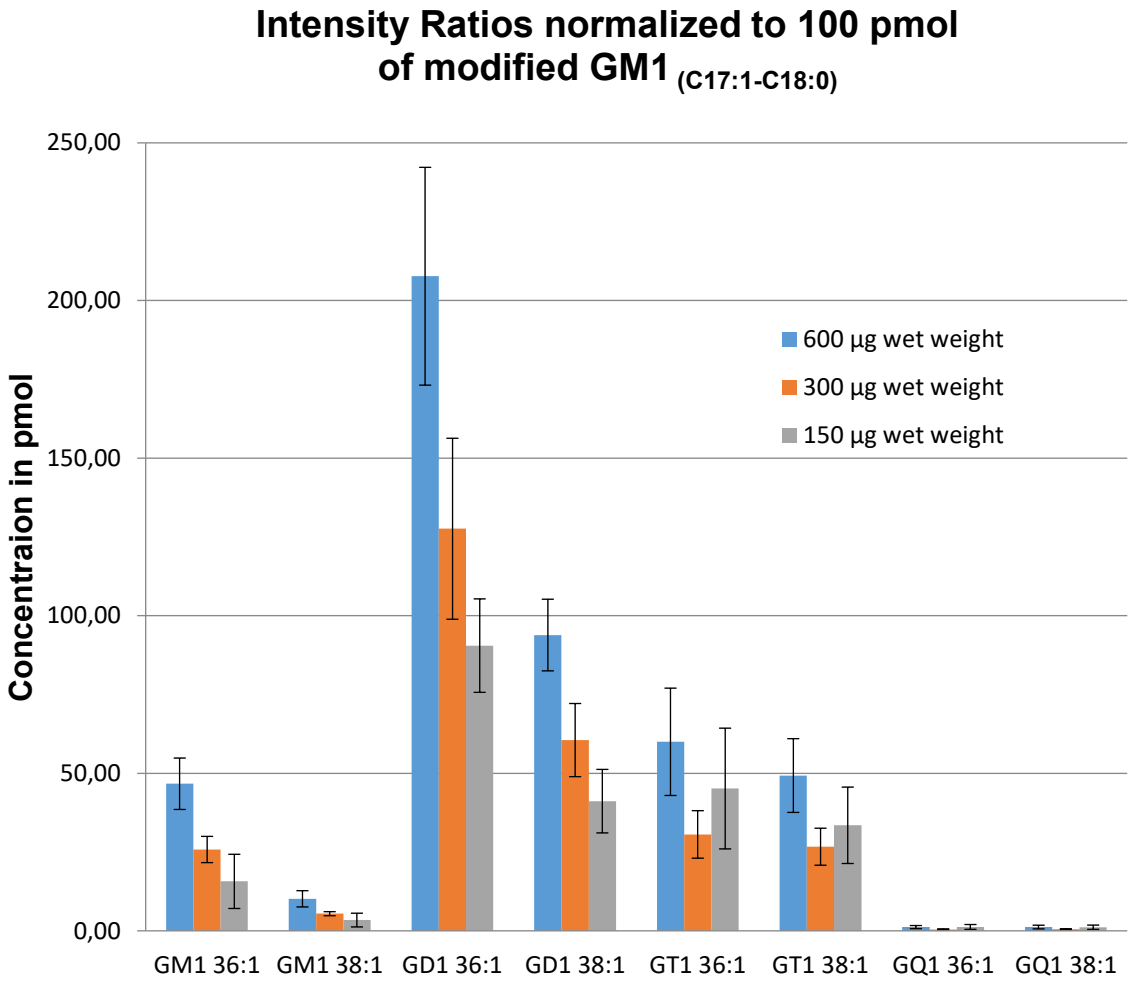

Figure 14. Brain tissue titration with evaluated (=old) protocol and all shown gangliosides species normalized to modified C17-GM1b. Y-Axis shows measured concentration in pmol. X-Axis shows mean values (triplicates) for the two dominant lipid species (36:1 and 38:1) for the four major mammal brain ganglioside classes. Error bars are +/- of Standard deviation (SD). Titration of wet weight mouse brain tissue was done with 600 µg (blue), 300 µg (orange) and 150 µg (grey) and in triplicates. The 2-fold increase of wet weight mouse brain tissue over the titration should also be reflected in a similar increase of measured ganglioside concentration. The stagnation for the 600 µg wet weight samples could be explained with matrix effects and a possible ion suppression in the ion trap by GD1. For GT1 36:1 and 38:1 with 300 µg of wet weight brain tissue the concentration was lower than for the 150 µg wet weight samples. A possible reason could be a non-homogenous distribution of sample material while pipetting, but this would have lowered the measured concentrations for the other ganglioside classes equally and not only for GT1.

At a later stage of the project, after also the modified ganglioside standards arrived for GD1a and GT1b, the above experiment was repeated, with a slightly broader titration range of the used mouse brain tissue amount: from 100 µg to 1000 µg wet weight (Figure 15), where again 100 µg of wet weight tissue would equal around 4600 pmol of total lipid. The final protocol was used to obtain these data, employing 100 pmol from each of the three modified ganglioside standards and SOLA™ plates in combination with the vacuum manifold. The measured quantities are in accordance to the findings of other studies (Ikeda et al., 2008; Fong et al., 2009). The error bars are clearly much smaller than in the previous experiment, which could not only be attributed to the fitting class standards, but also a result of the different acquisitional mass windows used in this experiment. If there is no fitting class standard with a mass over charge (m/z) ratio that lays close to the m/z ratio of the peaks of interest, it is necessary to either make a very broad acquisitional window that includes both, the standard as well as the peaks of interest, or make two individual windows. A broader acquisitional m/z window means a higher noise level. But the low abundance of GQ1b required as few background as possible, therefor two separate m/z acquisition windows were set, resulting in the standard peaks and the peaks of interest being measured separately from each other. The m/z of the double negatively charged modified C17-GM1b standard is at 764,92 and for 38:1 of GQ1b at 1.222,59, meaning the acquisitional window would need to span more than 457 Da (see Table 7) to measure the peaks of interest in one acquisition. Measuring in separate acquisitions commonly increases the spread in mass spectrometry.

The measured concentrations for GQ1b were also improved and reflected what was expected from the literature (Ikeda et al., 2008).

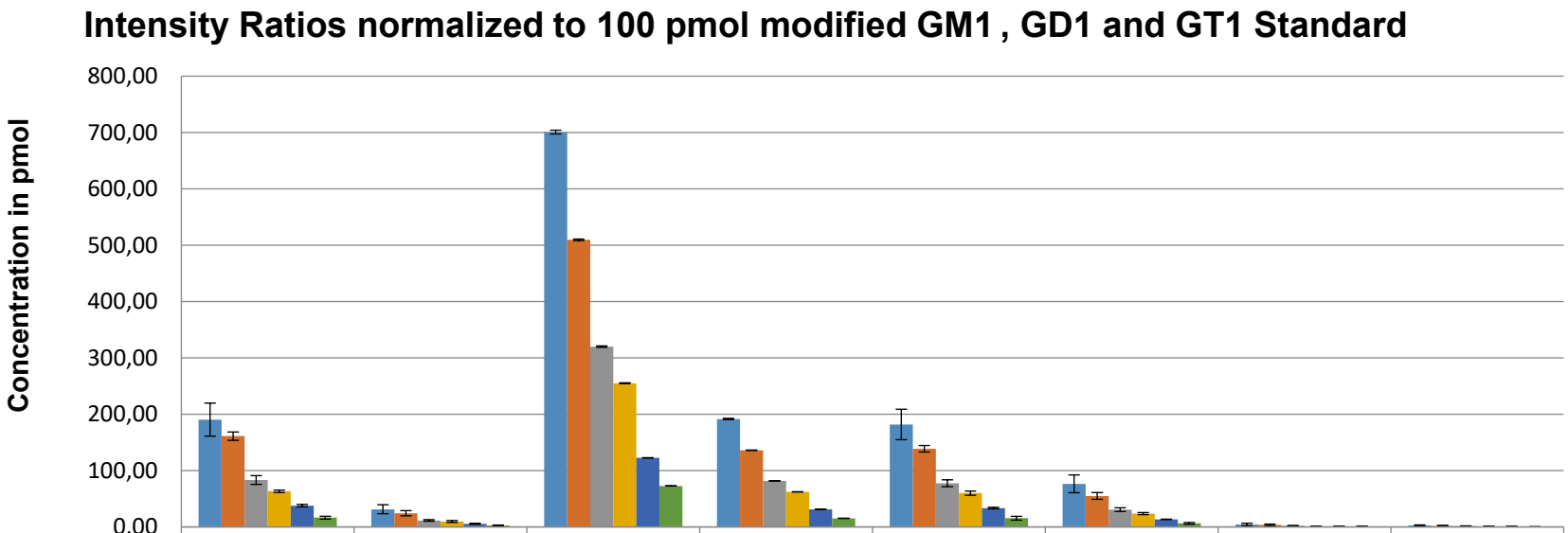

	GM1 36:1	GM1 38:1	GD1 36:1	GD1 38:1	GT1 36:1	GT1 38:1	GQ1 36:1	GQ1 38:1
1000 µg wet weight	190,46	31,41	700,78	191,56	181,86	76,51	4,52	2,44
800 µg wet weight	161,06	24,30	509,49	136,05	138,76	54,98	3,61	1,85
600 µg wet weight	83,26	11,48	319,97	81,80	77,56	30,74	2,14	1,56
400 µg wet weight	63,25	9,53	255,09	62,27	59,92	23,62	1,06	0,74
200 µg wet weight	37,74	5,52	122,57	31,14	33,39	13,37	0,87	0,64
100 µg wet weight	16,41	2,61	72,70	15,24	15,40	6,25	0,79	0,25

Figure 15. Brain tissue titration with evaluated (=old) protocol and all shown gangliosides species normalized to their respective modified C17-Standard, except for GQ1 which was normalized to modified C17-GT1b standard. Y-Axis shows measured concentration in pmol. X-Axis shows the mean values (triplicates) for the two dominant lipid species (36:1 and 38:1) for the four major mammal brain ganglioside classes. Error bars are +/- of Standard deviation (SD). Titration of wet weight whole mouse brain tissue was done with 1,000 µg, 800 µg, 600 µg, 400 µg, 200 µg and 150 µg wet weight in triplicates. Results improved considerably compared to the previous brain tissue titration with only modified C17-GM1 as internal standard.

3.9. Biological application: ganglioside measurement in murine cerebellum and hemispheres at different developmental stages

In a biological application the final version of the protocol was applied to two different brain areas, the cerebellum (cereb) and brain hemispheres (hemis), in mouse brains at five different developmental stages: postnatal day 4 (P4), day 14 (P14) and day 21 (P21), 8 weeks (8w) and 18 month (18m) after birth. The complexity of mammal brain gangliosides should be increasing over time (Fong et al., 2009) and the goal was to find out if we can measure this change in the different developmental stages and if we can observe a significant difference in between the two brain areas, not only for gangliosides, but for all lipid classes globally. Hence, we conducted first an exploratory experiment to get an idea of the total lipid amount per sample, where only phosphatidylcholine (PC) is measured for the same amount of tissue (wet weight). This is done to have comparable amounts of total lipid for the following experiment. Subsequently, the lipid composition at previously stated developmental time points and in the two brain areas is assessed. A general trend in the lipid class composition cannot be observed. Most abundant lipid class 4 days after birth (P4) is phosphatidylcholine (PC) and its percentage of total lipid goes down over time, while this trend can be observed in a reversed manner for cholesterol. Similarly, the percentage of total lipids is shifting between phosphatidylethanolamine (PE) and (PE O^-) with a lower abundance in the early days after birth, which is steadily increasing throughout first weeks after birth, thus making up an increasing fraction of the total lipids. For the other lipid classes, no clear trend can be observed (see Figure 16). The ganglioside classes are shown in more detail in Figure 17 and in Figures 19-21. At most of the time points measured from the hemisphere, gangliosides of the 36:1 species make up a bigger part of the total lipid than in the cerebellum. This trend seems to be reversed in the 38:1 ganglioside species, where the gangliosides make up a bigger part in the total lipids than in the hemisphere.

Contrary to our expectations, the amount of measured gangliosides reduces after birth over time, the same can be said for ceramide (Cer) and sphingomyelin (SM) in the cerebellum, but not for the hemispheres. The only sphingolipid class opposing this trend is hexosylceramide (HexCer) (Figure 16-17).

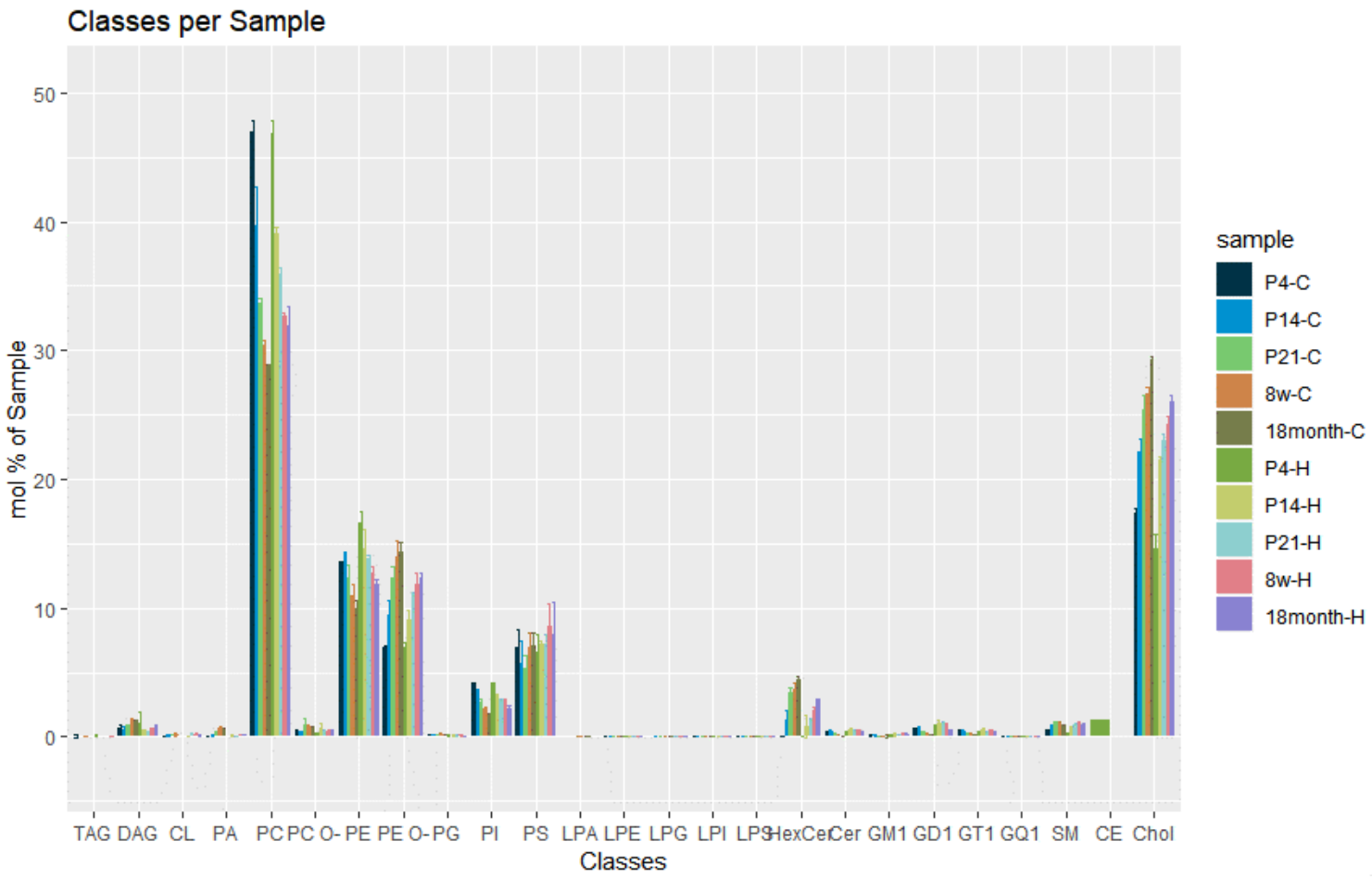

Figure 16. Lipid class composition of all lipids in mol% of total lipids Overall most abundant lipid class 4 days after birth (P4) is phosphatidylcholine (PC) and its percentage of total lipid goes down over time, while this trend can be observed in a reversed manner for cholesterol. Similarly, the percentage of total lipids is shifting between phosphatidylethanolamine (PE) and (PE O). For the other lipid classes, no clear trend can be observed. P4 = postnatal day 4; P14 = postnatal day 14; P21 = postnatal day 21; 8w = postnatal week 8; 18 months = postnatal month 18; C = Cerebellum; H = Hemisphere. Triplicates were measured for each sample, mean is shown, error bars are +/- SD. For a more detailed view regarding the sphingolipid classes see Figure 17.

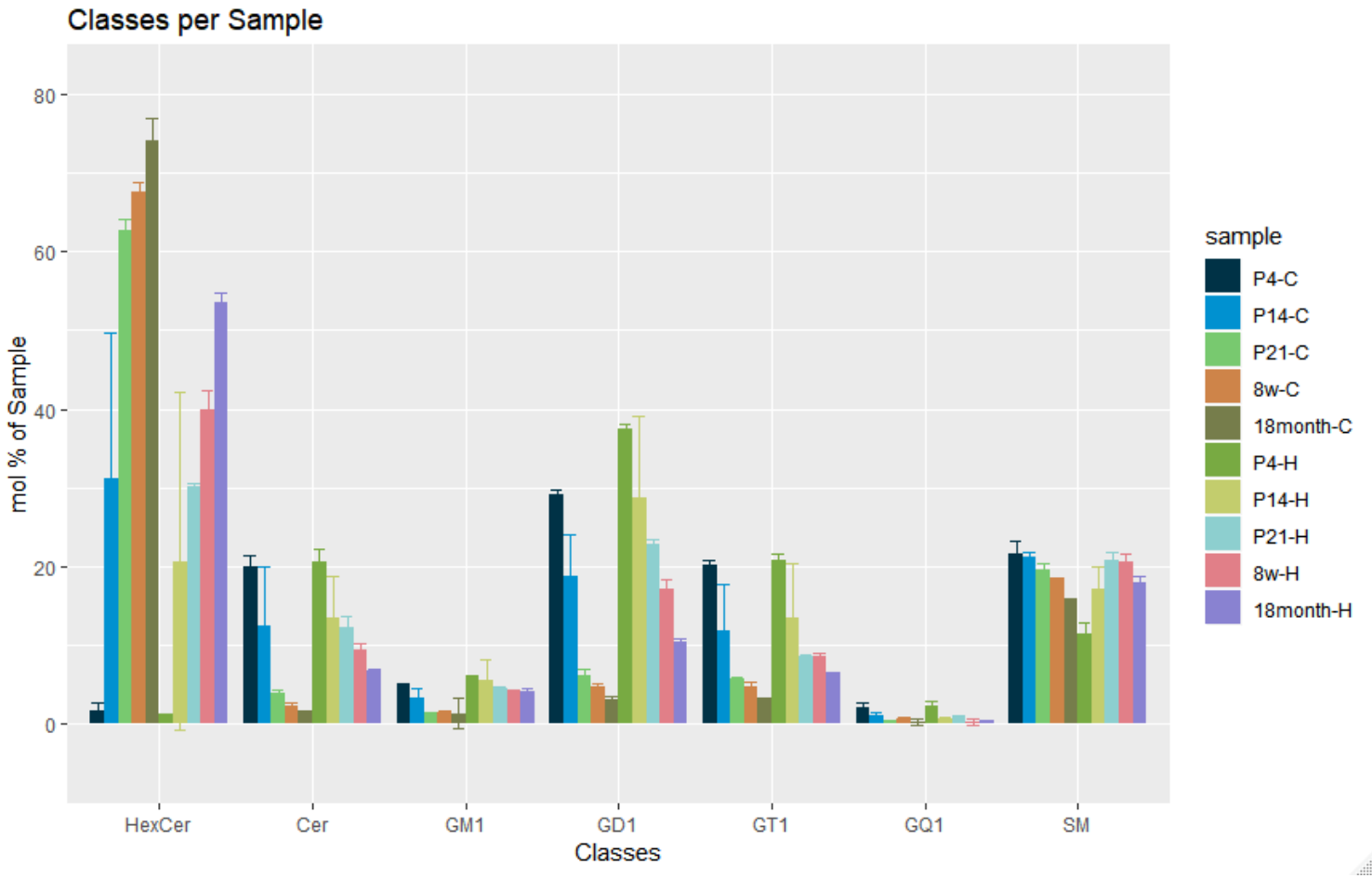

Figure 17. Lipid composition of sphingolipids classes in mol%; P4 = postnatal day 4; P14 = postnatal day 14; P21 = postnatal day 21; 8w = postnatal week 8; 18 months = postnatal month 18; C = Cerebellum; H = Hemisphere. Triplicates were measured for each sample, the values shown represent mean +/- SD. Remark: Only sphingolipids are observed in this graph, not the whole lipidome, therefor the given proportions apply to sphingolipids and not the whole lipidome. After birth the amount of gangliosides reduces over time, the same can be said for ceramide (Cer) and sphingomyelin (SM) in the cerebellum, but not for the hemispheres. The only sphingolipid class opposing this trend is HexCer.

Subsequently, a principal component analysis (PCA) was performed, which showed that the first principal component (PC) is the tissue of origin and the second PC is the developmental stage (see Figure 18), as to be expected. Generally, in PCAs, an orthogonal transformation is done to convert a set of observations of possibly correlated variables into a set of values of linearly uncorrelated variables, also called principal components. Usually, the PCA operation can be thought of as revealing the internal structure of the data in a way that best explains the variance in the data. If a dataset with several variants is visualized as a set of coordinates in a high-dimensional data space (1 axis per variable), PCA can supply the user with a lower-dimensional picture - a projection of this object when viewed from its most informative viewpoint. This is done by using only the first few principal components, so that the dimensionality of the transformed data is reduced.

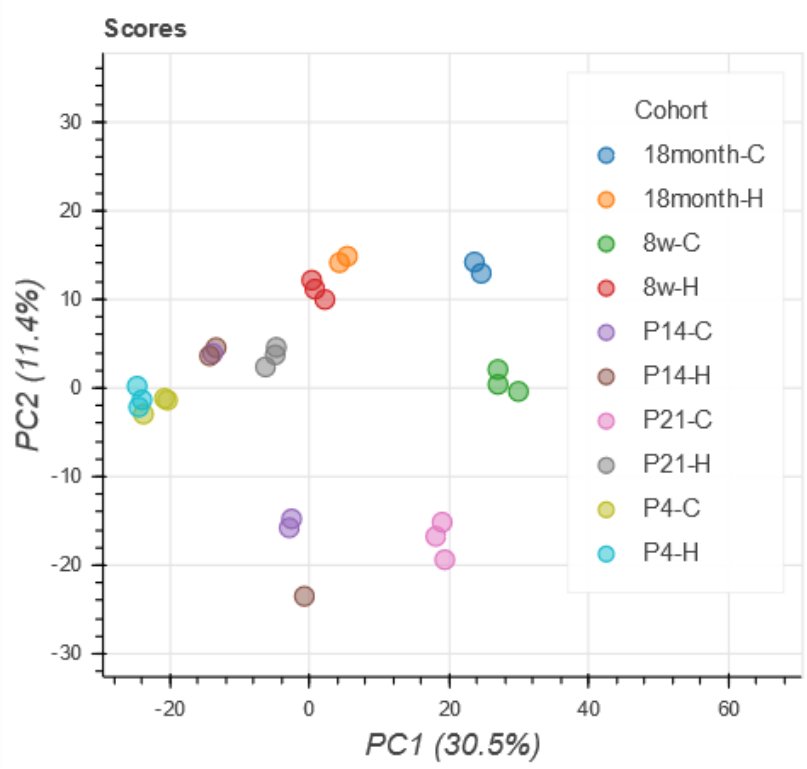

Figure 18. Principal component analysis (PCA) with tissue (PC1) and age (PC2) as principal components. Lipid class composition of all lipids in mol% of total lipids; P4 = postnatal day 4; P14 = postnatal day 14; P21 = postnatal day 21; 8w = postnatal week 8; 18 months = postnatal month 18; C = Cerebellum; H = Hemisphere. PCA is used as a statistical tool to prove if correlation between samples is given and as a test of plausibility the biological replicates need to cluster in the PCA. These data include the global lipid analysis combined with the ganglioside analysis. All samples were measured in Triplicates.

The chain length has significant impact on the properties of the fatty acid and the lipid itself. Generally, the longer an alkyl chain is, the higher the melting point of it. On the other hand, the shorter a fatty acid is less saturated the better is its fluidity, which is a common feature that animal cells require to maintain the fluidity of their cell membranes during varying temperatures. In Figure 19 the carbon chain length of the aliphatic head groups is shown.

The carbon chain length of fatty acids can also be of importance when it comes to extracellular export via micelles that can act as emulsifiers, e.g. to transport fat-soluble vitamins or other lipids. The same is true for the amount of double bonds (DB) within an alkyl chain. It may be saturated, meaning with no double bonds, or unsaturated, usually with one or two double bonds. Mostly occurring DBs in unsaturated fatty acids are in cis-formation and in polyunsaturated fatty acids generally separated by at least one methylene group. Unsaturated fatty acids have lower melting points than saturated fatty acids of the same length. Double bonds cause bending of the hydrocarbon chain, which is why the fatty acids cannot compact tightly together and the van der Waals interaction between the fatty acids are reduced. Hence, the number of DBs per ganglioside class may help to contribute to our understanding of the biological function of gangliosides in the central nervous system. The number of DBs at different developmental stages in the mouse brain was measured (see Figure 20).

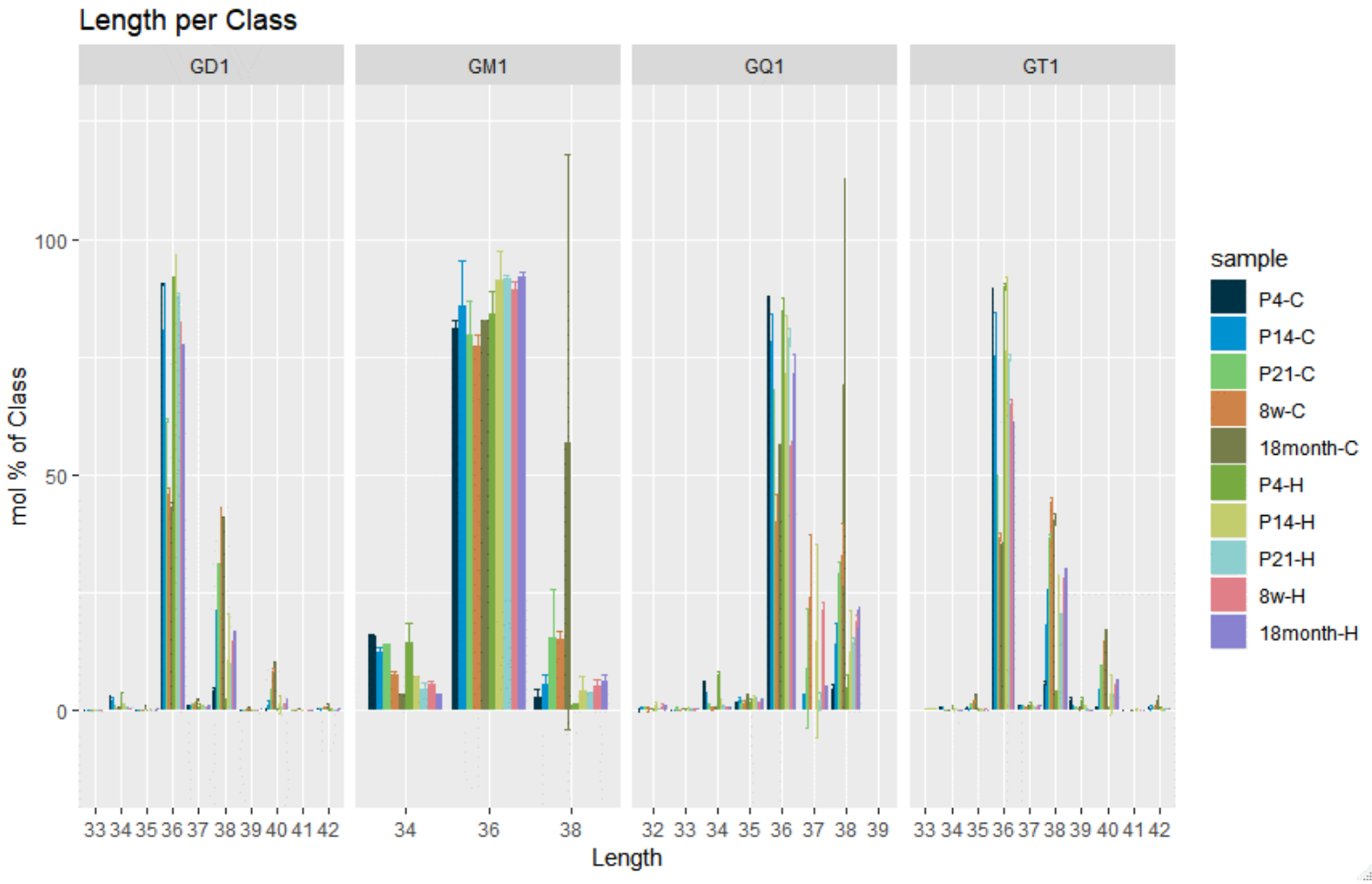

Figure 19. Carbon chain length of ganglioside classes shown in mol% per class; P4 = postnatal day 4; P14 = postnatal day 14; P21 = postnatal day 21; 8w = postnatal week 8; 18 month = postnatal month 18; C = Cerebellum; H = Hemisphere; Triplicates were measured for each sample, shown is mean +/- SD. Aliphatic chains in biological system usually contain mostly an even number of carbon atoms and are unbranched; For brain gangliosides there is usually one or two dominant chain lengths. As expected, the dominant ganglioside species that could be observed are 36:1 and 38:1 and to a lesser extent 40:1. The chain length and degree of saturation usually characterizes its properties of the fatty acid and lipids.

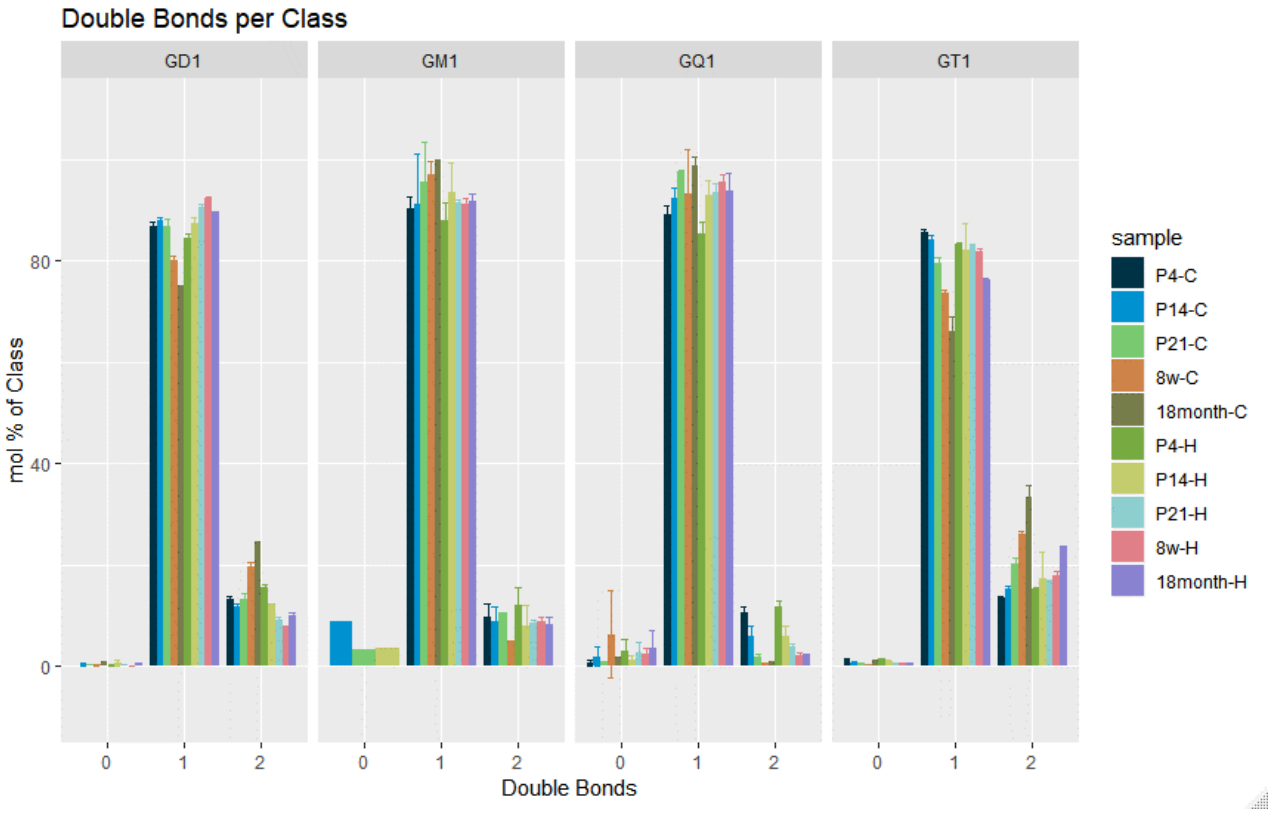

Figure 20. Number of double bonds (DB) per ganglioside lipid class; P4 = postnatal day 4; P14 = postnatal day 14; P21 = postnatal day 21; 8w = postnatal week 8; 18 months = postnatal month 18; C = Cerebellum; H = Hemisphere. Triplicates were measured for each sample, shown is mean +/- SD. The quantity of single DBs seams to increase over time for GM1 and GQ1, while the amount of two DBs stagnates (GM1) or is reducing (GQ1) with progressing age of the mice. For GT1 this trend seems to be reversed, the single DBs get less over time and the number of two DBs goes up with age. For GD1 a different trend in the two different tissue types can be observed, in the cerebellum the number of single DBs diminishes while the number of two DBs grows. In tissue coming from the hemisphere it is the opposite for GD1.

To provide even deeper characterization of the ganglioside classes across different developmental time-points of the mouse brain and to fully assess the possibilities of the final method of this protocol, in the next step also the hydroxyl groups of distinct ganglioside classes were quantified (Figure 21). The ganglioside class possess predominantly 2 hydroxyl groups (see Figure 21). While in GM1 and GQ1 no general trend is recognizable, the degree of hydroxylation in GT1 shifting from two hydroxyl groups to three. This can also be seen in the cerebellum in GD1. The amount of hydroxyl groups is important for the hydrophilic behavior of a molecule or the lack of such groups for its lipophilicity.

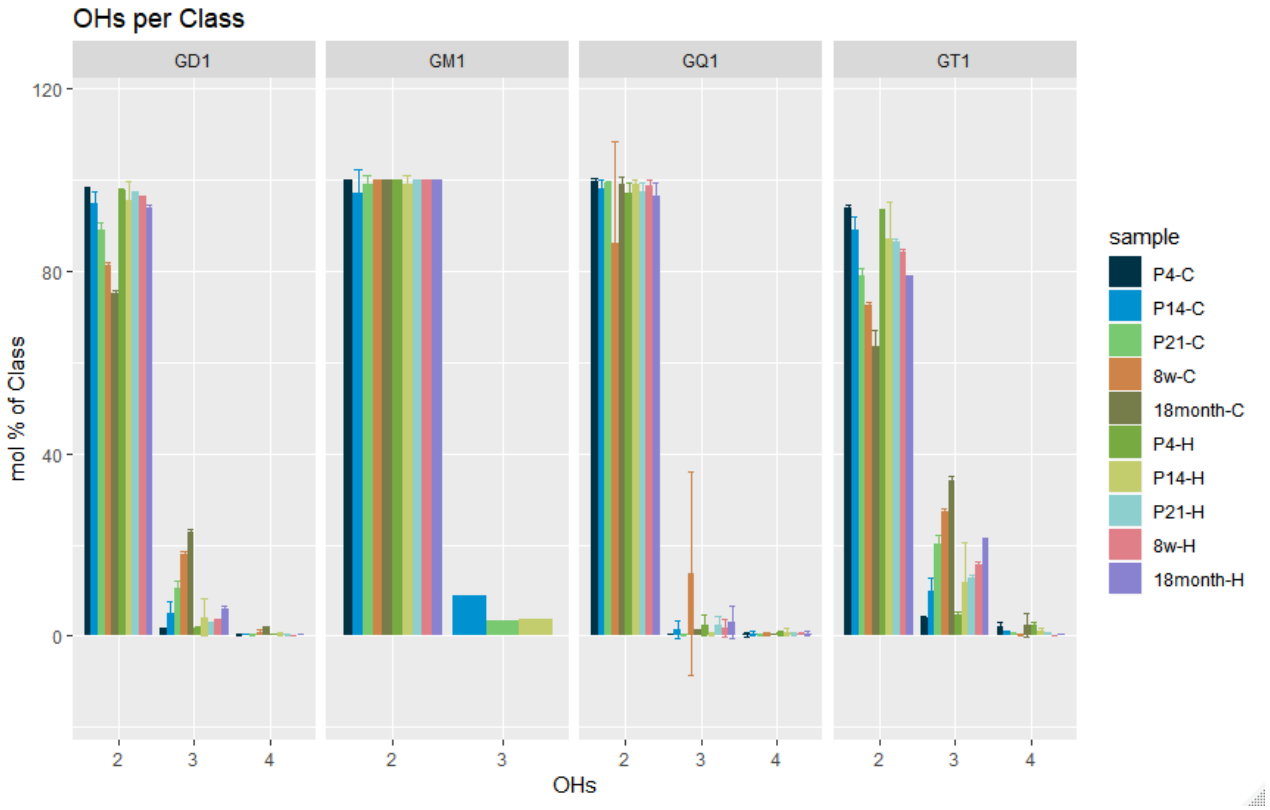

Figure 21. Degree of hydroxylation per ganglioside class shown in mol% per class; P4 = postnatal day 4; P14 = postnatal day 14; P21 = postnatal day 21; 8w = postnatal week 8; 18 months = postnatal month 18; C = Cerebellum; H = Hemisphere. Triplicates were measured for each sample, values represent mean +/- SD. Two hydroxyl groups prevail over all time points and in both tissues. In GT1 a general trend is recognizable with a shift from two hydroxyl groups to three. This can also be seen in the cerebellum in GD1.

4. Conclusion

Lipids have long been neglected. One barrier to overcome was the lack of analytical methodology that could come to grips with the broad spectrum of lipid molecules to be analyzed. This was solved by the introduction of mass spectrometry. Today there are two platforms that are mostly being used, namely LC-MS and direct infusion (shotgun). The field is still dominated by LC-MS but shotgun-MS is gaining ground. The reason for this development is that the latter method is faster and at the same time more quantitative than LC-MS.

One class of lipids that so far has not been included in the repertoire for shotgun-MS lipid analysis has been the gangliosides. They are exceptional in the sense that they are water-soluble, hence ending up in the water phase, after organic solvent extraction. They represent a poorly studied class of lipids because of the difficulty to analyze them with a resolution that extends the molecular level. Gangliosides are ubiquitous in their distribution over different tissues but show a higher concentration in the central nervous tissue and the liver (some refs).

Thus, the aim of this thesis was to add an analytical tool with a higher sensitivity and more complete acquisition than currently existing comparable methods can offer for ganglioside analysis. Additionally, the method should have a sample procession time and reproducibility, that is on level with previously reported studies for shotgun mass spectrometric analysis of lipids (Surma et al., 2015).

We wanted to achieve “complete acquisition” by measuring the gangliosides from the same sample as non-ganglioside lipids (Surma et al., 2015), thus opening new observation windows by increasing coverage. This was achieved by taking up the samples in 150 mM ammonium bi-carbonate and subsequently extracting with chloroform/methanol 10:1 followed by chloroform/methanol 2:1 (see 3.3 Final protocol) and after the organic solvent extractions were done and used for non-ganglioside lipids analysis, the remaining ammonium bi-carbonate phase was used for the ganglioside extraction.

This pursuit was successful. The method that we developed can be characterized as follows. The initial barrier that had to be overcome was to first standardize and subsequently automatize the extraction procedure as much as possible. Originally, the method started at the bi-phasic extraction protocol described by Svennerholm and Fredman (Svennerholm and Fredman, 1980), using chloroform/methanol/water 4:8:3. We ended up with a protocol, which included adjusting the salt concentration of the water phase during the extraction, increasing the number of sample loading on the C-18 resin columns as well as fixing the number of washing steps with H_2O of the columns. These experiments were done with bovine ganglioside standards (see Table 4) and with

the human erythroleukemia cells, HEL-SCR, that have such a low ganglioside abundance, that they can be considered ganglioside-free.

After the sensitivity yield was improved, the next phase of the project was to establish working internal standards to be able to quantify correctly the ganglioside concentration in complex biological samples. Deuterated ganglioside standards were not commercially available; hence the first experiments were carried out with internal standards used for the lipid class PE. Due to the different physio-chemical nature of this phospholipid compared to gangliosides, it could not be added at the beginning of the protocol. Additionally, PE did not bind to the C-18 resin columns, which is a necessary purification step of the protocol to separate the sialic acid carrying glycosphingolipids from the other polar lipids by means of their non-polar lipid head group. Therefore, the PE standard could not be used and had to be abandoned.

Class-specific internal standards for the three major brain ganglioside classes, GM1, GD1 and GT1 could be obtained from the Ludger Johannes lab at the Curie-Institute in Paris, France. Here we gained access to ganglioside standards with a C17-fatty acid in the ceramide head group of these gangliosides, which occurs naturally in such low abundance that it can be used as an internal standard. These standards are commercially not available. Since these standards could be added to the sample to be analyzed before extraction, it was possible to achieve quantification as was demonstrated earlier for the global analysis protocol (Surma et al. 2015).

Another important milestone for this thesis was the automatization of the protocol where it was feasible. Therefore, we switched from single C-18 resin spin columns to 96-well plates. This improved the processing speed of individual samples considerably. With the C-18 resin spin columns, it took approximately 16 hours to perform the whole protocol in one go and was additionally limited to 24 samples per processed batch. After the switch to 96-well plates, and the introduction of changes summed up in section 3.3 Final protocol, the processing time was reduced to 8.5 hours and the number of samples that can be processed simultaneously increased to 96. The acquisition at the MS data takes another 4 minutes per sample, resulting in an acquisition time of 6.4 hours for a whole 96-well plate.

To determine the amounts of gangliosides required in a sample, the limit of quantification (LOQ) needed to be assessed. With the limit of detection (LOD) the sensitivity of this developed method was assessed (see 3.6. Limit of detection (LOD) and limit of quantification (LOQ) for each ganglioside class) as well as and coefficient of variance (CV) (3.7. Technical variation). The LOD and LOQ were defined with dynamic range experiments, were a stable concentration of each modified C17-ganglioside class standard was titrated against a variety of concentrations from the

corresponding regular ganglioside standards of its respective matching class. For the final protocol with all three modified standards the LOD is 0.0081 µM (for GD1 36:1) to 0.137 µM (for GQ1 38:1) and the LOQ is 0.025 µM (for GD1 36:1) to 12.432 µM (for GQ1 38:1).

To be able to judge the effectiveness and parameters, e.g. sample amount, analysis time, LOD, LOQ, CV of a method, a comparison to other methods used to analyze gangliosides needs to be done. Fong *et al.* (2009) and Ikeda *et al.* (2008) are the benchmark studies for this purpose. In both publications LC-MS was used, which also reflects the predominant choice in the field, since LC-MS provides pre-separation of the lipids by chromatography and thus reduces the complexity of the mass spectrometric analysis. Typically, LC-MS has a higher sensitivity than Shotgun-MS, making it more suitable for analysis of low abundant classes of lipids – particularly with the use of LC-tandem mass spectrometry (LC-MS/MS) (Astarita et al., 2015). On the other hand, Shotgun-MS offers the advantages of simplicity, saves time (no column separation), and the quantification is more straightforward, since the internal standards are in the same sample matrix and measured together with the analytes. The internal standards experience the same ion suppression and matrix effects and this feature makes the shotgun platform better suited for quantitative, high-throughput and comprehensive lipid analysis than LC/MS/MS. The shotgun mass spectrometric method developed here clearly seems to be superior to the LC/MS/MS methods that we are using (for comparison see Table 14).

	Ikeda *et al.* 2008	**Fong *et al.* 2009**	**This Thesis**
Method	**LC/ESI – MS/MS**	**LC/ESI – MS/MS**	**Shotgun MS/MS**
Used sample amount	500 mg mouse brain (25 weeks old) in 16.6 ml	Left-brain hemisphere of 2 d (0.4 – 0.45 g) & 80 d (0.9 – 1 g) old rats in 5.05 ml Used 1/6 of extract (70 – 170 µg)	Variable (Tissue or cell culture) Minimum: 100 µg wet weight of brain tissue
Chromatographic retention time	Ca. 90 minutes	Ca. 25 minutes	0 minutes
Extraction	- Individual (C/M/W – 1:2:0.8) - Redisolve (C/M/W – 30:60:8) - Washing (C/M/W – 30:60:8)	- Mod. Svennerholm and Fredman (C/M/W – 4:8:3) Double Extraction 2 Phase partitioning with 0.01 M KCl	- 150 mM ABC with 5x volume of C/M 10:1 - 150 mM ABC with 5x volume of C/M 2:1 - SOLA™ column purification

	- Eluation (C/M/0.8M sodium acetate – 30:60:8 - Injection	Injection	- Evaporation - Taken up in 20 µl methylamine mix (see Table 5) - Injection
Mass Spectrometer	4000Q TRAP Quadrupole-linear Ion Trap hybrid MS	LTQ-Orbitrap™ Mass Spectrometer	Q Exactive™ Hybrid Quadrupole-Orbitrap Mass Spectrometer
Sensitivity	Not stated	Estimated via S/N ratio LOD = 0.146 – 1.78 µM LOQ = 0.459 – 5.31 µM	Final: LOD = 0.0081 – 0.137 µM LOQ = 0.025 – 0.41 µM
Technical variation: (Coefficiant of Variance = CV)	Not stated	CV: 4.8-12.3%	CV: 5.1 % (w/o GQ1b) 0.24% - 12.4 % (with GQ1b) (see Table 11 for details)

Table 14. Method comparison. Retention time: while Shotgun-MS has no retention time, the column purification is an additional step that LC-MS methods do not have. Hence, the time required for column purification in this method replaces the retention time of the LC-MS methods. Sensitivity: LOD/LOQ range is calculated for required minimal amount of the major mammal brain gangliosides for two dominant species (namely, 36:1 and 38:1), lowest and highest values are stated for all ganglioside classes combined (for more details see Table 11). In regard to the CV values of GQ1b it has to be pointed out, that no class specific internal standard was available for this class throughout the project and it had to be quantified via the modified C17-GT1b class standard. Therefore, the CV of GQ1b is higher.

Overall, the set goals for this method have been reached. It was possible to incorporate it into an pre-existing workflow (Surma et al., 2015) and have a higher sensitivity as well as shorter processing time than comparable method (see Table 14). Nevertheless, still a lot can be done to further enhance this protocol.

To broaden the coverage of this method, further modified C17-ganglioside standards for other classes are required. Here, of particular importance would be the gangliosides associated with malignant development, e.g. GD2 (see section 1.6). Enhancing the repertoire of ganglioside

standards and application of our method could offer a valuable contribution to cancer research and diagnostics and help us unravel the roles gangliosides play in cancer.

Finally, our method was on mouse brain tissue samples. The experiment, done with two different kinds of brain tissues (cerebellum and hemispheres) at different postnatal developmental stages, worked as a proof-of-concept in regard to the ability to perform a “complete acquisition”, by measuring for the first time the gangliosides and the non-ganglioside lipids simultaneously from the same sample. A complete acquisition platform now needs to be developed to establish a reliable combination of these two independently acquired data sets for studies of lipid biology and disease. Since no studies of this type have been done until now, it is not possible to compare our data with others. Importantly, is that ganglioside molecular species have not been quantitively measured in the brain or its individual regions so far.

Overall, the method that we have developed will enable the ganglioside field to move into the molecular species era of lipid research. Little is known yet about their function, especially their role in the nervous system where they are concentrated. This new avenue is exciting and holds great promises for the future of the field.

5. Summary

The goal of this thesis was to develop a high-throughput shotgun-MS lipidomics method to qualitatively and quantitively analyze the major mammalian brain ganglioside classes: GM1, GD1, GT1 and GQ1. As a starting point for the method to be developed, a modified ganglioside extraction method from Svennerholm and Ladisch was used (Svennerholm and Fredman, 1980; Ladisch and Gillard, 1985). The efficiencies and the impact of different extraction procedures to the overall performance were evaluated with a software called OptiVal™. The evaluation showed that the most important steps of the protocol are the salt concentration of the water phase during the 2-phase extraction, and 10 mM NaCl yielded the best sensitivity. Also, the number of washing steps with water during reverse solid phase extraction using C18 resin has a significant effect.

The next step was to find suitable standards for quantification of the individual ganglioside classes. Since deuterated and alike ganglioside standards were commercially not available, we initially used a deuterated PE standard with limited success.

A collaboration with the Ludger Johannes lab provided us with modified C17-ganglioside standards. The term “modified” describes the enzymatic exchange of the fatty acid in the hydrophobic tail by a 17-carbon atom long fatty acid. Since odd numbered fatty acids occur very rarely in nature, it is possible to use the measured intensity of the modified ceramide headgroup of 35:1 (Sphingosine C18:1 + Fatty Acid C17:0) to quantify natural gangliosides. Ideally, we would need to have a fitting modified C17-ganglioside standard for each class to be quantified. Since first only GM1 as a modified standard was available, it was necessary to determine response factors (RFs) for the ganglioside classes GD1, GT1 and GQ1. RFs were assessed empirically by titrating a variety of equimolar concentrations of the modified C17-GM1 standard versus wildtype standards of the other ganglioside classes. After establishment of the RFs it was possible to determine the limits of detection (LOD) and quantification (LOQ) for the ganglioside classes GD1, GT1 and GQ1 - with regard to the modified C17-GM1 standard.

When the modified C17-standards for GD1 and GT1 became available, I was able to find out whether the correct internal standards are superior to the proxy method via response factors. The results clearly showed that the use of a correct class standards is preferable. For GQ1 no modified C17-standard was obtainable, therefore this class still has to be quantified via RFs. Experiments showed that the modified C17-GT1 standard is best suited for that.

Another major goal was to integrate the ganglioside method into the general lipid analysis workflow of the high-throughput shotgun mass spectrometry platform that we were using. To achieve these goals adjustments on the evaluated (=old) protocol had to be done. These adjustments included

changes in the extraction steps from the Svennerholm & Ladisch more into the direction of a Bligh & Dyer based extraction method. This meant abandoning the 2-phase extraction step as well as the chloroform/methanol/water (C/M/W) 4:8:3 extraction, in favor of a C/M 10:1 followed by a C/M 2:1 extraction of 150 mM ammonium-bicarbonate water solution. The goal behind this was to enable a combination of the global lipidome extraction (Surma et al., 2015) with the ganglioside extraction.

Another important improvement was scaling up the extraction process. The use of standard single solid phase extraction (SPE) cartridges was limiting the extraction throughput to only 24 samples at a time, therefore the single SPE cartridges were replaced with the 96-well SPE SOLA™ plates. To process the SOLA™ plates it was necessary to establish the usage of a vacuum manifold. Combined, these changes lowered the overall process time of the protocol from nearly two working days to one working day, without significant loss of sensitivity regarding the measured sample concentrations. This was assessed by performing the mouse brain tissue titration experiment, with all three modified C17-ganglioside class standards GM1, GD1 and GT1.

Finally, the established method was applied to investigate the difference in ganglioside levels in the cerebellum compared to the brain hemispheres in mice of different age. First the C/M 10:1 and 2:1 extraction was done for the analysis of all non-ganglioside lipids in the sample. The leftover water phase was then loaded onto the SOLA™ plates and processed with the new protocol. The results matched the given goals - to establish a protocol to measure and quantify the four major brain ganglioside classes in combination with the global lipidomics in a high-throughput manner - and thus were a success.

To the best of our knowledge, this was the first time such a broad lipidomic measurement has been performed, hence no other studies exist to which the outcome could be compared.

6. Zusammenfassung

Das Ziel dieser Dissertation war es eine Hochdurchsatz-Shotgun-MS Methode zur qualitativen und quantitativen Analyse der vier wichtigsten Gehirngangliosid-Klassen, namens GM1, GD1, GT1 und GQ1, von Säugetieren zu entwickeln. Als Ausgangspunkt für die Protokollentwicklung dienten die modifizierten Extraktionsmethoden von Svennerholm und Ladisch (Svennerholm and Fredman, 1980; Ladisch and Gillard, 1985). Um die Effizienz sowie die Auswirkungen einzelner Extraktionsschritte auf die Sensitivität dieser Methode auszutesten wurde sie zunächst mit Hilfe der Software OptiVal™ evaluiert. Diese Evaluierung zeigte, dass den größten Einfluss auf die Sensitivität während der Extraktion die Salzkonzentration der wässrigen Phase während der 2-phasen Extraktion hat. Eine Salzkonzentration von 10mM NaCl zeigte die besten Resultate. Außerdem wurde offensichtlich, dass die Anzahl der Waschschritte mit Wasser während der umgekehrten Festphasenextraktion mit C18 Resin auch eine signifikante Rolle spielen mit der generellen Regel, je mehr Waschschritte umso besser das Ergebnis.

Der nächste Schritt war es passende Standards zur Quantifizierung der einzelnen Gangliosid-Klassen zu bekommen. Hierbei stellte es sich als Problem heraus, dass deuterierte oder vergleichbare Standards für diese Ganglioside kommerziell nicht verfügbar sind. Daher versuchten wir anfänglich einen deuterierten PE-Standard ersatzweise zu verwenden, mit begrenztem Erfolg.

Eine Kooperation mit dem Ludger Johannes Labor ermöglichte es uns modifizierte C17-Gangliosid-Standards zu erhalten. Mit dem Begriff „modifiziert“ ist gemeint, dass bei diesen Standards die Fettsäure aus der hydrophoben Ceramide-Kopfgruppe enzymatisch ausgetauscht wurde mit einer 17 Kohlenstoff Atom langen Fettsäure. Da Fettsäuren mit einer ungeraden Anzahl an Kohlenstoffatomen auf natürliche Weise nur äußerst selten vorkommen, ist es möglich einen solchen Standard mit einer 35:1 Kopfgruppe (Sphingosine C18:1 + Fettsäure C17:0) zur Quantifizierung von Gangliosiden zu verwenden. Ideal wäre es für jede Gangliosid-Klasse einen eigenen modifizierten Standard zu haben, aber zu Beginn war es nur möglich einen modifizierten Standard für GM1 zu bekommen. Um diesen Standard auch für die Gangliosid-Klassen GD1, GT1 und GQ1 nutzen zu können war es notwendig zunächst sogenannte „Response Factors“ (RFs) empirisch zu bestimmen, diese RFs sollen das unterschiedliche chemische und physikalische Verhalten, z.B. Ionisierungsfähigkeit der Moleküle, der unterschiedlichen Klassen wiederspiegeln. Hierzu wurden die Intensitätsmessungen von verschiedenen äquimolaren Konzentrationen des modifizierten Standards mit den nicht-modifizierten Standards der anderen Gangliosid-Klassen verglichen. Nach der Bestimmung der RFs war es möglich weitere Parameter wie den

Streuungskoeffizienten, sowie die quantifizierbaren und detektierbaren Grenzen für die anderen Gangliosid-Klassen in Bezug auf den modifizierten GM1 Standard zu bestimmen.

Mit der Zeit war es möglich auch noch modifizierte Standards für die Gangliosid-Klassen GD1 und GT1 zu erhalten und die Proxy-Ergebnisse via RFs mit den Messergebnissen passender Klassenstandards zu vergleichen. Das Ergebnis zeigte eindeutig, dass ein passender Klassenstandard zu bevorzugen ist, wo möglich. Für GQ1 war es nicht möglich einen solchen Standard zu bekommen, deswegen musste diese Klasse weiterhin mit Hilfe der RFs quantifiziert werden. Jedoch zeigte sich, dass der modifizierte GT1 Standard hierfür am besten geeignet ist.

Ein weiteres wichtiges Ziel dieser Dissertation war es diese Methode in einen routinemäßigen Arbeitsablauf zur allgemeinen Hochdurchsatz-Lipidanalyse zu integrieren. Um diese Ziele zu erreichen waren einige Änderungen am mit OptiVal™ evaluierten Protokoll notwendig. Diese Anpassungen beinhalteten die Änderung von einer auf Svennerholm und Ladisch basierenden Gangliosid-Extraktionsmethode mehr hin zu einer auf Bligh und Dyer zurückgehende Extraktionsmethode. Dies bedeutete die Abschaffung der 2-phasen Extraktion. Der Extraktionsschritt mit einem Mischungsverhältnisses von Chloroform/Methanol/Wasser (C/M/W) von 4:8:3 wurde ersetzt mit einer C/M 10:1 gefolgt von einer C/M 2:1 Extraktion von 150µl einer 150mM Ammonium-Bicarbonat wässrigen Lösung. Der Grund hierfür war es die Kombination einer bereits etablierten globalen Lipidanalyse-Methode (Surma et al., 2015) mit der hier etablierten Gangliosid-Analyse zu ermöglichen.

Da die Nutzung von einzelnen SPE-Säulen dem Hochdurchsatzansatz im Weg stand, mussten diese zugunsten von 96-well Platten ersetzt werden. SPE-SOLA™ Platten wurden ab sofort verwendet. Um die SOLA™ Platten besser prozessieren zu können war die Etablierung eines Vacuum Manifolds notwendig. Alles in allem brachten diese Veränderungen eine Verringerung der Arbeitszeit des Protokolls von rund 2 Arbeitstagen auf einen Arbeitstag und das ohne Einbußen der Sensitivität für die gemessenen Konzentrationen. Dies wurde auch nochmals überprüft durch die Wiederholung der Titration von Mäusegehirngewebe, dieses Mal mit allen 3 modifizierten Gangliosid-Standarden GM1, GD1 und GT1. Die Resultate dieses Versuches übertrafen die vorgegebenen Ziele und waren daher erfolgreich.

Schließlich wurde die entwickelte Methode verwendet um die unterschiedlichen Gangliosid-Level von Cerebellum und Gehirnhemisphären von Mäusen unterschiedlichen Alters zu verglichen. Das bedeutet eine C/M 10:1 gefolgt von einer 2:1 Extraktion, um damit die nicht-Gangliosid Lipide zu extrahieren und zu bestimmen. Die verbleibende wässrige Phase konnte direkt auf die SOLA™-Platten geladen und prozessiert werden, wie in 3.3 beschrieben.

Die Resultate waren in Übereinstimmung mit den vorgegebenen Zielen – ein Protokoll zu entwickeln mit dem die vier wichtigsten Gangliosid-Klassen in Gehirnen von Säugetieren gemessen und quantifiziert werden können, in Kombination mit der globalen Lipidomik-Analyse und in einem Hochdurchsatzverfahren – erreicht worden.

Nach meinem besten Wissen wurde bislang keine vergleichbar Lipidanalyse von Säugetiergehirnen durchgeführt, bei der so viele Lipidklassen inklusive der Ganglioside qualitativ und quantitativ gemessen werden konnten und zu der diese Ergebnisse verglichen werden könnten.

7. References:

Abrahamsson, S., Dahlén, B., Löfgren, H., Pascher, I., Sundell, S., 1977. Molecular Arrangement and Conformation of Lipids of Relevance to Membrane Structure, in: Abrahamsson, S., Pascher, I. (Eds.), Structure of Biological Membranes, Nobel Foundation Symposia. Springer US, Boston, MA, pp. 1–23. https://doi.org/10.1007/978-1-4684-8127-3_1

Ahmed, M., Cheung, N.-K.V., 2014. Engineering anti-GD2 monoclonal antibodies for cancer immunotherapy. FEBS Lett. 588, 288–297. https://doi.org/10.1016/j.febslet.2013.11.030

Alberts, B., Johnson, A., Lewis, J., Raff, M., Roberts, K., Walter, P., 2002. The Extracellular Matrix of Animals. Mol. Biol. Cell 4th Ed.

Allen, P.M., Roberts, I., Boulnois, G.J., Saunders, J.R., Hart, C.A., 1987. Contribution of capsular polysaccharide and surface properties to virulence of Escherichia coli K1. Infect. Immun. 55, 2662–2668.

Angata, T., Varki, A., 2002. Chemical Diversity in the Sialic Acids and Related α-Keto Acids: An Evolutionary Perspective. Chem. Rev. 102, 439–470. https://doi.org/10.1021/cr000407m

Aoki, K., Perlman, M., Lim, J.-M., Cantu, R., Wells, L., Tiemeyer, M., 2007. Dynamic Developmental Elaboration of N-Linked Glycan Complexity in the Drosophila melanogaster Embryo. J. Biol. Chem. 282, 9127–9142. https://doi.org/10.1074/jbc.M606711200

Ariga, T., Kobayashi, K., Hasegawa, A., Kiso, M., Ishida, H., Miyatake, T., 2001. Characterization of high-affinity binding between gangliosides and amyloid beta-protein. Arch. Biochem. Biophys. 388, 225–230. https://doi.org/10.1006/abbi.2001.2304

Ariga, T., McDonald, M.P., Yu, R.K., 2008. Thematic Review Series: Sphingolipids. Role of ganglioside metabolism in the pathogenesis of Alzheimer's disease—a review. J. Lipid Res. 49, 1157–1175. https://doi.org/10.1194/jlr.R800007-JLR200

Astarita, G., Kendall, A.C., Dennis, E.A., Nicolaou, A., 2015. Targeted lipidomic strategies for oxygenated metabolites of polyunsaturated fatty acids. Biochim. Biophys. Acta 1851, 456–468. https://doi.org/10.1016/j.bbalip.2014.11.012

Aureli, M., Grassi, S., Prioni, S., Sonnino, S., Prinetti, A., 2015. Lipid membrane domains in the brain. Biochim. Biophys. Acta BBA - Mol. Cell Biol. Lipids, Brain Lipids 1851, 1006–1016. https://doi.org/10.1016/j.bbalip.2015.02.001

Aureli, M., Loberto, N., Lanteri, P., Chigorno, V., Prinetti, A., Sonnino, S., 2011. Cell surface sphingolipid glycohydrolases in neuronal differentiation and aging in culture. J. Neurochem. 116, 891–899. https://doi.org/10.1111/j.1471-4159.2010.07019.x

Avdulov, N.A., Chochina, S.V., Igbavboa, U., O'Hare, E.O., Schroeder, F., Cleary, J.P., Wood, W.G., 1997. Amyloid beta-peptides increase annular and bulk fluidity and induce lipid peroxidation in brain synaptic plasma membranes. J. Neurochem. 68, 2086–2091.

Battula, V.L., Shi, Y., Evans, K.W., Wang, R.-Y., Spaeth, E.L., Jacamo, R.O., Guerra, R., Sahin, A.A., Marini, F.C., Hortobagyi, G., Mani, S.A., Andreeff, M., 2012. Ganglioside GD2 identifies breast cancer stem cells and promotes tumorigenesis. J. Clin. Invest. 122, 2066–2078. https://doi.org/10.1172/JCI59735

Baumgart, T., Hammond, A.T., Sengupta, P., Hess, S.T., Holowka, D.A., Baird, B.A., Webb, W.W., 2007. Large-scale fluid/fluid phase separation of proteins and lipids in giant plasma membrane vesicles. Proc. Natl. Acad. Sci. U. S. A. 104, 3165–3170. https://doi.org/10.1073/pnas.0611357104

Biswas, K., Richmond, A., Rayman, P., Biswas, S., Thornton, M., Sa, G., Das, T., Zhang, R., Chahlavi, A., Tannenbaum, C.S., Novick, A., Bukowski, R., Finke, J.H., 2006. GM2 Expression in Renal Cell Carcinoma: Potential Role in Tumor-Induced T-Cell

Dysfunction. Cancer Res. 66, 6816–6825. https://doi.org/10.1158/0008-5472.CAN-06-0250
Bligh, E.G., Dyer, W.J., 1959. A rapid method of total lipid extraction and purification. Can. J. Biochem. Physiol. 37, 911–917. https://doi.org/10.1139/o59-099
Boukhris, A., Schule, R., Loureiro, J.L., Lourenço, C.M., Mundwiller, E., Gonzalez, M.A., Charles, P., Gauthier, J., Rekik, I., Acosta Lebrigio, R.F., Gaussen, M., Speziani, F., Ferbert, A., Feki, I., Caballero-Oteyza, A., Dionne-Laporte, A., Amri, M., Noreau, A., Forlani, S., Cruz, V.T., Mochel, F., Coutinho, P., Dion, P., Mhiri, C., Schols, L., Pouget, J., Darios, F., Rouleau, G.A., Marques, W., Brice, A., Durr, A., Zuchner, S., Stevanin, G., 2013. Alteration of Ganglioside Biosynthesis Responsible for Complex Hereditary Spastic Paraplegia. Am. J. Hum. Genet. 93, 118–123. https://doi.org/10.1016/j.ajhg.2013.05.006
Brady, R.O., Murray, G.J., Moore, D.F., Schiffmann, R., 2001. Enzyme replacement therapy in Fabry disease. J. Inherit. Metab. Dis. 24 Suppl 2, 18–24; discussion 11-12.
Brown, D.A., Rose, J.K., 1992. Sorting of GPI-anchored proteins to glycolipid-enriched membrane subdomains during transport to the apical cell surface. Cell 68, 533–544.
Buccinnà, B., Piccinini, M., Prinetti, A., Scandroglio, F., Prioni, S., Valsecchi, M., Votta, B., Grifoni, S., Lupino, E., Ramondetti, C., Schuchman, E.H., Giordana, M.T., Sonnino, S., Rinaudo, M.T., 2009. Alterations of myelin-specific proteins and sphingolipids characterize the brains of acid sphingomyelinase-deficient mice, an animal model of Niemann-Pick disease type A. J. Neurochem. 109, 105–115. https://doi.org/10.1111/j.1471-4159.2009.05947.x
Carvalho, M., Sampaio, J.L., Palm, W., Brankatschk, M., Eaton, S., Shevchenko, A., 2012. Effects of diet and development on the Drosophila lipidome. Mol. Syst. Biol. 8, 600. https://doi.org/10.1038/msb.2012.29
Cayrol, R., Haqqani, A.S., Ifergan, I., Dodelet-Devillers, A., Prat, A., 2011. Isolation of Human Brain Endothelial Cells and Characterization of Lipid Raft-Associated Proteins by Mass Spectroscopy, in: Nag, S. (Ed.), The Blood-Brain and Other Neural Barriers: Reviews and Protocols, Methods in Molecular Biology. Humana Press, Totowa, NJ, pp. 275–295. https://doi.org/10.1007/978-1-60761-938-3_13
Chalat, M., Menon, I., Turan, Z., Menon, A.K., 2012. Reconstitution of Glucosylceramide Flip-Flop across Endoplasmic Reticulum. J. Biol. Chem. 287, 15523–15532. https://doi.org/10.1074/jbc.M112.343038
Chang, H.R., Cordon-Cardo, C., Houghton, A.N., Cheung, N.K., Brennan, M.F., 1992. Expression of disialogangliosides GD2 and GD3 on human soft tissue sarcomas. Cancer 70, 633–638.
Cheever, M.A., Allison, J.P., Ferris, A.S., Finn, O.J., Hastings, B.M., Hecht, T.T., Mellman, I., Prindiville, S.A., Steinman, R.M., Viner, J.L., Weiner, L.M., Matrisian, L.M., 2009. The Prioritization of Cancer Antigens: A National Cancer Institute Pilot Project for the Acceleration of Translational Research. Clin. Cancer Res. Off. J. Am. Assoc. Cancer Res. 15, 5323–5337. https://doi.org/10.1158/1078-0432.CCR-09-0737
Cheung, N.-K.V., Neely, J.E., Landmeier, B., Nelson, D., Miraldi, F., 1987. Targeting of Ganglioside GD2Monoclonal Antibody to Neuroblastoma. J. Nucl. Med. 28, 1577–1583.
Chou, H.-H., Hayakawa, T., Diaz, S., Krings, M., Indriati, E., Leakey, M., Paabo, S., Satta, Y., Takahata, N., Varki, A., 2002. Inactivation of CMP-N-acetylneuraminic acid hydroxylase occurred prior to brain expansion during human evolution. Proc. Natl. Acad. Sci. 99, 11736–11741. https://doi.org/10.1073/pnas.182257399
Christie, W.W., 1990. Has thin-layer chromatography had its day. Lipid Technol. 2, 22–3.
Cingolani, F., Futerman, A.H., Casas, J., 2016. Ceramide synthases in biomedical research. Chem. Phys. Lipids, Inhibitors of enzymes of lipid metabolism and their medical applications 197, 25–32. https://doi.org/10.1016/j.chemphyslip.2015.07.026
Cohen, M., Varki, A., 2010. The Sialome—Far More Than the Sum of Its Parts. OMICS J. Integr. Biol. 14, 455–464. https://doi.org/10.1089/omi.2009.0148

Crino, P.B., Ullman, M.D., Vogt, B.A., Bird, E.D., Volicer, L., 1989. Brain gangliosides in dementia of the Alzheimer type. Arch. Neurol. 46, 398–401.
D'Angelo, G., Polishchuk, E., Di Tullio, G., Santoro, M., Di Campli, A., Godi, A., West, G., Bielawski, J., Chuang, C.-C., van der Spoel, A.C., Platt, F.M., Hannun, Y.A., Polishchuk, R., Mattjus, P., De Matteis, M.A., 2007. Glycosphingolipid synthesis requires FAPP2 transfer of glucosylceramide. Nature 449, 62–67. https://doi.org/10.1038/nature06097
D'Angelo, G., Uemura, T., Chuang, C.-C., Polishchuk, E., Santoro, M., Ohvo-Rekilä, H., Sato, T., Di Tullio, G., Varriale, A., D'Auria, S., Daniele, T., Capuani, F., Johannes, L., Mattjus, P., Monti, M., Pucci, P., Williams, R.L., Burke, J.E., Platt, F.M., Harada, A., De Matteis, M.A., 2013. Vesicular and non-vesicular transport feed distinct glycosylation pathways in the Golgi. Nature 501, 116–120. https://doi.org/10.1038/nature12423
Daum, G., Lees, N.D., Bard, M., Dickson, R., n.d. Biochemistry, cell biology and molecular biology of lipids of Saccharomyces cerevisiae. Yeast 14, 1471–1510. https://doi.org/10.1002/(SICI)1097-0061(199812)14:16<1471::AID-YEA353>3.0.CO;2-Y
D'Autry, W., Wolfs, K., Yarramraju, S., Schepdael, A.V., Hoogmartens, J., Adams, E., 2010. Characterization and Improvement of Signal Drift Associated with Electron Ionization Quadrupole Mass Spectrometry. Anal. Chem. 82, 6480–6486. https://doi.org/10.1021/ac100780s
Davies, L.R.L., Varki, A., 2015. Why Is N-Glycolylneuraminic Acid Rare in the Vertebrate Brain? Top. Curr. Chem. 366, 31–54. https://doi.org/10.1007/128_2013_419
DeMarco, M.L., Woods, R.J., 2009. Atomic-resolution conformational analysis of the GM3 ganglioside in a lipid bilayer and its implications for ganglioside–protein recognition at membrane surfaces. Glycobiology 19, 344–355. https://doi.org/10.1093/glycob/cwn137
Dolgachev, V., Farooqui, M.S., Kulaeva, O.I., Tainsky, M.A., Nagy, B., Hanada, K., Separovic, D., 2004. De novo ceramide accumulation due to inhibition of its conversion to complex sphingolipids in apoptotic photosensitized cells. J. Biol. Chem. 279, 23238–23249. https://doi.org/10.1074/jbc.M311974200
Efthymiopoulos, I., Hellier, P., Ladommatos, N., Russo-Profili, A., Eveleigh, A., Aliev, A., Kay, A., Mills-Lamptey, B., 2018. Influence of solvent selection and extraction temperature on yield and composition of lipids extracted from spent coffee grounds. Ind. Crops Prod. 119, 49–56. https://doi.org/10.1016/j.indcrop.2018.04.008
Eggeling, C., Ringemann, C., Medda, R., Hein, B., Hell, S.W., 2009a. High-Resolution Far-Field Fluorescence STED Microscopy Reveals Nanoscale Details of Molecular Membrane Dynamics. Biophys. J. 96, 197a. https://doi.org/10.1016/j.bpj.2008.12.1058
Eggeling, C., Ringemann, C., Medda, R., Schwarzmann, G., Sandhoff, K., Polyakova, S., Belov, V.N., Hein, B., Middendorff, C. von, Schönle, A., Hell, S.W., 2009b. Direct observation of the nanoscale dynamics of membrane lipids in a living cell. Nature 457, 1159–1162. https://doi.org/10.1038/nature07596
Eich, C., Manzo, C., Keijzer, S. de, Bakker, G.-J., Reinieren-Beeren, I., García-Parajo, M.F., Cambi, A., 2016. Changes in membrane sphingolipid composition modulate dynamics and adhesion of integrin nanoclusters. Sci. Rep. 6, 20693. https://doi.org/10.1038/srep20693
Ejsing, C.S., Sampaio, J.L., Surendranath, V., Duchoslav, E., Ekroos, K., Klemm, R.W., Simons, K., Shevchenko, A., 2009. Global analysis of the yeast lipidome by quantitative shotgun mass spectrometry. Proc. Natl. Acad. Sci. U. S. A. 106, 2136–2141. https://doi.org/10.1073/pnas.0811700106
Evangelisti, E., Wright, D., Zampagni, M., Cascella, R., Fiorillo, C., Bagnoli, S., Relini, A., Nichino, D., Scartabelli, T., Nacmias, B., Sorbi, S., Cecchi, C., 2013. Lipid Rafts Mediate Amyloid-Induced Calcium Dyshomeostasis and Oxidative Stress in Alzheimer's Disease [WWW Document]. URL https://www.ingentaconnect.com/content/ben/car/2013/00000010/00000002/art00004 (accessed 2.28.19).

Fahy, E., Subramaniam, S., Brown, H.A., Glass, C.K., Merrill, A.H., Murphy, R.C., Raetz, C.R.H., Russell, D.W., Seyama, Y., Shaw, W., Shimizu, T., Spener, F., Meer, G. van, VanNieuwenhze, M.S., White, S.H., Witztum, J.L., Dennis, E.A., 2005. A comprehensive classification system for lipids. J. Lipid Res. 46, 839–862. https://doi.org/10.1194/jlr.E400004-JLR200

Folch, J., Lees, M., Stanley, G.H.S., 1957. A Simple Method for the Isolation and Purification of Total Lipides from Animal Tissues. J. Biol. Chem. 226, 497–509.

Fong, B., Norris, C., Lowe, E., McJarrow, P., 2009. Liquid chromatography-high-resolution mass spectrometry for quantitative analysis of gangliosides. Lipids 44, 867–874. https://doi.org/10.1007/s11745-009-3327-1

Fuchs, B., Süß, R., Nimptsch, A., Schiller, J., 2008. MALDI-TOF-MS Directly Combined with TLC: A Review of the Current State. Chromatographia 69, 95. https://doi.org/10.1365/s10337-008-0661-z

Futerman, A.H., Riezman, H., 2005. The ins and outs of sphingolipid synthesis. Trends Cell Biol. 15, 312–318. https://doi.org/10.1016/j.tcb.2005.04.006

Groux-Degroote, S., Guérardel, Y., Julien, S., Delannoy, P., 2015. Gangliosides in breast cancer: New perspectives. Biochem. Mosc. 80, 808–819. https://doi.org/10.1134/S0006297915070020

Hakomori, S., 2001. Tumor-associated carbohydrate antigens defining tumor malignancy: basis for development of anti-cancer vaccines. Adv. Exp. Med. Biol. 491, 369–402.

Hakomori, S., 1996. Tumor Malignancy Defined by Aberrant Glycosylation and Sphingo(glyco)lipid Metabolism. Cancer Res. 56, 5309–5318.

Halter, D., Neumann, S., van Dijk, S.M., Wolthoorn, J., de Mazière, A.M., Vieira, O.V., Mattjus, P., Klumperman, J., van Meer, G., Sprong, H., 2007. Pre- and post-Golgi translocation of glucosylceramide in glycosphingolipid synthesis. J. Cell Biol. 179, 101–115. https://doi.org/10.1083/jcb.200704091

Han, X., Yang, J., Cheng, H., Ye, H., Gross, R.W., 2004. Toward fingerprinting cellular lipidomes directly from biological samples by two-dimensional electrospray ionization mass spectrometry. Anal. Biochem. 330, 317–331. https://doi.org/10.1016/j.ab.2004.04.004

Han, X., Yang, K., Yang, J., Cheng, H., Gross, R.W., 2006. Shotgun lipidomics of cardiolipin molecular species in lipid extracts of biological samples. J. Lipid Res. 47, 864–879. https://doi.org/10.1194/jlr.D500044-JLR200

Hanada, K., 2006. Discovery of the molecular machinery CERT for endoplasmic reticulum-to-Golgi trafficking of ceramide. Mol. Cell. Biochem. 286, 23–31. https://doi.org/10.1007/s11010-005-9044-z

Hanada, K., Kumagai, K., Yasuda, S., Miura, Y., Kawano, M., Fukasawa, M., Nishijima, M., 2003. Molecular machinery for non-vesicular trafficking of ceramide. Nature 426, 803–809. https://doi.org/10.1038/nature02188

Hancock, J.F., 2006. Lipid rafts: contentious only from simplistic standpoints. Nat. Rev. Mol. Cell Biol. 7, 456–462. https://doi.org/10.1038/nrm1925

Harlalka, G.V., Lehman, A., Chioza, B., Baple, E.L., Maroofian, R., Cross, H., Sreekantan-Nair, A., Priestman, D.A., Al-Turki, S., McEntagart, M.E., Proukakis, C., Royle, L., Kozak, R.P., Bastaki, L., Patton, M., Wagner, K., Coblentz, R., Price, J., Mezei, M., Schlade-Bartusiak, K., Platt, F.M., Hurles, M.E., Crosby, A.H., 2013. Mutations in B4GALNT1 (GM2 synthase) underlie a new disorder of ganglioside biosynthesis. Brain 136, 3618–3624. https://doi.org/10.1093/brain/awt270

Hashimoto, N., Hamamura, K., Kotani, N., Furukawa, Keiko, Kaneko, K., Honke, K., Furukawa, Koichi, 2012. Proteomic analysis of ganglioside-associated membrane molecules: substantial basis for molecular clustering. Proteomics 12, 3154–3163. https://doi.org/10.1002/pmic.201200279

Hemsley, K.M., Hopwood, J.J., 2010. Lessons learnt from animal models: pathophysiology of neuropathic lysosomal storage disorders. J. Inherit. Metab. Dis. 33, 363–371. https://doi.org/10.1007/s10545-010-9078-6
Herzog, R., Schuhmann, K., Schwudke, D., Sampaio, J.L., Bornstein, S.R., Schroeder, M., Shevchenko, A., 2012. LipidXplorer: A Software for Consensual Cross-Platform Lipidomics. PLoS ONE 7. https://doi.org/10.1371/journal.pone.0029851
Herzog, R., Schwudke, D., Schuhmann, K., Sampaio, J.L., Bornstein, S.R., Schroeder, M., Shevchenko, A., 2011. A novel informatics concept for high-throughput shotgun lipidomics based on the molecular fragmentation query language. Genome Biol. 12, R8. https://doi.org/10.1186/gb-2011-12-1-r8
Ikeda, K., Shimizu, T., Taguchi, R., 2008. Targeted analysis of ganglioside and sulfatide molecular species by LC/ESI-MS/MS with theoretically expanded multiple reaction monitoring. J. Lipid Res. 49, 2678–2689. https://doi.org/10.1194/jlr.D800038-JLR200
Inoue, M., Fujii, Y., Furukawa, Keiko, Okada, M., Okumura, K., Hayakawa, T., Furukawa, Koichi, Sugiura, Y., 2002. Refractory Skin Injury in Complex Knock-out Mice Expressing Only the GM3 Ganglioside. J. Biol. Chem. 277, 29881–29888. https://doi.org/10.1074/jbc.M201631200
Ioannou, Y.A., Zeidner, K.M., Gordon, R.E., Desnick, R.J., 2001. Fabry Disease: Preclinical Studies Demonstrate the Effectiveness of α-Galactosidase A Replacement in Enzyme-Deficient Mice. Am. J. Hum. Genet. 68, 14–25.
Itokazu, Y., Tsai, Y.-T., Yu, R.K., 2017. Epigenetic regulation of ganglioside expression in neural stem cells and neuronal cells. Glycoconj. J. 34, 749–756. https://doi.org/10.1007/s10719-016-9719-6
IUPAC-IUB Joint Commission on Biochemical Nomenclature (JCBN) Nomenclature of glycolipids, 1998. . Eur. J. Biochem. 257, 293–298. https://doi.org/10.1046/j.1432-1327.1998.2570293.x
Ivanova, P.T., Milne, S.B., Myers, D.S., Brown, H.A., 2009. Lipidomics: a mass spectrometry based, systems level analysis of cellular lipids. Curr. Opin. Chem. Biol. 13, 526–531. https://doi.org/10.1016/j.cbpa.2009.08.011
Jacobson, K., Sheets, E.D., Simson, R., 1995. Revisiting the fluid mosaic model of membranes. Science 268, 1441–1442.
Jahnke, A., Holmbäck, J., Andersson, R.A., Kierkegaard, A., Mayer, P., MacLeod, M., 2015. Differences between Lipids Extracted from Five Species Are Not Sufficient To Explain Biomagnification of Nonpolar Organic Chemicals. Environ. Sci. Technol. Lett. 2, 193–197. https://doi.org/10.1021/acs.estlett.5b00145
Jin, H.J., Nam, H.Y., Bae, Y.K., Kim, S.Y., Im, I.R., Oh, W., Yang, Y.S., Choi, S.J., Kim, S.W., 2010. GD2 expression is closely associated with neuronal differentiation of human umbilical cord blood-derived mesenchymal stem cells. Cell. Mol. Life Sci. CMLS 67, 1845–1858. https://doi.org/10.1007/s00018-010-0292-z
Kailayangiri, S., Altvater, B., Meltzer, J., Pscherer, S., Luecke, A., Dierkes, C., Titze, U., Leuchte, K., Landmeier, S., Hotfilder, M., Dirksen, U., Hardes, J., Gosheger, G., Juergens, H., Rossig, C., 2012. The ganglioside antigen G(D2) is surface-expressed in Ewing sarcoma and allows for MHC-independent immune targeting. Br. J. Cancer 106, 1123–1133. https://doi.org/10.1038/bjc.2012.57
Kakio, A., Nishimoto, S., Yanagisawa, K., Kozutsumi, Y., Matsuzaki, K., 2001. Cholesterol-dependent Formation of GM1 Ganglioside-bound Amyloid β-Protein, an Endogenous Seed for Alzheimer Amyloid. J. Biol. Chem. 276, 24985–24990. https://doi.org/10.1074/jbc.M100252200
Kawai, H., Allende, M.L., Wada, R., Kono, M., Sango, K., Deng, C., Miyakawa, T., Crawley, J.N., Werth, N., Bierfreund, U., Sandhoff, K., Proia, R.L., 2001. Mice Expressing Only Monosialoganglioside GM3 Exhibit Lethal Audiogenic Seizures. J. Biol. Chem. 276, 6885–6888. https://doi.org/10.1074/jbc.C000847200

Klenk, E., 1942. Über die Ganglioside des Gehirns bei der infantilen amaurotischen Idiotie vom Typ Tay-Sachs. Berichte Dtsch. Chem. Ges. B Ser. 75, 1632–1636. https://doi.org/10.1002/cber.19420751231
Klose, C., Tarasov, K., 2016. Profiling of Yeast Lipids by Shotgun Lipidomics. Methods Mol. Biol. Clifton NJ 1361, 309–324. https://doi.org/10.1007/978-1-4939-3079-1_17
Koles, K., Repnikova, E., Pavlova, G., Korochkin, L.I., Panin, V.M., 2009. Sialylation in protostomes: a perspective from <Emphasis Type="Italic">Drosophila</Emphasis> genetics and biochemistry. Glycoconj. J. 26, 313. https://doi.org/10.1007/s10719-008-9154-4
Kolesnick, R., 2002. The therapeutic potential of modulating the ceramide/sphingomyelin pathway. J. Clin. Invest. 110, 3–8. https://doi.org/10.1172/JCI16127
Kracun, I., Kalanj, S., Cosovic, C., Talan-Hranilovic, J., 1990. Brain gangliosides in Alzheimer's disease. J. Hirnforsch. 31, 789–793.
Kraĉun, I., Rösner, H., Ćosović, C., Stavljenić, A., 1984. Topographical Atlas of the Gangliosides of the Adult Human Brain. J. Neurochem. 43, 979–989. https://doi.org/10.1111/j.1471-4159.1984.tb12833.x
Kracun, I., Rosner, H., Drnovsek, V., Heffer-Lauc, M., Cosovi?, C., Lauc, G., 2002. Human brain gangliosides in development, aging and disease. Int. J. Dev. Biol. 35, 289–295. https://doi.org/10.1387/ijdb.1814411
Kracun, I., Rosner, H., Drnovsek, V., Heffer-Lauc, M., Cosović, C., Lauc, G., 1991. Human brain gangliosides in development, aging and disease. Int. J. Dev. Biol. 35, 289–295.
Kwon, D.-N., Chang, B.-S., Kim, J.-H., 2014. Gene expression and pathway analysis of effects of the CMAH deactivation on mouse lung, kidney and heart. PloS One 9, e107559. https://doi.org/10.1371/journal.pone.0107559
Ladisch, S., Gillard, B., 1985. A solvent partition method for microscale ganglioside purification. Anal. Biochem. 146, 220–231.
Lammie, G., Cheung, N., Gerald, W., Rosenblum, M., Cordoncardo, C., 1993. Ganglioside gd(2) expression in the human nervous-system and in neuroblastomas - an immunohistochemical study. Int. J. Oncol. 3, 909–915.
Laurijssens, B., Aujard, F., Rahman, A., 2013. Animal models of Alzheimer's disease and drug development. Drug Discov. Today Technol. 10, e319-327. https://doi.org/10.1016/j.ddtec.2012.04.001
Ledesma, M.D., Prinetti, A., Sonnino, S., Schuchman, E.H., 2011. Brain pathology in Niemann Pick disease type A: Insights from the acid sphingomyelinase knockout mice. J. Neurochem. 116, 779–788. https://doi.org/10.1111/j.1471-4159.2010.07034.x
Levy, M., Futerman, A.H., 2010. Mammalian Ceramide Synthases. IUBMB Life 62, 347–356. https://doi.org/10.1002/iub.319
Li, M., Zhou, Z., Nie, H., Bai, Y., Liu, H., 2011. Recent advances of chromatography and mass spectrometry in lipidomics. Anal. Bioanal. Chem. 399, 243–249. https://doi.org/10.1007/s00216-010-4327-y
Liang, Y.-J., Ding, Y., Levery, S.B., Lobaton, M., Handa, K., Hakomori, S., 2013. Differential expression profiles of glycosphingolipids in human breast cancer stem cells vs. cancer non-stem cells. Proc. Natl. Acad. Sci. U. S. A. 110, 4968–4973. https://doi.org/10.1073/pnas.1302825110
Liebisch, G., Binder, M., Schifferer, R., Langmann, T., Schulz, B., Schmitz, G., 2006. High throughput quantification of cholesterol and cholesteryl ester by electrospray ionization tandem mass spectrometry (ESI-MS/MS). Biochim. Biophys. Acta 1761, 121–128. https://doi.org/10.1016/j.bbalip.2005.12.007
Liebisch, G., Ekroos, K., Hermansson, M., Ejsing, C.S., 2017. Reporting of lipidomics data should be standardized. Biochim. Biophys. Acta 1862, 747–751. https://doi.org/10.1016/j.bbalip.2017.02.013

Lingwood, D., Ries, J., Schwille, P., Simons, K., 2008. Plasma membranes are poised for activation of raft phase coalescence at physiological temperature. Proc. Natl. Acad. Sci. U. S. A. 105, 10005–10010. https://doi.org/10.1073/pnas.0804374105
Lingwood, D., Simons, K., 2010. Lipid Rafts As a Membrane-Organizing Principle. Science 327, 46–50. https://doi.org/10.1126/science.1174621
Lloyd, K.O., Old, L.J., 1989. Human Monoclonal Antibodies to Glycolipids and Other Carbohydrate Antigens: Dissection of the Humoral Immune Response in Cancer Patients. Cancer Res. 49, 3445–3451.
Marin, R., Rojo, J.A., Fabelo, N., Fernandez, C.E., Diaz, M., 2013. Lipid raft disarrangement as a result of neuropathological progresses: A novel strategy for early diagnosis? Neuroscience 245, 26–39. https://doi.org/10.1016/j.neuroscience.2013.04.025
Martinez, C., Hofmann, T.J., Marino, R., Dominici, M., Horwitz, E.M., 2007. Human bone marrow mesenchymal stromal cells express the neural ganglioside GD2: a novel surface marker for the identification of MSCs. Blood 109, 4245–4248. https://doi.org/10.1182/blood-2006-08-039347
Matsuzaki, K., Horikiri, C., 1999. Interactions of amyloid beta-peptide (1-40) with ganglioside-containing membranes. Biochemistry 38, 4137–4142. https://doi.org/10.1021/bi982345o
McLaurin, J., Franklin, T., Fraser, P.E., Chakrabartty, A., 1998. Structural Transitions Associated with the Interaction of Alzheimer β-Amyloid Peptides with Gangliosides. J. Biol. Chem. 273, 4506–4515. https://doi.org/10.1074/jbc.273.8.4506
Mennel, H.D., Bosslet, K., Wiegandt, H., Sedlacek, H.H., Bauer, B.L., Rodden, A.F., 1992. Expression of GD2-epitopes in human intracranial tumors and normal brain. Exp. Toxicol. Pathol. Off. J. Ges. Toxikol. Pathol. 44, 317–324. https://doi.org/10.1016/S0940-2993(11)80218-6
Möbius, W., Herzog, V., Sandhoff, K., Schwarzmann, G., 1999. Intracellular distribution of a biotin-labeled ganglioside, GM1, by immunoelectron microscopy after endocytosis in fibroblasts. J. Histochem. Cytochem. Off. J. Histochem. Soc. 47, 1005–1014. https://doi.org/10.1177/002215549904700804
Modak, S., Gerald, W., Cheung, N.-K.V., 2002. Disialoganglioside GD2 and a novel tumor antigen: potential targets for immunotherapy of desmoplastic small round cell tumor. Med. Pediatr. Oncol. 39, 547–551. https://doi.org/10.1002/mpo.10151
Mukherjee, P., Faber, A.C., Shelton, L.M., Baek, R.C., Chiles, T.C., Seyfried, T.N., 2008. Thematic Review Series: Sphingolipids. Ganglioside GM3 suppresses the proangiogenic effects of vascular endothelial growth factor and ganglioside GD1a. J. Lipid Res. 49, 929–938. https://doi.org/10.1194/jlr.R800006-JLR200
Müller, W.E., Koch, S., Eckert, A., Hartmann, H., Scheuer, K., 1995. beta-Amyloid peptide decreases membrane fluidity. Brain Res. 674, 133–136.
Neoh, S.H., Gordon, C., Potter, A., Zola, H., 1986. The purification of mouse monoclonal antibodies from ascitic fluid. J. Immunol. Methods 91, 231–235.
Ngamukote, S., Yanagisawa, M., Ariga, T., Ando, S., Yu, R.K., 2007. Developmental changes of glycosphingolipids and expression of glycogenes in mouse brains. J. Neurochem. 103, 2327–2341. https://doi.org/10.1111/j.1471-4159.2007.04910.x
Norton, W.T., Poduslo, S.E., 1973. Myelination in rat brain: changes in myelin composition during brain maturation. J. Neurochem. 21, 759–773.
O'Brien, J.S., Sampson, E.L., 1965. Lipid composition of the normal human brain: gray matter, white matter, and myelin. J. Lipid Res. 6, 537–544.
Okerblom, J.J., Schwarz, F., Olson, J., Fletes, W., Ali, S.R., Martin, P.T., Glass, C.K., Nizet, V., Varki, A., 2017. Loss of CMAH during Human Evolution Primed the Monocyte-Macrophage Lineage toward a More Inflammatory and Phagocytic State. J. Immunol. Baltim. Md 1950 198, 2366–2373. https://doi.org/10.4049/jimmunol.1601471

Pati, S., Nie, B., Arnold, R.D., Cummings, B.S., 2016. Extraction, chromatographic and mass spectrometric methods for lipid analysis. Biomed. Chromatogr. BMC 30, 695–709. https://doi.org/10.1002/bmc.3683
Patterson, M.C., Vecchio, D., Prady, H., Abel, L., Wraith, J.E., 2007. Miglustat for treatment of Niemann-Pick C disease: a randomised controlled study. Lancet Neurol. 6, 765–772. https://doi.org/10.1016/S1474-4422(07)70194-1
Peterson, B.L., Cummings, B.S., 2006. A review of chromatographic methods for the assessment of phospholipids in biological samples. Biomed. Chromatogr. BMC 20, 227–243. https://doi.org/10.1002/bmc.563
Pettus, B.J., Chalfant, C.E., Hannun, Y.A., 2002. Ceramide in apoptosis: an overview and current perspectives. Biochim. Biophys. Acta 1585, 114–125.
Pike, L.J., 2006. Rafts defined: a report on the Keystone Symposium on Lipid Rafts and Cell Function. J. Lipid Res. 47, 1597–1598. https://doi.org/10.1194/jlr.E600002-JLR200
Platt, F., Walkley, S. (Eds.), 2004. Lysosomal Disorders of the Brain: Recent Advances in Molecular and Cellular Pathogenesis and Treatment. Oxford University Press, Oxford, New York.
Platt, F.M., 2014. Sphingolipid lysosomal storage disorders. Nature 510, 68–75. https://doi.org/10.1038/nature13476
Platt, F.M., Lachmann, R.H., 2009. Treating lysosomal storage disorders: Current practice and future prospects. Biochim. Biophys. Acta BBA - Mol. Cell Res., Lysosomes 1793, 737–745. https://doi.org/10.1016/j.bbamcr.2008.08.009
Poliak, S., Peles, E., 2003. The local differentiation of myelinated axons at nodes of Ranvier. Nat. Rev. Neurosci. 4, 968–980. https://doi.org/10.1038/nrn1253
Potapenko, M., Shurin, G.V., de León, J., 2007. Gangliosides as immunomodulators. Adv. Exp. Med. Biol. 601, 195–203.
Proia, R.L., 2004. Gangliosides help stabilize the brain. Nat. Genet. 36, 1147–1148. https://doi.org/10.1038/ng1104-1147
Proia, R.L., 2003. Glycosphingolipid functions: insights from engineered mouse models. Philos. Trans. R. Soc. B Biol. Sci. 358, 879–883. https://doi.org/10.1098/rstb.2003.1268
Ravindranath, M.H., Muthugounder, S., Presser, N., Ye, X., Brosman, S., Morton, D.L., 2005. Endogenous immune response to gangliosides in patients with confined prostate cancer. Int. J. Cancer 116, 368–377. https://doi.org/10.1002/ijc.21023
Reddy, A., Caler, E.V., Andrews, N.W., 2001. Plasma Membrane Repair Is Mediated by Ca2+-Regulated Exocytosis of Lysosomes. Cell 106, 157–169. https://doi.org/10.1016/S0092-8674(01)00421-4
Repnikova, E., Koles, K., Nakamura, M., Pitts, J., Li, H., Ambavane, A., Zoran, M.J., Panin, V.M., 2010. Sialyltransferase Regulates Nervous System Function in Drosophila. J. Neurosci. 30, 6466–6476. https://doi.org/10.1523/JNEUROSCI.5253-09.2010
Roth, G.S., Joseph, J.A., Mason, R.P., 1995. Membrane alterations as causes of impaired signal transduction in Alzheimer's disease and aging. Trends Neurosci. 18, 203–206.
Sa, G., Das, T., Moon, C., Hilston, C.M., Rayman, P.A., Rini, B.I., Tannenbaum, C.S., Finke, J.H., 2009. GD3, an Over-Expressed, Tumor-Derived Ganglioside, Mediates the Apoptosis of Activated But Not Resting T cells. Cancer Res. 69, 3095–3104. https://doi.org/10.1158/0008-5472.CAN-08-3776
Sales, S., Graessler, J., Ciucci, S., Al-Atrib, R., Vihervaara, T., Schuhmann, K., Kauhanen, D., Sysi-Aho, M., Bornstein, S.R., Bickle, M., Cannistraci, C.V., Ekroos, K., Shevchenko, A., 2016. Gender, Contraceptives and Individual Metabolic Predisposition Shape a Healthy Plasma Lipidome. Sci. Rep. 6, 27710. https://doi.org/10.1038/srep27710
Sampaio, J.L., Gerl, M.J., Klose, C., Ejsing, C.S., Beug, H., Simons, K., Shevchenko, A., 2011. Membrane lipidome of an epithelial cell line. Proc. Natl. Acad. Sci. U. S. A. 108, 1903. https://doi.org/10.1073/pnas.1019267108

Sandhoff, K., Harzer, K., 2013. Gangliosides and Gangliosidoses: Principles of Molecular and Metabolic Pathogenesis. J. Neurosci. 33, 10195–10208. https://doi.org/10.1523/JNEUROSCI.0822-13.2013
Sandhoff, K., Kolter, T., 2003. Biosynthesis and degradation of mammalian glycosphingolipids. Philos. Trans. R. Soc. B Biol. Sci. 358, 847–861. https://doi.org/10.1098/rstb.2003.1265
Sastry, P.S., 1985. Lipids of nervous tissue: Composition and metabolism. Prog. Lipid Res. 24, 69–176. https://doi.org/10.1016/0163-7827(85)90011-6
Sato, T., Zakaria, A.M., Uemura, S., Ishii, A., Ohno-Iwashita, Y., Igarashi, Y., Inokuchi, J.-I., 2005. Role for up-regulated ganglioside biosynthesis and association of Src family kinases with microdomains in retinoic acid-induced differentiation of F9 embryonal carcinoma cells. Glycobiology 15, 687–699. https://doi.org/10.1093/glycob/cwi055
Scandroglio, F., Venkata, J.K., Loberto, N., Prioni, S., Schuchman, E.H., Chigorno, V., Prinetti, A., Sonnino, S., 2008. LIPID CONTENT OF BRAIN, OF BRAIN MEMBRANE LIPID DOMAINS, AND OF NEURONS FROM ACID SPHINGOMYELINASE DEFICIENT MICE (ASMKO). J. Neurochem. 107, 329–338. https://doi.org/10.1111/j.1471-4159.2008.05591.x
Schnaar, R.L., Gerardy-Schahn, R., Hildebrandt, H., 2014. Sialic Acids in the Brain: Gangliosides and Polysialic Acid in Nervous System Development, Stability, Disease, and Regeneration. Physiol. Rev. 94, 461–518. https://doi.org/10.1152/physrev.00033.2013
Schneider, M.C., Exley, R.M., Ram, S., Sim, R.B., Tang, C.M., 2007. Interactions between Neisseria meningitidis and the complement system. Trends Microbiol. 15, 233–240. https://doi.org/10.1016/j.tim.2007.03.005
Schuhmann, K., Almeida, R., Baumert, M., Herzog, R., Bornstein, S.R., Shevchenko, A., 2012. Shotgun lipidomics on a LTQ Orbitrap mass spectrometer by successive switching between acquisition polarity modes. J. Mass Spectrom. 47, 96–104. https://doi.org/10.1002/jms.2031
Schultz, M.L., Tecedor, L., Chang, M., Davidson, B.L., 2011. Clarifying lysosomal storage diseases. Trends Neurosci. 34, 401–410. https://doi.org/10.1016/j.tins.2011.05.006
Schwudke, D., Liebisch, G., Herzog, R., Schmitz, G., Shevchenko, A., 2007. Shotgun lipidomics by tandem mass spectrometry under data-dependent acquisition control. Methods Enzymol. 433, 175–191. https://doi.org/10.1016/S0076-6879(07)33010-3
Sedel, F., 2007. [Niemann-Pick diseases in adults]. Rev. Med. Interne 28 Suppl 4, S292-293. https://doi.org/10.1016/j.revmed.2007.09.017
Sewell, G.W., Hannun, Y.A., Han, X., Koster, G., Bielawski, J., Goss, V., Smith, P.J., Rahman, F.Z., Vega, R., Bloom, S.L., Walker, A.P., Postle, A.D., Segal, A.W., 2012. Lipidomic profiling in Crohn's disease: abnormalities in phosphatidylinositols, with preservation of ceramide, phosphatidylcholine and phosphatidylserine composition. Int. J. Biochem. Cell Biol. 44, 1839–1846. https://doi.org/10.1016/j.biocel.2012.06.016
Sezgin, E., Kaiser, H.-J., Baumgart, T., Schwille, P., Simons, K., Levental, I., 2012. Elucidating membrane structure and protein behavior using giant plasma membrane vesicles. Nat. Protoc. 7, 1042–1051. https://doi.org/10.1038/nprot.2012.059
Shah, A., Chen, D., Boda, A.R., Foster, L.J., Davis, M.J., Hill, M.M., 2015. RaftProt: mammalian lipid raft proteome database. Nucleic Acids Res. 43, D335–D338. https://doi.org/10.1093/nar/gku1131
Sharma, P., Varma, R., Sarasij, R.C., Ira, null, Gousset, K., Krishnamoorthy, G., Rao, M., Mayor, S., 2004. Nanoscale organization of multiple GPI-anchored proteins in living cell membranes. Cell 116, 577–589.
Simons, K., Ikonen, E., 1997. Functional rafts in cell membranes. Nature 387, 569–572. https://doi.org/10.1038/42408
Simons, K., van Meer, G., 1988. Lipid sorting in epithelial cells. Biochemistry 27, 6197–6202.

Simpson, M.A., Cross, H., Proukakis, C., Priestman, D.A., Neville, D.C.A., Reinkensmeier, G., Wang, H., Wiznitzer, M., Gurtz, K., Verganelaki, A., Pryde, A., Patton, M.A., Dwek, R.A., Butters, T.D., Platt, F.M., Crosby, A.H., 2004. Infantile-onset symptomatic epilepsy syndrome caused by a homozygous loss-of-function mutation of GM3 synthase. Nat. Genet. 36, 1225–1229. https://doi.org/10.1038/ng1460

Singer, S.J., Nicolson, G.L., 1972. The fluid mosaic model of the structure of cell membranes. Science 175, 720–731.

Sonnino, S., Aureli, M., Grassi, S., Mauri, L., Prioni, S., Prinetti, A., 2014. Lipid rafts in neurodegeneration and neuroprotection. Mol. Neurobiol. 50, 130–148. https://doi.org/10.1007/s12035-013-8614-4

Sturgeon, C.M., Viljoen, A., 2011. Analytical error and interference in immunoassay: minimizing risk. Ann. Clin. Biochem. 48, 418–432. https://doi.org/10.1258/acb.2011.011073

Surma, M.A., Herzog, R., Vasilj, A., Klose, C., Christinat, N., Morin-Rivron, D., Simons, K., Masoodi, M., Sampaio, J.L., 2015. An automated shotgun lipidomics platform for high throughput, comprehensive, and quantitative analysis of blood plasma intact lipids. Eur. J. Lipid Sci. Technol. 117, 1540–1549. https://doi.org/10.1002/ejlt.201500145

Svennerholm, L., 1994. Gangliosides--a new therapeutic agent against stroke and Alzheimer's disease. Life Sci. 55, 2125–2134.

Svennerholm, L., Fredman, P., 1980. A procedure for the quantitative isolation of brain gangliosides. Biochim. Biophys. Acta 617, 97–109.

The Evolution of Thin-Layer Chromatography, 2008. , in: Chapters in the Evolution of Chromatography. PUBLISHED BY IMPERIAL COLLEGE PRESS AND DISTRIBUTED BY WORLD SCIENTIFIC PUBLISHING CO., pp. 208–220. https://doi.org/10.1142/9781860949449_0017

Thermo Scientific SOLA SPE cartridges and plates Technical Guide, n.d. 20.

Thompson, T.E., Tillack, T.W., 1985. Organization of glycosphingolipids in bilayers and plasma membranes of mammalian cells. Annu. Rev. Biophys. Biophys. Chem. 14, 361–386. https://doi.org/10.1146/annurev.bb.14.060185.002045

Tidhar, R., Futerman, A.H., 2013. The complexity of sphingolipid biosynthesis in the endoplasmic reticulum. Biochim. Biophys. Acta 1833, 2511–2518. https://doi.org/10.1016/j.bbamcr.2013.04.010

Tsubuki, S., Takaki, Y., Saido, T.C., 2003. Dutch, Flemish, Italian, and Arctic mutations of APP and resistance of Abeta to physiologically relevant proteolytic degradation. Lancet Lond. Engl. 361, 1957–1958.

Tsuchida, T., Saxton, R.E., Morton, D.L., Irie, R.F., 1989. Gangliosides of human melanoma. Cancer 63, 1166–1174.

Ungerer, J.P.J., Pretorius, C.J., Dimeski, G., O'Rourke, P.K., Tyack, S.A., 2010. Falsely elevated troponin I results due to outliers indicate a lack of analytical robustness. Ann. Clin. Biochem. 47, 242–247. https://doi.org/10.1258/acb.2010.010012

van der Beek, N.A., de Vries, J.M., Hagemans, M.L., Hop, W.C., Kroos, M.A., Wokke, J.H., de Visser, M., van Engelen, B.G., Kuks, J.B., van der Kooi, A.J., Notermans, N.C., Faber, K.G., Verschuuren, J.J., Reuser, A.J., van der Ploeg, A.T., van Doorn, P.A., 2012. Clinical features and predictors for disease natural progression in adults with Pompe disease: a nationwide prospective observational study. Orphanet J. Rare Dis. 7, 88. https://doi.org/10.1186/1750-1172-7-88

van Meer, G., Hoetzl, S., 2010. Sphingolipid topology and the dynamic organization and function of membrane proteins. FEBS Lett. 584, 1800–1805. https://doi.org/10.1016/j.febslet.2009.10.020

Varki, A., 2010. Uniquely human evolution of sialic acid genetics and biology. Proc. Natl. Acad. Sci. U. S. A. 107, 8939–8946. https://doi.org/10.1073/pnas.0914634107

Varki, A., 2009. Multiple changes in sialic acid biology during human evolution. Glycoconj. J. 26, 231–245. https://doi.org/10.1007/s10719-008-9183-z

Varki, A., 2008. Sialic acids in human health and disease. Trends Mol. Med. 14, 351–360. https://doi.org/10.1016/j.molmed.2008.06.002
Vimr, E.R., Kalivoda, K.A., Deszo, E.L., Steenbergen, S.M., 2004. Diversity of Microbial Sialic Acid Metabolism. Microbiol. Mol. Biol. Rev. 68, 132–153. https://doi.org/10.1128/MMBR.68.1.132-153.2004
Vitner, E.B., Futerman, A.H., 2013. Neuronal forms of Gaucher disease. Handb. Exp. Pharmacol. 405–419. https://doi.org/10.1007/978-3-7091-1511-4_20
Vitner, E.B., Platt, F.M., Futerman, A.H., 2010. Common and Uncommon Pathogenic Cascades in Lysosomal Storage Diseases. J. Biol. Chem. 285, 20423–20427. https://doi.org/10.1074/jbc.R110.134452
Wang, B., Brand-Miller, J., 2003. The role and potential of sialic acid in human nutrition. Eur. J. Clin. Nutr. 57, 1351–1369. https://doi.org/10.1038/sj.ejcn.1601704
Wu, Z.-L., Schwartz, E., Seeger, R., Ladisch, S., 1986. Expression of GD2 Ganglioside by Untreated Primary Human Neuroblastomas. Cancer Res. 46, 440–443.
Xu, Y.-H., Barnes, S., Sun, Y., Grabowski, G.A., 2010. Multi-system disorders of glycosphingolipid and ganglioside metabolism. J. Lipid Res. 51, 1643–1675. https://doi.org/10.1194/jlr.R003996
Yamashita, T., Wada, R., Sasaki, T., Deng, C., Bierfreund, U., Sandhoff, K., Proia, R.L., 1999. A vital role for glycosphingolipid synthesis during development and differentiation. Proc. Natl. Acad. Sci. U. S. A. 96, 9142–9147.
Yanagisawa, K., McLaurin, J., Michikawa, M., Chakrabartty, A., Ihara, Y., 1997. Amyloid beta-protein (A beta) associated with lipid molecules: immunoreactivity distinct from that of soluble A beta. FEBS Lett. 420, 43–46.
Yanagisawa, K., Odaka, A., Suzuki, N., Ihara, Y., 1995. GM1 ganglioside-bound amyloid beta-protein (A beta): a possible form of preamyloid in Alzheimer's disease. Nat. Med. 1, 1062–1066.
Yanagisawa, M., Yoshimura, S., Yu, R.K., 2011. Expression of GD2 and GD3 gangliosides in human embryonic neural stem cells. ASN NEURO 3. https://doi.org/10.1042/AN20110006
Yanagisawa, M., Yu, R.K., 2007. The expression and functions of glycoconjugates in neural stem cells. Glycobiology 17, 57R-74R. https://doi.org/10.1093/glycob/cwm018
Yang, K., Han, X., 2016. Lipidomics: Techniques, Applications, and Outcomes Related to Biomedical Sciences. Trends Biochem. Sci. 41, 954–969. https://doi.org/10.1016/j.tibs.2016.08.010
Yang, K., Han, X., 2011. Accurate quantification of lipid species by electrospray ionization mass spectrometry - Meet a key challenge in lipidomics. Metabolites 1, 21–40. https://doi.org/10.3390/metabo1010021
Yu, R.K., Itokazu, Y., 2014. Glycolipid and glycoprotein expression during neural development. Adv. Neurobiol. 9, 185–222. https://doi.org/10.1007/978-1-4939-1154-7_9
Yu, R.K., Macala, L.J., Taki, T., Weinfield, H.M., Yu, F.S., 1988. Developmental changes in ganglioside composition and synthesis in embryonic rat brain. J. Neurochem. 50, 1825–1829.
Yu, R.K., Nakatani, Y., Yanagisawa, M., 2009. The role of glycosphingolipid metabolism in the developing brain. J. Lipid Res. 50, S440–S445. https://doi.org/10.1194/jlr.R800028-JLR200
Yu, R.K., Tsai, Y.-T., Ariga, T., Yanagisawa, M., 2011. Structures, biosynthesis, and functions of gangliosides—An overview. J. Oleo Sci. 60, 537–544.
Yuki, N., 2007. Ganglioside mimicry and peripheral nerve disease. Muscle Nerve 35, 691–711. https://doi.org/10.1002/mus.20762
Yuki, N., Hartung, H.-P., 2012. Guillain–Barré Syndrome. N. Engl. J. Med. 366, 2294–2304. https://doi.org/10.1056/NEJMra1114525

Zarbo, R.J., Jones, B.A., Friedberg, R.C., Valenstein, P.N., Renner, S.W., Schifman, R.B., Walsh, M.K., Howanitz, P.J., 2002. Q-tracks: a College of American Pathologists program of continuous laboratory monitoring and longitudinal tracking. Arch. Pathol. Lab. Med. 126, 1036–1044. https://doi.org/10.1043/0003-9985(2002)126<1036:QT>2.0.CO;2
Zellmer, S., Lasch, J., 1997. Individual variation of human plantar stratum corneum lipids, determined by automated multiple development of high-performance thin-layer chromatography plates. J. Chromatogr. B. Biomed. Sci. App. 691, 321–329. https://doi.org/10.1016/S0378-4347(96)00470-7
Zeng, B.J., Torres, P.A., Viner, T.C., Wang, Z.H., Raghavan, S.S., Alroy, J., Pastores, G.M., Kolodny, E.H., 2008. Spontaneous appearance of Tay-Sachs disease in an animal model. Mol. Genet. Metab. 95, 59–65. https://doi.org/10.1016/j.ymgme.2008.06.010
Zervas, M., Somers, K.L., Thrall, M.A., Walkley, S.U., 2001. Critical role for glycosphingolipids in Niemann-Pick disease type C. Curr. Biol. CB 11, 1283–1287.
Zhang, S., Cui, W., 2014. Sox2, a key factor in the regulation of pluripotency and neural differentiation. World J. Stem Cells 6, 305–311. https://doi.org/10.4252/wjsc.v6.i3.305
Zhang, T., Chen, S., Liang, X., Zhang, H., 2015. Development of a mass-spectrometry-based lipidomics platform for the profiling of phospholipids and sphingolipids in brain tissues. Anal. Bioanal. Chem. 407, 6543–6555. https://doi.org/10.1007/s00216-015-8822-z
Ziak, M., Qu, B., Zuo, X., Zuber, C., Kanamori, A., Kitajima, K., Inoue, S., Inoue, Y., Roth, J., 1996. Occurrence of poly(alpha2,8-deaminoneuraminic acid) in mammalian tissues: widespread and developmentally regulated but highly selective expression on glycoproteins. Proc. Natl. Acad. Sci. 93, 2759–2763. https://doi.org/10.1073/pnas.93.7.2759

Anlage 1

Technische Universität Dresden

Medizinische Fakultät Carl Gustav Carus

Promotionsordnung vom 24. Juli 2011

Erklärungen zur Eröffnung des Promotionsverfahrens

1. Hiermit versichere ich, dass ich die vorliegende Arbeit ohne unzulässige Hilfe Dritter und ohne Benutzung anderer als der angegebenen Hilfsmittel angefertigt habe; die aus fremden Quellen direkt oder indirekt übernommenen Gedanken sind als solche kenntlich gemacht.

2. Bei der Auswahl und Auswertung des Materials sowie bei der Herstellung des Manuskripts habe ich Unterstützungsleistungen von folgenden Personen erhalten:
.....
.....

3. Weitere Personen waren an der geistigen Herstellung der vorliegenden Arbeit nicht beteiligt. Insbesondere habe ich nicht die Hilfe eines kommerziellen Promotionsberaters in Anspruch genommen. Dritte haben von mir weder unmittelbar noch mittelbar geldwerte Leistungen für Arbeiten erhalten, die im Zusammenhang mit dem Inhalt der vorgelegten Dissertation stehen.

4. Die Arbeit wurde bisher weder im Inland noch im Ausland in gleicher oder ähnlicher Form einer anderen Prüfungsbehörde vorgelegt.

5. Die Inhalte dieser Dissertation wurden in folgender Form veröffentlicht:
.....
.....

6. Ich bestätige, dass es keine zurückliegenden erfolglosen Promotionsverfahren gab.
.....

7. Ich bestätige, dass ich die Promotionsordnung der Medizinischen Fakultät der Technischen Universität Dresden anerkenne. 8. Ich habe die Zitierrichtlinien für Dissertationen an der Medizinischen Fakultät der Technischen Universität Dresden zur Kenntnis genommen und befolgt.

Ort, Datum

Unterschrift des Doktoranden:

(Diese Erklärungen sind an das Ende der Arbeit einzubinden) Formblatt 1.2.1, Seite 1-1, erstellt 18.10.2013

Anlage 2

Hiermit bestätige ich die Einhaltung der folgenden aktuellen gesetzlichen Vorgaben im Rahmen meiner Dissertation

- das zustimmende Votum der Ethikkommission bei Klinischen Studien, epidemiologischen Untersuchungen mit Personenbezug oder Sachverhalten, die das Medizinproduktegesetz betreffen
  Aktenzeichen der zuständigen Ethikkommission

  ……..……..……...

- die Einhaltung der Bestimmungen des Tierschutzgesetzes
  Aktenzeichen der Genehmigungsbehörde zum Vorhaben/zur Mitwirkung

  ……..……...

- die Einhaltung des Gentechnikgesetzes
  Projektnummer ……..……..……..

- die Einhaltung von Datenschutzbestimmungen der Medizinischen Fakultät und des Universitätsklinikums Carl Gustav Carus.

Dresden, den

Unterschrift des Doktoranden:

Formblatt 1.1, Seite 1-1, erstellt 27.05.2015

(Anlage 1 und 2 sind an das Ende der Dissertation einzubinden)